Mass balances of Yala and Rikha Samba ~~Glacier~~glaciers, Nepal from 2000 to 2017

Dorothea Stumm[1,2], Sharad Prasad Joshi[2], Tika Ram Gurung[2], Gunjan Silwal[2,3]

[1]Independent consultant, 8184 Bachenbülach, Switzerland
[2]ICIMOD, G.P.O. Box 3226, Kathmandu, 44600, Nepal
[3]Department of Earth and Atmospheric Sciences, University of Alberta, Edmonton, Alberta, T6G 2E3, Canada

Correspondence to: Dorothea Stumm (stummd@gmail.com)

Abstract. The glacier mass balance is an important variable to describe the climate system, and is used for various applications like water resource management or runoff modelling. The direct or glaciological ~~method is~~and the geodetic method are the standard methods to quantify glacier mass changes, and both methods are an integral part of international glacier monitoring strategies~~, and the mass balance is an essential variable to describe the climate system and model runoff.~~. In 2011, we established two glacier mass~~-~~-balance programmes on Yala and Rikha Samba ~~Glacier~~glaciers in the Nepal Himalaya. Here we present the methods and data ~~that we ingested into the database of the World Glacier Monitoring Service. We present~~ for glacier length changes and the directly measured annual mass balances for the first six mass~~-~~-balance years for both glaciers. For Yala Glacier we additionally present the ~~mass balance of~~directly measured seasonal ~~in situ measurements~~mass balance, and the mass balance from 2000 to 2012 analysed with the geodetic method. The annual mass~~-~~-balance rates of Yala Glacier from 2000 to 2012 and from 2011 to 2017 are -0.74 ±0.53 m and -0.~~74~~80 ±0.28 m w.e. a^{-1}, and for Rikha Samba Glacier from 2011 to 2017 -0.39 ±0.32 m w.e. a^{-1}. The cumulative mass loss for the period 2011 to 2017 for Yala and Rikha Samba ~~Glacier~~glaciers is -4.~~44~~80 ±0.69 m w.e. and -2.34 ±0.79 m w.e., respectively. The winter balance of Yala Glacier is positive in every investigated year, but the negative summer balance determines the annual balance. ~~The~~Compared to regional mean geodetic mass~~-~~-balances rates in the Nepalese Himalaya, the mean mass-balance rate of Rikha Samba Glacier is in a similar range, and the mean mass-balance rate of Yala Glacier is more negative ~~than on other glaciers in the region, mostly~~ because of the small and low~~-~~-lying accumulation area. ~~The mass balance of Rikha Samba Glacier is more positive than the other glaciers in the region, likely because of~~ During the ~~large and high lying accumulation area.~~study period, a change of Yala Glacier's surface topography has been observed with glacier thinning and downwasting. Due to the topography, the retreat rates of Rikha Samba Glacier are ~~much~~ higher than for Yala Glacier. From 1989 to 2013, Rikha Samba retreated 431 m (-18.0 m a^{-1}), and from 1974 to 2016 Yala Glacier retreated 346 m (-8.2 m a^{-1}). ~~During~~The data of the ~~study period, a change of Yala Glacier's surface topography has been observed with glacier thinning~~annual and ~~downwasting, which indicates the likely disappearance of Yala Glacier within this century. The datasets~~seasonal mass balances, point mass balance, geodetic mass balance and length changes are ~~freely~~ accessible from WGMS (~~2020a~~2021): Fluctuations of Glaciers Database. World Glacier Monitoring Service, Zurich, Switzerland~~.~~, http://dx.doi.org/10.5904/wgms-fog-~~2020-08.~~2021-xx.

1 Introduction

Glaciers are an essential climate variable (ECV) that contribute to understand and describe the global climate system (IGOS, 2007; Bojinski et al., 2014, Haeberli et al., 2000). The glacier mass balance is one of the seven headline indicators for global climate monitoring (Trewin et al., 2021) and one of the products of the ECV glacier, besides area and glacier thickness changes (GCOS, 2016). ~~The~~ Mass-balance monitoring with the glaciological method ~~for glacier mass balance monitoring~~ is an integral part of international glacier monitoring strategies ~~and a significant component~~(Haeberli et al., 2007; Trewin et al. 2021). The glacier mass balance is relevant in various regards, such as climate indicator, for glacier process understanding, the hydrological cycle and modelling, hazards and contribution to ~~estimate global~~ sea level rise~~, regional river runoff and local~~

~~hazards.~~. As an ~~important~~input variable the mass balance is used to model the water availability and its change, and runoff scenarios for glacierized catchments and downstream livelihoods and ecosystems (Huss and Hock, 2018; Immerzeel et al., 2012; Kaser et al~~.~~., 2010). The World Glacier Monitoring Service (WGMS) manages the ~~data warehouse~~database for glacier monitoring data including mass balance and frontal variation data, and runs the Global Terrestrial Network for Glaciers (GTN-G) in collaboration with partners~~.~~ (IGOS, 2007; WGMS, 2020b). GTN-G is the framework for the internationally coordinated monitoring of the ECV glacier, and ~~supports~~in support of the United Nations Framework Convention on Climate Change (UNFCCC).

In the Fourth Assessment Report of the Intergovernmental Panel on Climate Change (Cruz et al., 2007; Cogely et al., 2010), misinformation was published about an extreme above global average shrinkage of Himalayan glaciers. This led to the question about the actual status and future development of the glaciers in the Himalayas. The current contribution of glaciers in the Hindu Kush Himalayan (HKH) region to the water availability downstream and sea level rise still involve~~ still~~ large uncertainties (Zemp et al., 2020; Immerzeel et al., 2019; Azam et al., 2018; Lutz et al., 2014, Marzeion et al., 2012; Bolch et al., 2012). Still only few~~ long-term~~ programmes are established to monitor the in situ glacier mass balance and length changes on clean glaciers in Bhutan, China, India, Nepal and Pakistan (e.g. Azam et al., 2018; Wagnon et al., 2020; Tshering and Fujita, 2016; Dobhal et al., 2013), and only few include seasonal measurements (Wagnon et al., 2013; Azam et al., 2016; Sherpa et al., 2017). On a regional scale glacier mass balances have been estimated by remote sensing techniques (e.g. Abdullah et al., 2020; Maurer et al., 2019; Gardelle et al., 2013; Vincent et al., 2013; Kääb et al., 2012; Berthier et al., 2007) and modelling (Fujita et al., 2011; Shea et al., 2015a; Tawde et al., 2017). However, due to the remoteness, high altitude topography and logistical challenges there is still a lack of in situ measurements to validate and calibrate such studies. Some studies ~~focus~~focused on ablation and runoff on a high spatial and temporal resolution~~, especially~~ on clean and debris covered glaciers (Litt et al., 2019; Pratap et al., 2019; Pratap et al., 2015; Immerzeel et al., 2014; Fujita and Sakai, 2014~~; Lutz et al., 2014~~), but rarely ~~measure~~measured precipitation and snow accumulation in high altitudes due to challenges such as harsh conditions for precipitation measurements or difficult access to the accumulation zone.

A detailed review on the status and mass changes of Himalayan glaciers has been provided by Azam et al. (2018). They found that up to the year 2000, the mean glacier mass balance was in a similar range as the global average, but likely less negative after 2000. The longest time series with direct glaciological measurements ~~are~~is found for Chhota Shigri Glacier, India, with measurements since 2002 (Mandal et al., 2020; Wagnon et al., 2007; Azam et al., 2012, 2014 and 2016). Other investigated glaciers in the Indian Himalaya ~~partly with ongoing monitoring~~ are for example Dokriani, Gara, Gor Garang, Naradu, Neh Nar, Shaune Garang and Tipra Bank (Dobhal et al., 2008; Vincent et al., 2013; Pratap et al., 2015; Azam et al. 2018; WGMS, 2020a). In the Chinese Himalaya, ~~glaciological and dGPS mass balance records~~geodetic mass-balance data measured with differential global navigation satellite system (dGNSS) surveys are available from 1991 to 1993 and 2007 to 2010 for Kangwure Glacier, north of Mt Shisha Pangma and Langtang Valley, and from 2006 to 2010 on Naimona 'Nyi Glacier, in an upper tributary of the Ganges (Liu et al. 1996; Tian et al., 2014; WGMS, 2020a). ~~Glaciological and in situ geodetic mass~~ Additionally, glaciological mass-balance data are available for Kangwure Glacier from 1991 to 1993, and Naimona 'Nyi Glacier from 2006 to 2010. Glaciological and dGNSS mass-balance measurements have been carried out in Bhutan on Gangju La Glacier from 2003-2014 (Tshering and Fujita, 2016) and Thana Glacier since 2012 by the National Center for Hydrology and Meteorology by the Government of Bhutan, and the partners ICIMOD and the Norwegian Water Resources and Energy Directorate. In Afghanistan, ~~index~~point measurements were initiated in 2017 on Pir Yakh Glacier and are continued by the University of Kabul, the Ministry of Energy and Water and supported by ICIMOD (WGMS, 2020b).

In the Nepal Himalaya extensive glaciological measurements have been carried out by Japanese researchers on Rikha Samba Glacier, Hidden Valley and AX010 in Shorong Himal since the ~~1970's~~1970s, and on Yala Glacier, Langtang Valley since the ~~1980's~~1980s (e.g. Ageta and Higuchi, 1984; Fujii et al., 1996; Fujita et al., 1998; Fujita et al., 2001; Sugiyama et al., 2013). Mass~~-~~-balance programmes were established on Mera Glacier in Hinku Valley, Pokalde and West Changri Nup ~~Glacier~~glaciers in Khumbu Valley in 2007, 2009 and 2010, respectively (Wagnon et al., 2013; Sherpa et al., 2017). Wagnon et al. (2020) ~~use a comprehensive monitoring approach for Mera Glacier by reanalysing~~reanalysed the mass-balance data ~~and calibrating~~of Mera Glacier by using geodetic mass balances to calibrate the glaciological measurements from 2007 to 2019. Various researchers used the geodetic method with remote sensing products ~~or in situ surface surveys~~ to calculate thickness changes (e.g. Bolch et al., 2008; Bolch et al., 2011; Nuimura et al., 2012; Lindenmann, 2012; Ragettli et al., 2016).

On Rikha Samba Glacier, the first glaciological fieldwork was carried out in 1974 by Japanese researchers as part of the Glaciological Expedition of Nepal (GEN) (Fujii et al., 1976). Further fieldwork was carried out in October 1995, including terminus surveys, glacier surface profiles, flow measurements, ice core drilling and meteorological observations (Fujii et al., 1996; Fujita et al., 1997a; Shrestha et al., 1976). In October 1998 and 1999, stakes were installed and measured for direct point mass-balance measurements (Fujita et al., 2001). Terminus position changes and surface flow velocities were also measured and weather data collected. In 2010, the glacier surface was again surveyed ~~with dGPS~~by dGNSS and the geodetic mass balances calculated (Fujita and Nuimura, 2011) and meteorological data collected.

Yala Glacier was selected for the Himalayan Glacier Boring Project based on a GEN reconnaissance flight in Langtang Valley because it was the only one without debris cover and ~~it had~~offered easy access to the glacier and the accumulation area (Watanabe et al., 1984). Comprehensive studies were carried out with a wide range of measurements~~, for example glacier processes~~ in the field of glaciology, meteorology~~,~~ and geomorphology ~~and photogrammetry~~ (e.g. Murakami et al., 1989; Ono, 1985; Yokohama, 1984). Stake measurements were taken in September and October 1982 (Ageta et al., 1984), and from summer 1985 to spring 1986 (Iida et al., 1987). In the accumulation area, Okawa (1991), Iida et al~~.,~~. (1984), Watanabe et al. (1984), and Steinegger et al. (1993) investigated the snow cover, boreholes, crevasses and ice cliffs to better understand the processes including mass balance, hydrology and snow metamorphosis. Fujita et al. (1998) carried out further glaciological measurements in 1994 and 1996 and documented an accelerated retreat and surface lowering of Yala Glacier in the 1990s and decreasing flow velocities. Various studies ~~(e.g.~~assessed historic and recent glacier fluctuations at Yala Glacier and in the Langtang Valley (e.g. Shiraiwa and Watanabe, 1991; Ono, 1985; Yamada et al., 1992; Kappenberger et al., 1993~~) document historic and recent glacier fluctuations at Yala Glacier and for Langtang Valley.~~). Hydro-meteorological observations were made by Japanese researchers in 1982, 1985 to 1986, 1989 to 1991, and 2008 to 2011 (Yamada et al., 1992; Takahashi et al., 1987a; 1987b; Fujita et al., 1997b; Shiraiwa et al., 1992; unpublished data). Based on sensitivity studies and observational data from Yala and other Himalayan glaciers Fujita (2008a, 2008b) highlights the importance of precipitation seasonality on the climatic sensitivity of glacier mass balance, besides air temperature changes.

In 2011 the HKH-Cryosphere Monitoring Project was initiated in Nepal by ICIMOD, and its partners the Department of Hydrology and Meteorology of the Government of Nepal, Kathmandu University and Tribhuvan University. The project goal was to improve the knowledge and understanding of the cryosphere in relation to climate change and impact on water resources in the HKH region and capacity building. Within this framework mass-balance monitoring programmes were established on Yala and Rikha Samba glaciers. An integral part of the project were~~In the Fourth Assessment Report of the Intergovernmental Panel on Climate Change (Cruz et al., 2007; Cogely et al., 2010), misinformation was published about an extreme above global average shrinkage of Himalayan glaciers. This led to the question about the actual status and future development of the glaciers in the Himalayas. Since then, many studies have been published on the glacier status and changes with remote sensing techniques and modelling approaches. However, in situ monitoring programmes of glacier mass balances and high-altitude weather stations are still rare. The main objective of this study was to establish sustainable and long-term glacier mass balance programmes on Yala and Rikha Samba Glacier and submit the standardized data to the World Glacier Monitoring Service (WGMS, 2015; 2017; 2020a; 2020b). An integral part of the programme was to conduct~~ trainings every year on the easily accessible Yala Glacier for a few dozens of students and professionals from the Himalayan countries, on one hand to build capacity for sustainable and consistent measurements, and on the other hand to promote the development of further mass-balance programmes in other parts of the ~~Hindu Kush Himalayan~~HKH Region. Students from Kathmandu University utilized preliminary mass~~-~~-balance data for their Master ~~theses'~~theses (Baral et al., 2014; Gurung et al., 2016; Acharya and Kayastha, 2019).

Here we focus on the mass balance of Yala and Rikha Samba glaciers. At Yala Glacier ~~where combined bi-annual~~we measured the mass balance twice a year in the field ~~measurements and~~ from 2011 to 2017, with remote sensing ~~approaches allowed to assess the mass balance of this glacier~~ from 2000 to ~~2017~~2012, and assessed glacier length changes from 1974 ~~onwards~~to 2016. On Rikha Samba Glacier we assess the annual mass balances and glacier length changes from 2011 to 2017, and 1989 ~~onwards~~to 2013, respectively. The methods are documented for ~~the~~ these measurements and data submitted to the WGMS Fluctuations of Glaciers (FoG) database (WGMS, ~~2020a; 2020b). The descriptions of challenges, methods and decisions confronted within a Himalayan context may serve as reference for colleagues starting new glacier monitoring programmes in the Himalayas.~~2021), and other supporting data beyond the scope of the WGMS FoG database.

2 Study areas and climatic setting

Yala Glacier is a small and debris-free glacier in central Nepal in Langtang Valley, and Rikha Samba Glacier is a valley glacier with a moderate altitude range located in western Nepal, in the Hidden Valley in Lower Mustang (Fig. 1, Table 1). Both glaciers are under the influence of the ~~South~~ Indian summer monsoon~~. However,~~, but Rikha Samba Glacier lies behind the main weather divide in the rain shadow zone and receives less precipitation. ~~Yala Glacier has been studied since 1981 (Higuchi et al., 1984), and Rikha Samba Glacier already in 1974 and from 1994 onwards, with long gaps (Fujita et al., 1997a). In 2011, for both glaciers, monitoring programmes were re-started, in the framework of the HKH-Cryosphere Monitoring Project (CMP), by ICIMOD, and its partners the Department of Hydrology and Meteorology of the Government of Nepal, Kathmandu University and Tribhuvan University.~~Both glaciers are summer-accumulation type glaciers (Ageta and Higuchi, 1984), which are characterized by an overlapping main accumulation and ablation season during the monsoon season (Fig. S1). A brief description of summer-accumulation type glaciers and mass-balance measurements is provided in the Supplement (section S1).

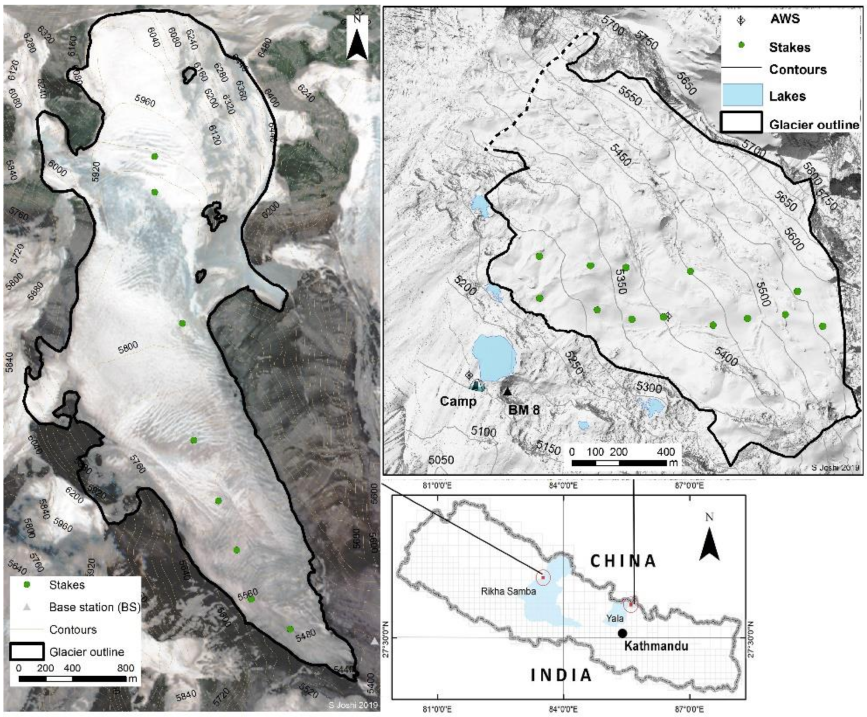

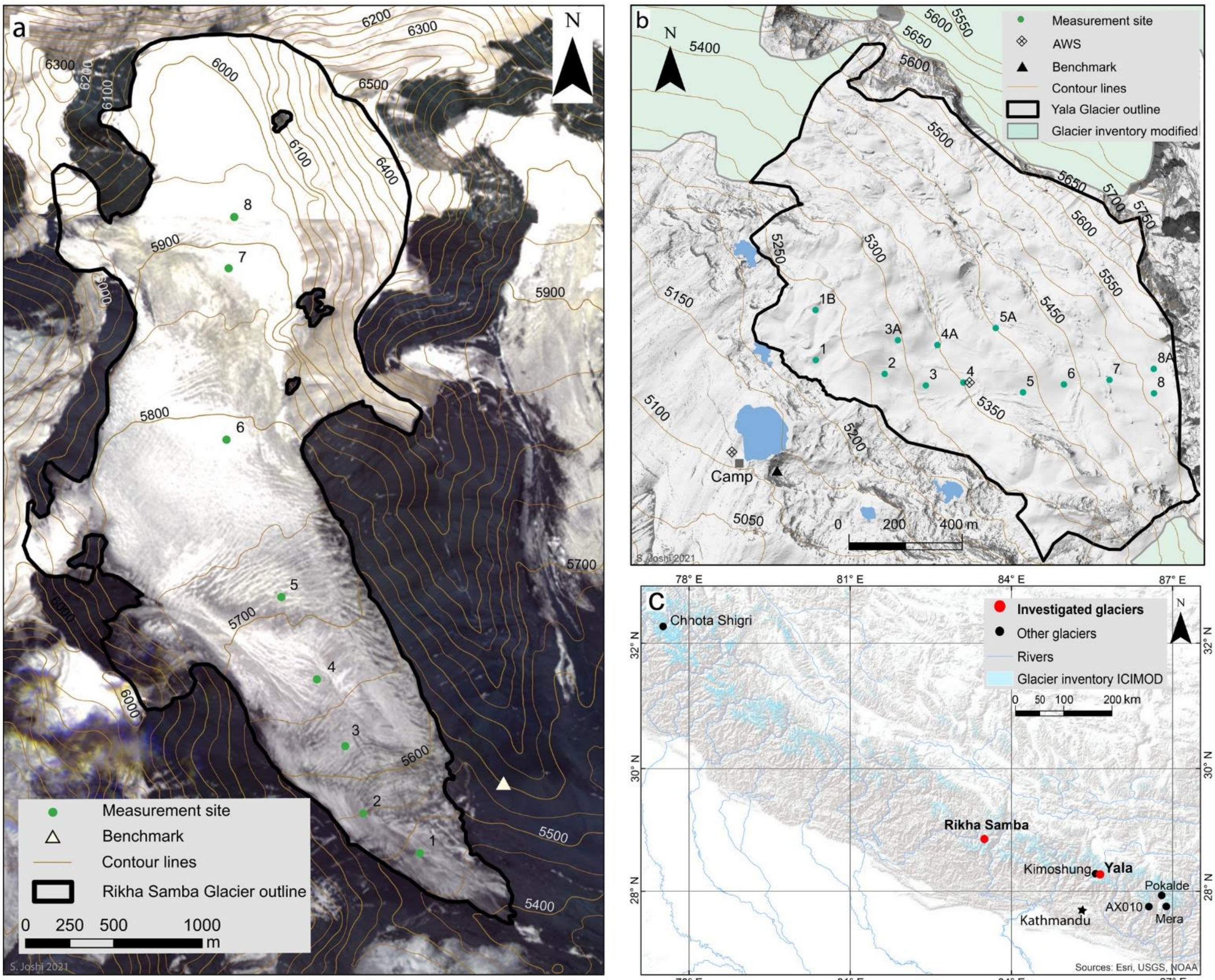

Figure 1: ~~Study~~The study sites Rikha Samba ~~(left)~~ and Yala ~~Glacier (right),~~glaciers showing the measurement ~~network and glacier boundaries~~sites and their location in the Himalayas. At all measurements sites stakes were installed. Snow pits were dug at the top stakes and at selected lower stakes provided snow was present. (a) For Rikha Samba Glacier RapidEye orthoimages from April 2010 ~~(Rikha Samba) and 2012 (Yala). The~~ were used for the background ~~images~~image and glacier outlines. The contour lines are ~~the hill-shaded DEM~~ derived from the SRTM-3 ~~and~~DEM. (b) For Yala Glacier GeoEye-1 ~~image of~~ orthoimages from January 2012 ~~for Rikha Samba and Yala Glacier, respectively.~~were used for the background image and in combination with dGNSS data for the glacier outlines. The contour lines are derived from the DEM2012 generated from the GeoEye-1 stereo images. (c) The overview map shows the location of the two investigated glaciers and other glaciers mentioned in the discussion section. The glacier inventory is from ICIMOD (Bajracharya et al., 2014).

Table 1. Geographic and topographic features of Yala Glacier in Langtang Valley and Rikha Samba Glacier in the Hidden Valley. **The balanced-budget equilibrium line altitude and accumulation area ration are denoted as ELA$_0$ and AAR$_0$.**

General features of	Yala Glacier	Rikha Samba Glacier
Country, region	Nepal, Rasuwa district	Nepal, Mustang district
Mountain range	Langtang Himal, Central Nepal Himalaya	Dhaulagiri, Western Nepal Himalaya
River system	Trisuli basin, Ganges river	Kali Gandaki basin, Ganges river
Climate	Indian monsoon zone	~~Rain~~Indian monsoon zone, rain shadow
Glacier type	Summer-accumulation type	Summer-accumulation type
Glacier characteristics ~~and mass balance information~~		
Latitude/ Longitude	28° 14' N, 85° 34' E	28° 50' N, 83° 30' E
Elevation range	5168–5661 m a.s.l.	5416–6515 m a.s.l.
Glacier area/length	1.61 km^2/1.4 km (2012, GeoEye-1)	5.7 km^2/5.4 km (2010, ~~Rapid Eye~~RapidEye)
Orientation	South-west	South-east
~~ELA$_0$~~Average slope	~~~5380 m a.s.l.~~25°	~~~5760~~5416–6000 m a.s.l.: 10° 6000–6515 m a.s.l.: 36°
~~AAR$_0$~~	~~49 %~~	~~66 %~~
Measurement information		
Maximum number of measurement sites	14 (between 5175–5483 m a.s.l.)	8 (between 5437–5900 m a.s.l.)
Measurement frequency	~~Biannually~~Twice a year in May and November (pre- and post-monsoon)	Annually in October (post-monsoon)
Mass-balance information		
ELA$_0$	~5380 m a.s.l.	~5760 m a.s.l.
AAR$_0$	0.49	0.66

2.1 Yala and Rikha Samba ~~Glacier~~glaciers

Yala Glacier (28° 14' N, 85° 36' E) is located in the Rasuwa district, Central Nepal about 70 km north of Kathmandu, draining into Langtang River which feeds the Trisuli, and then Ganges River. It is a plateau-shaped glacier, ranging from 5168 m to 5661 m a.s.l, and with a length and area of about 1.4 km and 1.61 km^2, respectively~~.~~ (Fig 1). The ~~glacier~~ice body extends further to north-west~~, however, for~~ on a similar elevation range, with steep slopes, ice cliffs and rockfall areas. For the mass-balance analyses, ~~the glacier has been~~ Yala Glacier's drainage basin was separated from the adjacent ice body along the flowline~~, based on the surface contour line method.~~ .

The ~~slopes of the~~ glacier ~~face~~faces mainly ~~southwest,~~south-west and ~~have numerous~~the average slope is 25°. Numerous ice cliffs and steep slopes ~~steeper than 50° that make up 5 % of~~are distributed over the glacier area, ~~whereas the vertical cliffs cannot be quantified~~but mainly in the ~~DEM~~northern part of the glacier. The mean and maximum ice thickness measured by ground penetrating radar (GPR) was 36 m and 61 m in 2009, and the glacier bed topography indicates several small overdeepenings (Sugiyama et al., 2013). The glacier is polythermal (Okawa, 1991; Sugiyama et al., 2013), has clean ice with little debris and small proglacial ponds.

In the 2015 Nepal earthquake, rockfall covered parts of the ~~glacier~~ice body, which ~~are outside~~is next to the defined outlines~~.~~ of Yala Glacier. In these parts we find a transition from ~~glacier ice with~~ debris~~ cover~~-covered glacier to possible permafrost with refrozen meltwater and buried ice. Yala Glacier sits on a gneiss bedrock shelf, which forms part of the base from which ~~the earth's largest~~a large landslide ~~in a crystalline environment~~ slipped (Weidinger et al., 2002, Takagi et al., 2007). Weidinger et al. (2002) suggest that the landslide was a mountain of about 8000 m height, which collapsed about 51 ±13 ~~Ka~~ka ago (Takagi et al., 2007). The dislocated mass lies ~~southwest~~south-west of Yala Glacier and has largely been eroded in the most recent high glaciation. The landslide left behind an open topography, ~~which together~~ with ~~the southwest aspect of the glacier allows~~ Yala Glacier ~~to receive a lot of solar radiation. The~~located within and sheltered by the surrounding high mountains of the Langtang range (>6500 m a.s.l.~~) possibly shelter Yala Glacier from strong high winds and precipitation.~~).

Rikha Samba Glacier (28° 50' N, 83° 30' E) is located in the Hidden Valley on the north side of the main range, and is part of Lower Mustang. The Sangda River drains the Hidden Valley and joins the Kali Gandaki River further down. The glacier ~~is polythermal (Gilbert et al., 2020), ranges from~~ has an elevation range of 5416 m to 6515 m a.s.l. and ~~has~~ a length and area of 5.4 km and 5.7 km^2. The ice is polythermal and the maximum ice thickness measured is 178 ±2 m (Gilbert et al., 2020). At about 6000 m at the head of the valley, the glacier is wide and flows down with a gentle slope of ~10° on average, facing mainly south, and ~~southeast~~south-east at the glacier tongue. Above 6000 m a.s.l, the glacier is steep with an average slope of ~36° making up 19 % of the glacier area, and flowing down from the sides of the valley. ~~The climate at Rikha Samba and in the Hidden Valley is drier and windier.~~

2.2 Climate

The Himalayan mountains are an orographic barrier causing strong north-south, but also altitudinal temperature and precipitation gradients. Nepal is under the influence of the Indian summer monsoon that brings the majority of the annual precipitation, and receives in winter some precipitation from westerlies (Bookhagen and Burbank, 2010). The ~~inter-annual~~interannual variability of precipitation is much larger in winter than in summer, caused by westerly disturbances and occasional cyclones originating in the Bay of Bengal (Seko and Takahashi, 1991; Fujita et al., 1997b). However, climate information from high elevations in the HKH ~~are~~is sparse. The few high-altitude climate stations are mostly situated in valley floors and satellite derived products are less reliable (Salerno et al., 2015; Shea et al., 2015b; Ménégoz et al., 2013). Snowfall studies quantifying timing and amounts are sparse but critical (Litt et al., 2019), and automated snowfall measurements are challenging because undercatch can be up to 20 to 50 % in windy conditions (Rasmussen et al., 2012). Meteorological data from Rikha Samba Glacier, Yala Glacier and other automatic weather stations (AWS) in the Langtang and Dudh Koshi catchments were compared by Shea et al. (2015b). They analysed temperature, incoming radiation, wind, precipitation and other parameters from December 2012 to December 2013, as far as data were available.

Precipitation has been analysed for the Langtang Valley and Rikha Samba Glacier based on reanalysis data and field measurements (Immerzeel et al~~.~~., 2012; Racoviteanu et al., 2013; Fujita et al., 2001). Immerzeel et al. (2012) found that the upper Langtang ~~Khola~~ catchment received 814 mm of precipitation per year, and 77 % of it during monsoon from June to September based on ERA40 data from ~~1957-~~1957 to 2002. The ~~climate~~automatic weather station nearest to Yala Glacier with long-term data is in Kyangjing at 3,920 m a.s.l., which is about 6 km horizontal distance and south~~-~~-west from Yala Glacier. Racoviteanu et al. (2013) analysed the ~~climate station~~AWS data at Kyangjing between 1988 and 2006 and found ~~an average~~a mean annual precipitation of 647 mm. Fujita & Nuimura (2011) estimated the long-term annual mean precipitation at Yala Glacier to be 772 mm. From December 2012 to November 2013, Shea et al. (2015) measured 924 mm precipitation in Kyangjing, which includes an extreme precipitation event in October 2013. The conditions at the leeside of the main mountain range at Rikha Samba Glacier are much drier. Precipitation measured with a totalizer and a tipping bucket in the vicinity of the terminus of Rikha Samba Glacier (5267 m a.s.l.) amounted to about 450 mm from October 1998 to September 1999 (Fujita et al., 2001). The precipitation measured from October to April is minimal and likely indicates underrepresented snowfall. Fujita and Nuimura (2011) estimated at least 370 mm of long-term mean annual precipitation at Rikha Samba Glacier, and Shrestha et al., (1976) measured 203 mm of precipitation at 5055 m a.s.l. in the Hidden Valley during monsoon from July to early September 1974.

The mean annual air temperature in Kyangjing was about 4 °C from 1988 to 2012. Near Rikha Samba Glacier's terminus, the mean annual ~~mean~~ air temperatures were –4.6° C and –5° C, at 5267 m a.s.l. in 1999 and at 5310 m a.s.l. in 2014, respectively (Fujita et al., 2001; Gilbert et al., 2020). Temperature lapse rates vary with the season, with largest and smallest lapse rates in winter and summer, respectively (Immerzeel et al., 2015). The diurnal temperature variabilities are smallest during monsoon (Shea et al., 2015b).

~~Generally,~~The sky in the Nepal Himalaya ~~the sky~~ is generally clear in the post-monsoon and winter season~~, indicated by the incoming solar radiation.~~ (Fujita et al., 2001). Cloudiness increases during pre-monsoon and reaches a maximum during monsoon. During monsoon, the cloudiness at Yala Glacier is much higher than at Rikha Samba Glacier, which can be explained by the valley circulation and cloud formation patterns in Langtang and the leeside location of Rikha Samba Glacier (Fujita et al., 2001; Shea et al., 2015b; Litt et al., 2019). During post-monsoon and winter, the incoming solar radiation is higher at Yala Glacier, which can be explained by the south-west aspect of the glacier and the open topography left behind by the landslide. The wind directions at the Yala Base Camp station show a dominance of bimodal valley winds (Shea et al., 2015b). The Rikha Samba station is additionally exposed to synoptic-scale flows. Throughout the year, the wind velocities at Rikha Samba Glacier are higher and with a larger variability than at Yala Glacier. ~~(Shea et al., 2015b).~~ The highest wind speeds are recorded in winter from October to May, with strong wind events with >8 ms^{-1} (Fujita et al., 2001). Winter wind velocities measured at Rikha Samba Glacier are very high and ~~possibly caused by strong~~result from the channelling of synoptic-scale winds ~~associated to the subtropical jet stream (Ding and Sikka, 2006).~~(Shea et al., 2015b). The winter wind speeds at Yala Glacier are much smaller, ~~possibly~~probably because Yala Glacier is better sheltered by surrounding high mountains. During monsoon from June to September the ~~windspeeds~~wind speeds at both glaciers are lower with a smaller variability.

3 Data and methods

The mass balance of the two glaciers ~~is~~was monitored from 2011 to 2017 with the direct, glaciological method using stakes, snow pits and cores, and for Yala Glacier also with the geodetic method from 2000 to 2012. The frontal variations were evaluated based on satellite images, ~~GPS and dGPS~~dGNSS and global positioning system (GPS) data.

3.1 Data collection

The in situ measurements ~~of the HKH-CMP~~ started in autumn 2011 and are conducted ~~biannually~~twice a year on Yala and annually on Rikha Samba ~~Glacier~~glaciers. On Yala Glacier, the annual/summer balance ~~measurement~~measurements were taken in November. The winter balance was measured in late April or early May, and in 2015 in early June due to the major earthquake in Nepal on 25 April 2015. On Rikha Samba Glacier, in the first years the measurements were carried out in September, which is rather early because still under the influence of the monsoon. In the following years, the measurements were carried out in October or November. Generally, October and November are ideal periods for mass~~-~~ balance measurements in the central Nepal Himalaya, but coincide with the main festival season in Nepal. The festival season is of great religious importance, lasts for several weeks, and varies every year by weeks. This makes it hard to plan fieldwork at fixed dates and find people to conduct measurements. The autumn expeditions with trainings on Yala Glacier were conducted after the last festival ended to allow training participation from various institutions and universities.

3.1.1 In situ mass balance

The in situ mass balance was measured following Kaser et al. (2003), taking into consideration aspects in the ablation and accumulation area specific to summer-accumulation type glaciers (for details see Supplement, section S1). In the ablation area, the mass balance is measured with bamboo stakes. If snow is present, its depth is usually measured at each measurement site, and at selected ~~sakes~~stakes the snow density and profile are also recorded. In the accumulation area, ~~bamboo~~snow pits are dug or cores taken, and the snow profile, depth and density recorded. Additionally, several snow probing measurements are taken. Bamboo stakes mainly mark the measurements sites, but in absence of snow pit data they are also used for the mass~~-~~ balance calculation, in particular in the case of a negative mass balance. The snow pit measurements are only reliable if the previous measurement ~~horizon~~surface can be clearly ~~be~~ identified, e.g. when marked with a sawdust layer. Difficulties arise in the accumulation area, if the cumulative ablation ~~and~~temporarily exceeds the cumulative accumulation ~~occur in~~during the

~~same~~measurement period~~. If there is ablation before new accumulation, this~~ (Fig. S2). The exceeding ablation is not represented in a snow pit measurement and likely impacts the sawdust layer. Stake readings are less reliable because the underlying snow and firn layers compact over time and may push or pull the stake up or down.

On Yala Glacier, the ~~measurement network stretches~~measurements stretch along a line ~~that has been measured~~established in the past by Japanese ~~Researchers~~researchers (Fujita et al., 1998). In the lower part a few stakes were initially added in a transect. Since the glacier has been shrinking, a second row of stakes was installed parallel to the original line in November 2016, in an attempt to maintain measurements also in future when the glacier retreats beyond the current stake locations. ~~Large~~In the northern and highest parts of the glacier ~~are difficult to access~~ no measurements were taken because ~~of ice cliffs, crevasses, and~~ steep terrain~~. There is likely high ablation at the ice cliffs~~, crevasses and ~~steep slopes, which creates a bias that cannot be quantified.~~ice cliffs make access difficult.

On Rikha Samba Glacier, eight stakes are installed along the approximate glacier ~~flowline~~centre line with some deviation, which follow roughly the stake setup of the Japanese researchers (Fujita et al., 2001). In the first year, the lower five stakes were installed, and in 2012 additional 3 measurement sites ~~established.~~were established. Snow depth was probed, and the density measured in snow pits, but sawdust was spread only during few occasions and found only once, making accumulation measurements challenging. In 2011 and 2014, the conditions on the glacier were very difficult and the higher part of the glacier could not be reached~~. Snow depth, and snow pits with density were measured, but sawdust was spread only during few occasions and found only once, making accumulation measurements challenging.~~

~~At Yala Glacier, the measured average densities with standard deviation for snow and firn were 336 kg m^{-3} (±81 kg m^{-3}) and 562 kg m^{-3} (±128 kg m^{-3}). However, harder firn layers were difficult to measure and dependent of the site and conditions, firn densities were estimated between 550 kg and 700 kg m^{-3}. For ice we assumed a density of 900 kg m^{-3}. At Rikha Samba Glacier, the average snow density measured was 399 kg m^{-3} with a standard deviation of ±70 kg m^{-3}.~~

3.1.2 ~~GPS~~GNSS surveys

Differential ~~GPS (dGPS) were~~GNSS was used to survey the glacier termini, measurement sites, benchmarks, thickness changes along profiles, and surface velocities (Table S1). The devices were dual frequency ~~dGPS,~~dGNSS units from Topcon and Magellan ProMark 3, and used in real time kinematic (RTK) mode. The instrument accuracy is within a 10 mm range in RTK mode after post-processing. In the field the antenna was kept vertical in the backpack as much as possible and thus the accuracy is estimated to be ±0.3 m~~ at worst. At every visit, the measurement sites were also surveyed with handheld Garmin GPS, occasionally also the glacier terminus. The elevations of the handheld GPS were not used because of the higher uncertainty and inconsistent geoid correction by various users. At Yala Glacier, the number of visible satellites was normally very high, possibly due to the open topography, hence the GPS data often have a relatively high accuracy for a handheld GPS~~. Yala Glacier's terminus was mapped with a handheld Garmin GPS unit in November 2012 and dGNSS Topcon units in May 2014 and 2016. On Rikha Samba Glacier, the terminus was surveyed with a dGNSS Topcon unit in September 2013.

~~Yala Glacier's terminus is very broad and hence the terminus has been mapped covering the lowest part of the glacier, and beyond in an attempt to map part of the glacier outlines. The mapping was done with a Garmin GPS in November 2012 and a Topcon dGPS in May 2014 and 2016. On Rikha Samba Glacier, the terminus was surveyed with a Topcon dGPS in September 2013.~~

The glacier surface profiles of Yala and Rikha Samba ~~Glacier~~glaciers were repeatedly surveyed with ~~dGPS~~dGNSS, along a longitudinal profile and three and two cross-profiles, respectively, but only data from May 2012 from Yala Glacier are presented here. Already Sugiyama et al., (2013) surveyed the profile line in 2009. The repeated measurements provide the opportunity to further analyse the mass balance with an independent complementing method (Wagnon et al., 2013, 2020). Annual surface velocities were derived from stake ~~displacement~~displacements between 8 May 2012 and 5 May 2014 on Yala Glacier.

3.2 Maps, satellite images and DEMs

For Yala Glacier, various maps ~~have been~~were compared and evaluated for their suitability for area, volume and frontal change analysis. The maps include the Survey of India, the so-called Schneider and the Nepal topographical maps published in 1965, 1990 and 1995, the map by the Japanese Glaciological Expedition Nepal (GEN) map (Yokoyama, 1984) and glacier outlines from the ICIMOD glacier inventory of Nepal (Bajracharya et al., 2014; Table S2). The GEN map and glacier inventory data were used; however, despite good quality no other maps could be used because of transformation issues and inconsistencies. The GEN map is based on a ground photogrammetric field survey in 1981 ~~and has a scale of 1:5,000~~ (Yokoyama, 1984). The photo point was about 2 km from the glacier terminus in 1981 on a lower location; consequently, the exposing axis is almost parallel to the glacier surface. We found a distortion and ~~mismatch~~mismatches at the ridge and at the ~~southeast~~south-east and ~~northwest~~north-west side of the glacier. ~~To calculate the frontal variations, we~~We georeferenced the map with the GeoEye-1 orthoimage from 2012 to calculate the frontal variations but did not use it for area or geodetic mass-balance analyses.

Satellite images were used to delineate glacier outlines~~,~~ and termini~~, and other tasks for~~ of both glaciers, and to calculate the geodetic mass balance of Yala Glacier (Table S3). ~~For the glacier-wide geodetic mass balance analysis, stereo satellite images were evaluated with a date overlapping with the fieldwork period either in October/November or April/May, or in early winter when there is little new accumulation and ablation, clear sky conditions, and ideally few shadows.~~

The SRTM-3 DEM (SRTM-3) is the third version of the DEM from the Shuttle Radar Topography Mission (SRTM) and is generated based on data from 2000. The spatial resolution is about 90 m, with an absolute vertical accuracy of ±16 m and a vertical reference to the WGS 84 EGM96 geoid (Rabus et al., 2003). The penetration of the SRTM C-band beam in snow, firn and glacier ice is an issue that results in a lower accuracy especially in the accumulation area (Kääb et al., 2012, Berthier et al., 2006). SRTM-3 was resampled to 30 m for the geodetic mass~~-~~-balance calculation of Yala Glacier. The SRTM-1 DEM was used for the mass~~-~~-balance analysis of Rikha Samba Glacier. It is based on the SRTM-3 data from 2000 but ~~has been~~was released with an improved resolution of about 30 m. ~~Aster images were also evaluated but clouds and fresh snow made the products unsuitable for use.~~

The GeoEye-1 is a commercial high-resolution stereo satellite image with 0.5 m spatial and 8 bits per pixel radiometry resolutions. The stereoscopic images from 15 January 2012 were used to generate a DEM (DEM2012) for Yala Glacier to calculate the glacier-wide geodetic mass balance~~. The~~, and the orthoimage ~~from GeoEye-1~~ was used ~~in combination with dGPS data~~ to delineate the outlines ~~of Yala Glacier~~.

We ~~analysed~~used Landsat images ~~from several generations of Landsat, which are American Earth observation satellites. Landsat 4 has a resolution of 79 m, and the later Landsat 5 Thematic Mapper (TM) and Landsat 7 Enhanced Thematic Mapper (EMT+) have a resolution of 30 m. The~~for various purposes. A Landsat 8 ~~was made available for the public since 2013. It has eleven bands panchromatic, multispectral and thermal with spatial resolutions of 15 m, 30 m and 100 m respectively and the panchromatic band 8 has 0.500 – 0.680 µm radiometric resolution. The visible band of the~~ image acquired on 18 November 2013 ~~has been~~was used to collect horizontal reference (x, y) and the SRTM-3 for the vertical reference (z) for ground control points (GCP) to georeference the GeoEye-1 images, and tie points for DEM generation for Yala Glacier. ~~The ICIMOD glacier inventory for Nepal (Bajracharya et al., 2014) is based on Landsat 7~~ A Landsat 7 Enhanced Thematic Mapper (ETM~~+ images~~+) image from 2000~~, and~~ helped to identify the outlines of Yala Glacier ~~have been used and modified based on the original data. The outlines have been used~~ for the geodetic mass balance and to analyse frontal ~~variation analyses. The inventory outline data from the years 1980, 1990 and 2010 were not used because of the coarse resolution of the base images, partial snow cover and high uncertainty of ±30-60 m.~~variations. We ~~used~~analysed terminus changes of Rikha Samba Glacier using a Landsat 4, Landsat 7 ETM+ and two Landsat 5 Thematic Mapper (TM) images from the years 1989, 2001, 2006 and 2011~~ to analyse terminus changes of Rikha Samba Glacier.~~, respectively. RapidEye images from 25 and 27 April 2010 were used to delineate the outlines of Rikha Samba Glacier.

A Hexagon KH-9 ~~images~~image from November 1974 ~~were~~was used for a frontal variation analysis of Yala Glacier~~ but~~. Other Hexagon images were found unsuitable for area and volume analysis because of void areas, or cloud and snow cover in the images at other times of the year. Additionally, it was difficult to delineate the glacier at the north-west and south-east side without contour lines to derive the flowlines at that time.

For this study, we adopt the projection system WGS 1984, UTM Zone 44N and 45N for Rikha Samba and Yala ~~Glacier~~glaciers, respectively. ~~The~~We used the local projection ~~is the~~system called Modified Transverse Mercator, with false easting 500,000 m and scale factor of 0.9999 at the central meridian 84° E and 87° E for Rikha Samba and Yala ~~Glacier~~glaciers, respectively.

3.3 DEM generation

The DEM generation from GeoEye-1 stereo images from 2012 involved four steps, following Holzer et al. (2015): collection of ~~ground control points (~~GCPs~~),~~, extraction of the DEM, and the two post-processing steps to clean DEM areas of low quality and to co-register the DEM. The DEM was used ~~for~~to analyse the mass balance ~~analysis~~of Yala Glacier with the geodetic and glaciological method.

Eight ~~ground control points (~~GCPs~~)~~ were used to georeference the GeoEye-1 stereo satellite images. The GCPs were obtained from stable terrain and are evenly distributed. The x and y coordinates of the GCPs were measured from a Landsat 8 image from November 2013, and the z-values were taken from the SRTM-3 DEM. All GCPs were cross-checked in Google Earth™. For the DEM extraction from the GeoEye-1 stereo images OrthoEngine from PCI Geomatica 2013 software was used. The DEM was derived using the Rational Function model with first-order RPC adjustments from ephemeral data and GCPs. We applied the Wallis filtering to locally enhance the contrast of the image to improve the image matching. The DEM derived from the forward- and backward-looking images has a resolution of 2 m.

In the next step, DEM areas with low quality were removed. First the SRTM-3 DEM and the GeoEye-1 DEM were resampled from 90 to 30 m, and from 2 to 5 m, respectively, and aligned to a raster grid of same extent and cell alignment. Then the noises in the GeoEye-1 DEM were eliminated applying the expand-sink-expand tool and a median filter (5 x 5 m). With the hillshade of the GeoEye-1 DEM we visually checked the DEM. To evaluate the image matching, PCI produces a so-called score channel image, which we used to identify DEM areas of poor quality and set the values to "no data". Especially a small part of the north-eastern glacier area at Yala ridge had to be discarded due to a very low DEM quality.

In the DEM co-registration process, the SRTM-3 is the reference (master) DEM to which the ~~Geoeye~~GeoEye-1 slave DEM is co-registered. For the horizontal DEM co-registration, first we calculated the elevation difference of the GeoEye-1 DEM relative to the SRTM-3. We excluded non-stable terrain such as glaciers and landslide areas and use only terrain with a slope between 10° and 45° in SRTM-3. The SRTM-3 had initially a much coarser resolution than the GeoEye-1 DEM, leading to a resolution-induced bias at topographic extremes with strong curvature (Berthier et al. 2006; Paul, 2008; Gardelle et al., 2012). To account for such curvature effects and most extreme outliers in particular at steep slopes, we identified and removed DEM difference values in the 5 % and 95 % quantiles, as well as pixels outside the two-tailed 1.5 times interquartile range (Pieczonka et al., 2013). The horizontal shift between the two DEMs we corrected manually due to the small study area, followed by a two-dimensional spatial trend correction. For the vertical DEM co-registration of the GeoEye-1 DEM, the flat areas less than 10° of the SRTM-3 were used, avoiding steeper terrain with decreasing accuracy in SRTM-3. The DEM2012 was resampled to a resolution of 5 m for the geodetic method and 30 m for the glaciological method.

3.4 Analysis of glacier changes and uncertainties

3.4.1 Point and ~~glacierwide~~glacier-wide mass balance

The glacier-wide mass balances, the equilibrium line altitude (ELA) and accumulation area ratio (AAR) were calculated based on the interpolated mass~~-~~-balance gradient derived from the point measurements following a similar method used by Wagnon et al. ~~(2013).~~(2013). The mass-balance gradients were derived from the linear regression lines of the point measurements. The elevations of the DEMs of Yala and Rikha Samba glaciers were applied to the regression equations to calculate the glacier-wide mass balance.

~~The point mass balances are easy to calculate where ablation dominates, and are alike for measurements from multiple older stakes at the same location. In the accumulation area the analysis of the point data tends to be difficult because of the above described challenges during data collection. In such cases, each stake and snow pit measurement were assessed, and the main processes ablation and accumulation reconstructed.~~For Yala Glacier, characteristic gradients for the ablation area were identified, and separately analysed for the annual and seasonal mass balances, with the winter and summer season starting in November and May or June, respectively. In the accumulation area, there are fewer measurements with large uncertainties because of the challenging measurement conditions described earlier and in Supplement section S1. This inhibited not only to identify characteristic gradients in the accumulation area, but also to define a fixed mass balance that could be applied in the accumulation area from a defined elevation. As consequence, a single gradient was used for the glacier-wide mass balance. The interpolation approach is simple and introduces a systematic error for the mass balance in the accumulation area. The part of the accumulation area without measurements for the respective elevations bands makes up 15 % of the glacier area for an elevation range of about 160 m (~5500 m to 5662 m a.s.l.).

For Rikha Samba Glacier two characteristic annual gradients were identified, with a large gradient in the lower ablation area and a medium gradient in the transition between ablation and accumulation area. Based on the assumption that the mass-balance gradients remain very similar in different mass-balance years, gradients were reconstructed for Rikha Samba Glacier for years with limited point measurements (2011/12, 2013/14, and 2014/15). The intersection points of the lower (large) and upper (medium) gradients were identified and reconstructed based on a regression line for sections without measurements. For the accumulation area, no characteristic gradients could be identified because only few measurements were available. The elevation range without measurements is about 650 m (~5900 m to 6545 m a.s.l.) and makes up 36 % of the glacier area. At about 6000 m, the topography steepens (Fig 1). Using the upper gradient to interpolate the mass balance to the accumulation area would have resulted in much overestimated positive mass balances. Instead we considered it plausible to assume a fixed mass balance at high elevations, based on the steep slopes and the typically small gradient in accumulation areas. We assumed the lower elevation for a fixed mass-balance value between 5850 m and 5950 m a.s.l., guided by the upper gradient. For the mass-balance year 1998/99, the point measurements collected by Fujita et al. (2001) were used. The ELA and AAR were calculated based on the mass-balance gradients, whereas for Rikha Samba Glacier the upper gradient was used.

The errors of the point measurements were assessed by analysing the random errors for each measurement from density σ_d, ice surface roughness σ_{rough} mainly in the ablation area, varying snow depth σ_{depth} mainly in the accumulation area, stake reading σ_{read}, errors due to the sawdust spread for snow pit measurements σ_{sawd} and movement of the stake in the firn area σ_{firn}. The error of an individual point measurement σ_{point} was calculated:

$$\sigma_{point} = \sqrt{\sigma_d^2 + \sigma_{rough}^2 + \sigma_{depth}^2 + \sigma_{read}^2 + \sigma_{sawd}^2 + \sigma_{firn}^2} \qquad (1).$$

At few sites with minimal flow, two measurements from older and newer stakes allowed a comparison. In most cases the measurements were within the calculated error. Otherwise, if no explanation was found for differing values, the standard deviation of the two values was taken as error. ~~The error of the point measurements for a specific elevation band~~ ~~σ_{point_elevb} was calculated by considering n point measurements in the respective elevation band:~~

$$\sigma_{point\_elevb} = \sqrt{\sum_{point=1}^{n} \sigma_{point}^2} / \sqrt{n} \qquad (2).$$

~~The mass balance gradients were derived from the regression lines of the point measurements and applied to the DEMs of Yala and Rikha Samba glacier. For Yala Glacier, a gradient for the ablation area was identified, and separately analysed for~~

~~the annual and seasonal mass balances, with the winter and summer season starting in November and May or June, respectively. Too few measurements in the accumulation area inhibited to identify a gradient for the accumulation area. For Rikha Samba Glacier three characteristic annual gradients were identified, with a large gradient in the ablation area, a medium gradient in the transition between ablation and accumulation area, and a very small or no gradient in the accumulation area.~~

~~Based on the assumption that the mass balance gradients remain very similar in different mass balance years, gradients were reconstructed for Rikha Samba Glacier for years with limited point measurements (2012, 2014, and 2015). The intersection points of the lower and middle gradients were identified and reconstructed based on a regression line for sections without measurements. In the accumulation area, the starting elevation for a gradient of 0 m w.e. (100 m)$^{-1}$ was assumed between 5850 and 5950 m, based on the measurements and topographical setting. For the mass balance year 1999, the point measurements collected by Fujita et al. (2001) were used.~~

To assess the error σ_{final} of the mass balance for ~~elevation bands and~~ the entire glacier and elevation bands of 50 m, the errors of the point measurements σ_{point_elevb} and interpolation method σ_{int} were analysed. Due to a lack of updated glacier surface and outline data, the reference-surface balance was calculated (Elsberg et al., 2001), and the systematic errors caused by the changing glacier geometry were disregarded. Also, the systematic errors caused by stakes placed at unrepresentative locations or even lack of point measurements were not evaluated due to a lack of respective information.

The overall error σ_{final} for the mass balance for the glacier-wide balance and elevation bands was calculated:

$$\sigma_{final} = \sqrt{\sigma_{point\_elevb}^2 + \sigma_{int}^2} \qquad (2).$$

The error of the point measurements for a specific elevation band σ_{point_elevb} was calculated by considering n point measurements in the respective elevation band:

$$\sigma_{point\_elevb} = \sqrt{\textstyle\sum_{point=1}^{n} \sigma_{point}^2} / \sqrt{n} \qquad (3).$$

To calculate the systematic error caused by the interpolation method σ_{int}, we estimated the maximum difference in mass balance for 50 m elevation bands. The standard deviation of this value and the calculated mass balance was assumed as the error from the interpolation method.

~~The overall error σ_{final} for the mass balance for elevation bands and the glacier-wide balance was calculated:~~

$$\cancel{\sigma_{final} = \sqrt{\sigma_{point\_elevb}^2 + \sigma_{int}^2} \qquad (3).}$$

The error of the cumulative mass balance σ_{cumul} for n years was calculated:

$$\sigma_{cumul} = \sqrt{\textstyle\sum_{years=1}^{n} \sigma_{final}^2} \qquad (4),$$

And the error of the mean annual mass~~-~~ balance rate $\overline{\sigma_{cumul}}$ for n years was calculated:

$$\overline{\sigma_{cumul}} = \sqrt{\textstyle\sum_{years=1}^{n} \sigma_{final}^2} / \sqrt{n} \qquad (5).$$

~~The ELA and AAR were calculated based on the mass balance gradients, whereas for Rikha Samba Glacier the gradient of the mid-section of the glacier was used.~~ The accuracy of the ELA and AAR were estimated ~~based on the variation of~~by shifting the regression lines ~~caused by outlying~~ based on point measurements~~.~~ deviating from the initial regression line. For Rikha Samba Glacier the calculation of the ELA and AAR for the years ~~2012,~~ 2011/12, 2013/14 and 2014 ~~and 2015~~/15 were omitted due to the very few measurements.

3.4.2 Glacier area and length

The ~~glacier~~ area of Yala Glacier ~~has been~~was defined based on the GeoEye-1 ~~Image~~orthoimage from 15 January 2012, and GPS data of the terminus from 3 November 2012. On the north-west side, the ~~glacier~~glacier's drainage basin has been separated from the adjacent ice body along the flowline, ~~based on~~using flow vectors drawn perpendicular to the contour ~~line method~~lines derived from the DEM2012~~.~~ (Cuffey and Paterson, 2010). A section detached from the main glacier on the south-east side was excluded. For the analysis of the geodetic mass balance, the glacier outline is based on the Landsat 7 ETM+ image from February 2000 (Table S3).

The glacier frontal variations of Yala Glacier were analysed with satellite images, maps and field-based data (Table S1, S2, S3). Yala Glacier is very wide and the terminus is not constrained by a valley. Hence it is difficult to identify a central glacier flowline, and the general glacier flow direction was delineated instead. We applied the 'rectilinear box method' described by Lea et al. (2014) and Koblet et al. (2010). In this method an arbitrary rectangular box is drawn along the flowline. Perpendicular to the flowline and at the maximum extent of the Hexagon KH-9 1974 glacier outline, a straight arbitrary baseline was drawn. Perpendicular to the baseline and in flow direction, 26 parallel lines at 50 m intervals were drawn to quantify the glacier terminus changes. At each parallel line we ~~measure~~measured the frontal variation and averaged the values for the final frontal variation of that period. There are big outliers, and some of the mapped termini were not covered by all 26 parallel lines. Therefore, for the final calculation only 9 parallel lines which cover the lowest parts of the glacier were considered.

For Rikha Samba Glacier, the glacier outline was delineated from ~~Rapid Eye~~RapidEye images from 25 and 27 April 2010~~ for the mass balance analysis, and SRTM-1 was used for the mass balance calculation~~. The frontal variations are quantified along the central glacier flowline that was derived from SRTM-1. The glacier termini are based on Landsat images from 1989, 2001, 2006, 2011 and a ~~dGPS~~dGNSS survey from 2013 (Table S1). Uncertainties of glacier termini and outlines are estimated half to one pixel dependent on the quality of the source image or map scale, or according to the ~~dGPS~~dGNSS settings and field conditions.

3.4.3 Geodetic mass~~-~~-balance calculation

The geodetic mass~~-~~-balance calculation for Yala Glacier is based on the subtraction of the SRTM-3 from the DEM2012 from the years 2000 and 2012, respectively, which results in a map of elevation differences (Δh). Data gaps smaller than 0.01 km^2 in the elevation difference map, were filled with a mean filter of surrounding height change (Δh) values. The accumulation and ablation areas were separated by ~~the~~an estimated ELA of 5350 m a.s.l~~, which is based on field observations and the balanced ELA calculated from the field-based mass balance measurements~~. Outliers and voids larger than 0.01 km^2 occurred only in the accumulation area. The largest data gaps we found at the edge of the glacier at Yala ridge, where fresh snow in the GeoEye-1 image compromised the quality of the DEM2012. However, no plausible statistical value could replace the data voids and outliers, therefore, the mode value from the accumulation area was taken, assuming only minor elevation changes in these areas (Schwitter and Raymond, 1993). Assuming an average density of 850 kg m^{-3} (Huss, 2013) for the entire glacier, the elevation change was converted into mass change. Since the accumulation area was small, only a single density value was used. The glacier area was defined by the larger extent from the Landsat 7 image from February 2000. Additionally, the glacier surface elevation changes of Yala Glacier were analysed along ~~a~~the profile line surveyed by ~~dGPS~~dGNSS in May 2012, and compared to SRTM-3.

The SRTM-3 C-band potentially underestimates the glacier elevations because of radar penetration into the upper snow, firn and ice layers on the glacier (Kääb et al., 2012; Gardelle et al., 2012). In winter in the Karakoram, Gardelle et al. (2012) found a penetration on glacier of a couple of metres below 5300 m, which increases to about 5 m at 5700 m and more above. They emphasise that these values can vary in different regions, decreasing penetration in wetter and warmer snow and dirtier ice. Bolch et al. (2016) use a mean average penetration correction of 2.4 ±1.4m to address this issue in the Karakoram. The Landsat 7 image from February 2000 showed some snow cover. In this study, we assume that the SRTM-3 DEM represents the glacier surface from early 2000 because we expect on average only a small snow cover. Additionally, the accumulation area on Yala Glacier is small and on low elevation, reducing the effect of the penetration.

To assess the uncertainty of the geodetic mass~~-~~-balance calculation, we estimated the vertical DEM precision by calculating the normalized median absolute deviation (NMAD), which is 7.4 m, following the method by Holzer et al. (2015), and considering the density deviation of ±60 kg m^{-3} (Huss, 2013). Errors due to different spatial scale, sensors, resolutions and area of Yala ~~glacier~~Glacier are not considered.

4 Results

4.1 Mass balances, ELA, AAR and gradients

The glacier-wide annual mass balances of Yala and Rikha Samba ~~Glacier~~glaciers were negative for all years, except in ~~2013~~2012/13 when Yala Glacier was almost in balance (-0.01 ±0.29 m w.e.), and Rikha Samba Glacier had a slightly positive balance (0.12 ±0.32 m w.e.), reported in Table 2 and 3, and Fig. 2~~, 3~~ and ~~4~~3. The most negative annual balances on Yala Glacier occurred in ~~2015 and 2017 with -1.18 ±0.26 m~~2016/17 and 2014/15 with -1.54 ±0.20 m and -1.18 ±0.~~20~~26 m~~-~~ w.e. ~~In 2015, a very negative summer balance, overcompensated the very positive winter balance with extraordinary snowfall (Fujita et al., 2017). On Rikha Samba Glacier, 2012 was the most negative year (-0.72 ±0.34 m w.e.), followed by 2015 (-0.63 ±0.35 m w.e.). During the Nepal earthquakes in April and May 2015, Langtang was heavily affected by ice avalanches, landslides,~~In the years 2011/12, 2013/14 and ~~as well as rockfalls on the glacier in the immediate vicinity of the study area (Kargel et al., 2016, Fujita et al., 2017). Direct effects of the earthquake on the glacier could not be measured, however the climate station on and near the glacier were destroyed likely because of air blasts from ice avalanches.~~ 2015/16~~The effect of the air blasts on the snow cover of Yala Glacier is not known, however, it is possible that snow was blown away and partly sublimated. The air in the valley was filled with dust and it is probable that more dust than usual settled on Yala Glacier, increasing ablation. In the years 2012, 2014 and 2016~~ the values were similarly negative for ~~the~~ Yala Glacier (-0.86 ±0.40 m, -0.61 ±0.27 m and -0.61 ±0.23 m w.e.). ~~For Rikha Samba Glacier~~On Rikha Samba Glacier, 2011/12 was the most negative year (-0.72 ±0.34 m w.e.), followed by 2014/15 (-0.63 ±0.35 m w.e.). In the years 2011/12, 2013/14 and 2014/15, the balances were similarly negative ~~for the years 2012, 2014 and 2015~~ (-0.72 ±0.34 m, -0.55 ±0.34 m and -0.63 ±0.35 m w.e.), followed by less negative years in ~~2016~~2015/16 and ~~2017~~2016/17 (-0.33 ±0.27 m and -0.23 ±0.31 m w.e.). The mean annual mass-balance rate and cumulative balance of Yala and Rikha Samba glaciers from 2011 to 2017 are -0.80 ±0.28 m w.e. a^{-1}, -4.80 ±0.69 m w.e., and -0.39 ±0.32 m w.e. a^{-1}, and -2.34 ±0.79 m w.e., respectively. The most negative point mass balances of -3.75 ±0.05 m w.e. and -4.12 ±0.04 m w.e., respectively, were measured at the lowest stakes (5175 m and 5437 m a.s.l.) of Yala and Rikha Samba ~~Glacier~~glaciers in ~~2012~~2011/12.

Table 2: Mass balance (B) measured with the glaciological method, winter balance (B_W), summer balance (B_S), ELA, AAR and mass ~~-~~balance gradient for Yala Glacier from 2011/12 to ~~2017~~2016/17.

~~**Yala Glacier**~~

B year	B (m w.e.)	B_W	B_S	B_W+B_S	ELA (m a.s.l.)	AAR	db/dz (m w.e. (100 m)$^{-1}$)
~~1999~~	-	-	-	-	-	-	-
~~2012~~2011/12	-0.86 ±0.40	0.16	-0.20	-0.03	5454 ±30	0.28	1.14
~~2013~~2012/13	-0.01 ±0.29	0.36	-0.35	0.01	5380 ±20	0.48	0.99
~~2014~~2013/14	-0.61 ±0.27	0.27	-0.99	-0.73	5431 ±20	0.35	1.18
~~2015~~2014/15	-1.18 ±0.26	0.54	-1.12	-0.59	5510 ±40	0.13	0.90
~~2016~~2015/16	-0.61 ±0.23	0.19	-0.79	-0.60	5444 ±20	0.31	0.93
~~2017~~2016/17	-1.~~18~~54 ±0.20	0.20	-1.~~39~~75	-1.~~19~~54	~~5486~~5518 ±20	0.~~19~~12	1.10
Mean	-0.~~74~~80 ±0.28	0.29	-0.~~81~~87	-~~0.52~~1.10	~~5451~~5456	0.~~29~~28	1.04
STD	0.~~44~~53	0.14	0.~~46~~56	-0.~~45~~69	~~45~~52	0.~~12~~14	0.12
2011–2017	-4.~~44~~80 ±0.69	1.72	-~~4.85~~5.21	-~~3.13~~6.60			

Table 3: Mass balance (B) measured with the glaciological method, ELA, AAR and the lower and upper mass~~-~~-balance gradient for Rikha Samba Glacier for the mass-balance years 1998/99, and from 2011/12 to ~~2017~~2016/17. We did not calculate the ELA and AAR for Rikha Samba Glacier for ~~2012,~~2011/12, 2013/14 and 2014~~ and 2015~~/15 due to the very few data points. For the mass-balance year 1998/99, the point measurements collected by Fujita et al. (2001) were used.

~~**Rikha Samba Glacier**~~

B year	B (m w.e.)	ELA (m a.s.l.)	AAR	db/dz (lower) (m w.e. (100 m)$^{-1}$)	db/dz at ELA (upper) (m w.e. (100 m)$^{-1}$)
~~1999~~1998/99	-0.18	5790 ±50	0.49	1.27	0.25
~~2012~~2011/12	-0.72 ±0.34	-	-	1.13	
~~2013~~2012/13	0.12 ±0.32	5724 ±20	0.75	1.57	0.37
~~2014~~2013/14	-0.55 ±0.34	-	-	1.36	
~~2015~~2014/15	-0.63 ±0.35	-	-	1.48	
~~2016~~2015/16	-0.33 ±0.27	5872 ±50	0.41	1.64	0.36
~~2017~~2016/17	-0.23 ±0.31	5862 ±50	0.54	1.89	0.46
Mean	-0.39 ±0.32	5807	0.55	1.48	0.36
STD	0.31	63	0.15	0.25	0.09
2011–2017	-2.34 ±0.79				

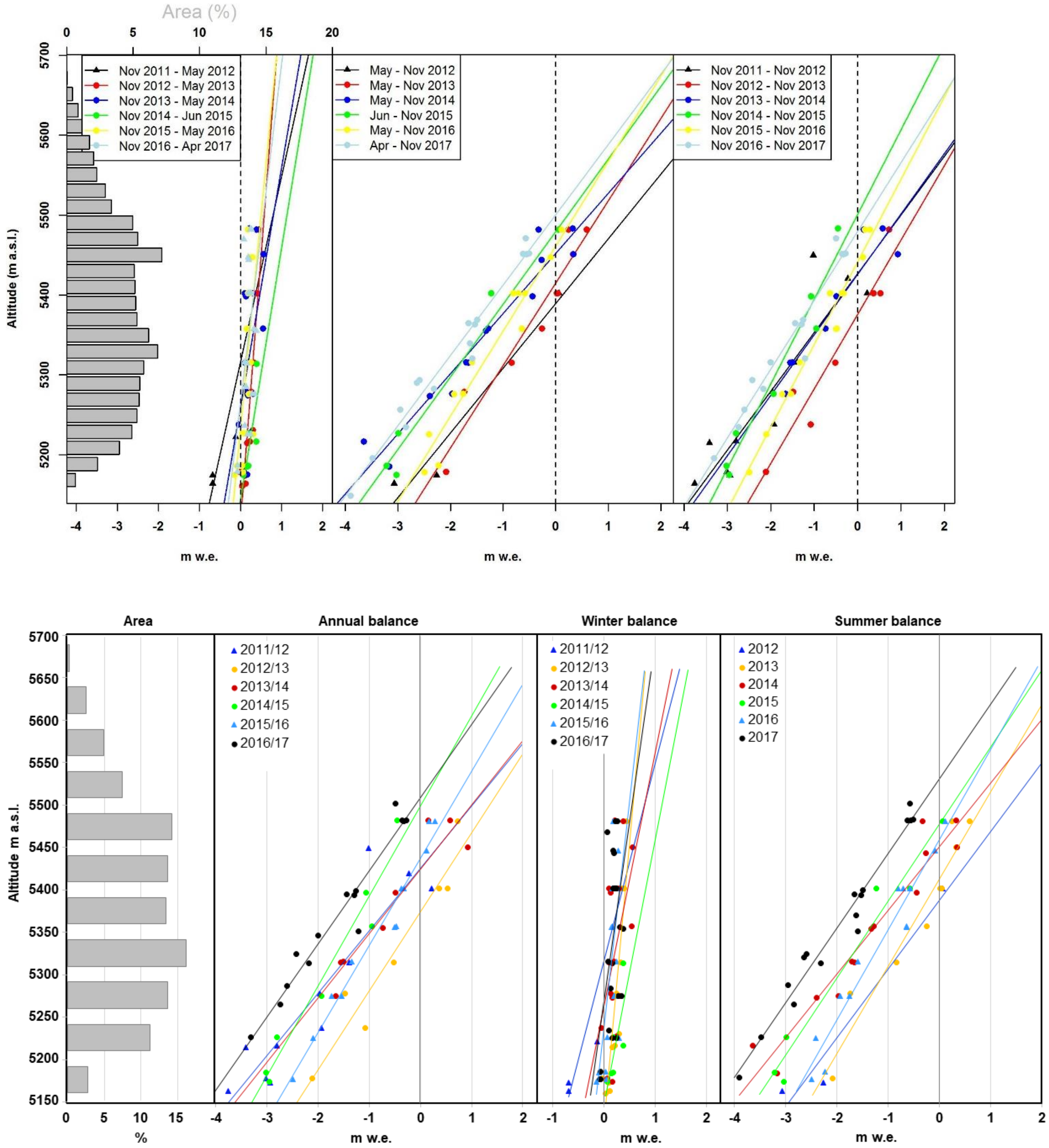

Figure 2: Mass ~~balance~~balances and gradients for the annual, winter ~~(left),~~and summer ~~(right) and annual~~ mass balance for Yala Glacier from 2011–2017, and the glacier hypsography (far left).

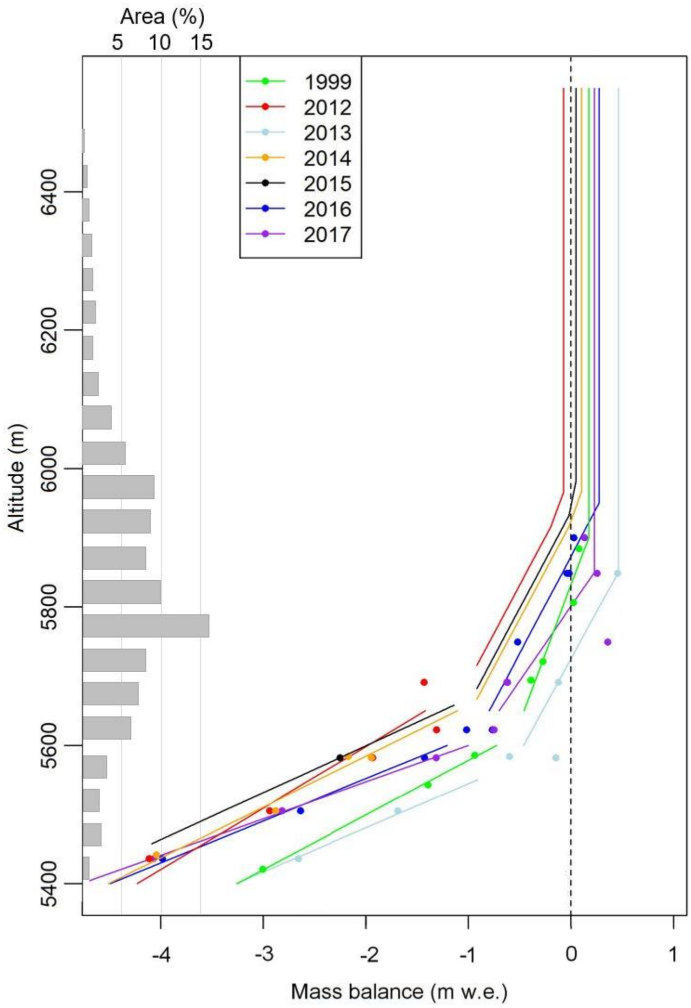

Figure 3: Point mass balance, gradients and hypsography of Rikha Samba Glacier for the mass~~-~~-balance years ~~1999~~1998/99, and ~~2012~~2011/12 to ~~2017~~2016/17.

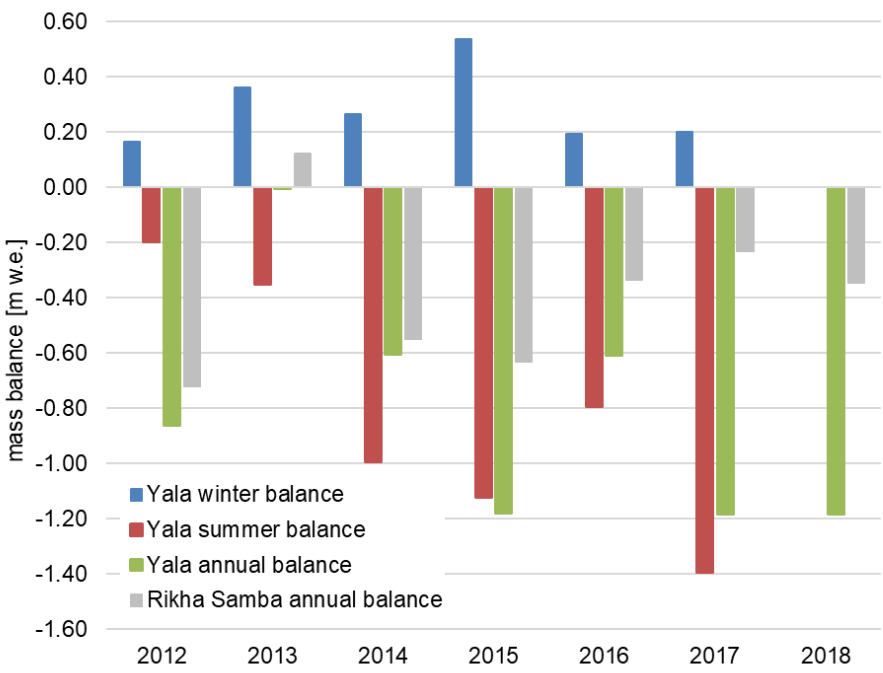

The seasonal mass balances on Yala Glacier are shown in Table 2 and Fig 4. The average winter and summer balances were 0.29 m and -0.87 m w.e. with standard deviations of 0.14 m w.e. and 0.56 m w.e., respectively. The winter balance is low in most years, except in 2014/15 when the accumulation was very positive (0.54 m w.e.). The summer balance of 2017 is the most negative balance (-1.75 m w.e.) followed by the summer balances of 2015 and 2014 (-1.12 m and -0.99 m w.e.). In autumn 2012 we calculated the least negative summer balance (-0.35 m w.e.), based on only three measurements. The extreme precipitation events from the cyclones Phailin and Hudhud in October 2013 and 2014, respectively, contributed to the summer balance. The cumulated winter and summer balances largely sum up to the annual mass balances, except in 2011/12 and 2014/15 when the cumulated winter and summer balances underestimate the annual mass loss by -0.83 m and -0.59 m w.e.

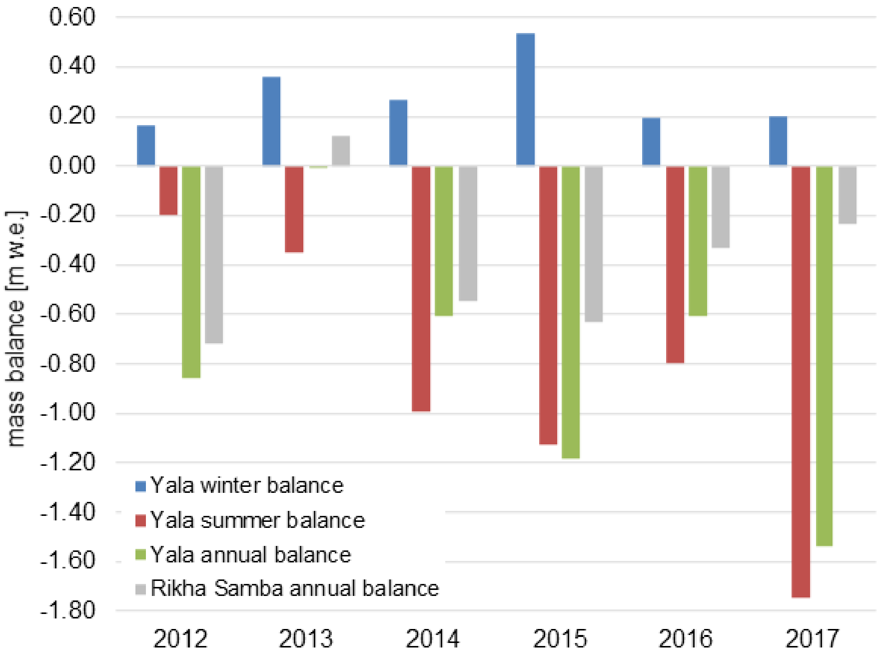

Figure 4: Winter, summer and annual mass balance of Yala Glacier and annual balance of Rikha Samba Glacier, calculated based on the respective gradients. In the mass~~-~~ balance years ~~2012~~2011/12 and ~~2015~~2014/15, the sum of winter and summer balances differ significantly from the annual balances, likely due to a lack of data in higher elevations.

The uncertainties in the accumulation area are larger than in the ablation area because the processes in the snowpack are more complex, influence each other and are difficult to measure~~.~~ (Fig. S3, S4, S5 and S6). The possible causes for these variations are manifold, from snow/firn compaction, spatial variability of the glacier surface due to varying accumulation and ablation, sawdust promoting local melt, bamboo stakes being pushed up or down and superimposed ice. In some years, the surface roughness was very large in the ablation area, resulting in large errors. Errors for the density of metamorphed snow tended to be larger than for fresh snow because it was harder to measure. At Yala Glacier, the error was largest in the highest elevation bands that make up 15 % of the glacier area because the lack of measurements prevented the calculation of a reliable gradient in the accumulation area. Similarly, at Rikha Samba Glacier, the sparse measurements in the accumulation area and in particular in its steep slopes (~~19~~36 % of the area) resulted in large errors that were difficult to estimate.

At Yala Glacier, the measured average densities with standard deviation for snow and firn were 336 kg m^{-3} (±81 kg m^{-3}) and 562 kg m^{-3} (±128 kg m^{-3}). However, harder firn layers were difficult to measure~~ and~~. Dependent on the site and firn conditions, and based on snow pit profiles and field observations we estimated firn density between 550 kg m^{-3} and 700 kg m^{-3}~~, dependent on the site and firn condition~~. At Rikha Samba Glacier, the average snow density measured was 399 kg m^{-3} with a standard deviation of ±70 kg m^{-3}. For ice we assumed a density of 900 kg m^{-3} (Cogley et al., 2011).

The calculated balanced-budget equilibrium line altitude (ELA_0) and balanced-budget accumulation area ration (AAR_0) for Yala and Rikha Samba ~~Glacier~~glaciers are 5378 m a.s.l., 5758 m a.s.l., 0.49~~%~~ and 0.66~~%~~ respectively (Fig. 5). From 2011 to 2017 the ELA ranged at Yala Glacier between 5380 m and 5510 m a.s.l. with uncertainties of ±20 m to ±40 m, and at Rikha Samba Glacier between 5724 m and 5872 m with uncertainties of ±20 m to ±50 m (Fig. 2 and 3, Table 2 and 3). The AAR range from 0.13~~%~~ to 0.48~~%~~ and from 0.41~~%~~ to 0.75~~%~~ for Yala and Rikha Samba ~~Glacier~~glaciers, respectively~~. The snow line was not a reliable indicator for the ELA, as characteristic for summer accumulation and ablation type glaciers~~.

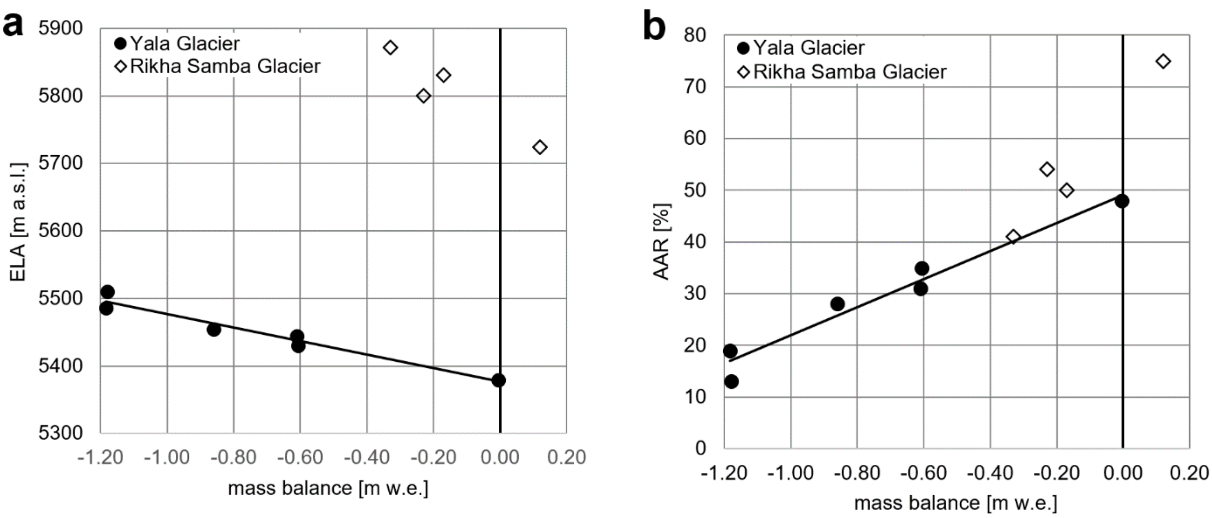

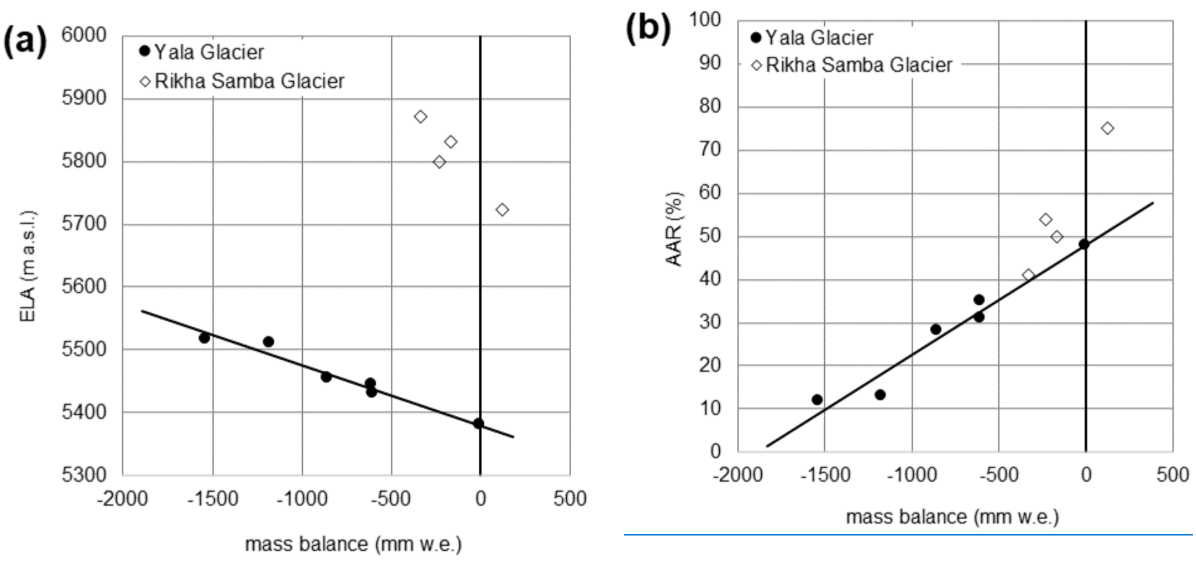

Figure 5: The ELA (a) and AAR (b) of Yala and Rikha Samba ~~Glacier~~glaciers against the mass balance. The ELA_0 and AAR_0 for the glaciers are 5377 m~~,~~ a.s.l., 5760 m~~,~~ a.s.l., 0.49 ~~%~~ and 0.66 ~~%~~ for Yala and Rikha Samba ~~Glacier~~glaciers, respectively.

The point mass balances are shown in Fig. 2 and 3 as function of elevation and with linear regression lines that are used to derive the mass~~-~~ balance gradients for Yala and Rikha Samba ~~Glacier~~glaciers, respectively. ~~The~~ For Yala and Rikha Samba glaciers, the mean mass~~-~~ balance gradient at the ELA are 1.04 m and 0.36 m w.e. (100 m)$^{-1}$, ~~for Yala and Rikha Samba Glacier,~~ respectively~~.~~ (Table 2 and 3). The gradients ~~are~~show a relatively ~~consistent over the years~~low interannual variability with standard deviations of 0.12 m and 0.9 m w.e. (100 m)$^{-1}$, respectively. In the lower part of Rikha Samba Glacier, the gradient is much larger with a mean value and standard deviation of 1.48 m and 0.25 m w.e. (100 m)$^{-1}$. ~~The mass balance~~Figure 2 shows the characteristic gradients for the annual and seasonal balances of Yala Glacier ~~are very consistent for the seasonal and annual balance, with only a single gradient observed for the glacier. Additional~~that remain relatively constant over the investigated time period. However, additional measurements in higher elevations ~~likely~~ would have allowed to identify a ~~smaller~~ gradient in the accumulation area for the annual and the summer balance. For the winter balance, a small gradient was identified, which is overestimated for years when ablation already set in on the lower part of the glacier. This is the case for the year ~~2012~~2011/12 when ablation possibly set in earlier, and ~~2015~~2014/15 when the stakes were measured a month later than normally, and in both ~~cases~~years without measurements in higher elevations. For these years, the winter mass~~-~~-balance gradient in the accumulation area is likely smaller than in the ablation area and generally the mass balance is overestimated above about 5500 m a.s.l.

~~In most years, the winter balances show a slight mass gain on Yala Glacier, which happens mainly from January to May when snowfall sets in. The average winter balance was 0.29 m w.e. with a standard deviation of 0.14 m w.e. However, in winter 2014/2015 an exceptional amount of precipitation was measured at various climate stations. In that winter local people in Langtang reported many Yaks dying in the snow, and during the Gorkha Earthquake in April extreme avalanches were triggered (Fujita et al., 2017). Above average accumulation (0.54 m w.e.) was calculated for the winter 2015 mass balance despite a delay of measurements by a month. However, the uncertainty is higher because of lacking measurements in higher elevations. The summer balances indicate an average mass loss of -0.81 m w.e. and standard deviation of 0.46 m w.e. In early October 2013 and 2014, the Central Himalayas received large amounts of precipitation brought by the cyclones Phailin and Hudhud (Shea et al. 2015b; Necker et al., 2015). These precipitation events in form of snow contributed to the summer balance since the measurements were taken after the cyclones passed.~~

~~We identify distinct snow and ice layers only after some winters, such as in April 2017 (Fig. 6).~~ In autumn, often only a very fresh layer of snow was clearly detectable over the entire glacier, and in some years the sawdust marking the ~~previous measurement~~reference surface was removed by ablation before accumulation. ~~Without the sawdust found~~ Distinct snow and ice layers we identified only after some winters, such as in April 2017 (Fig. 6). In April 2017, sawdust at the bottom of the ~~snowpits at S6, S7 and S8~~snow pits or the glacier ice indicated the reference surface. Without the sawdust marking, the lowest layer of darker coarse snow could ~~be~~have been mistaken for snow from the monsoon season. The amount of snow accumulation depended mainly on the elevation, but also aspect, slope and exposure. Maximum accumulation we typically measured at stake ~~7~~S7, which is less exposed than the stakes ~~6~~S6 and ~~8~~S8. In April 2014, we measured superimposed ice, which formed at the glacier surface below the snow from the cyclone Phailin. ~~The cumulated winter and summer balances largely sum up to the annual mass balances, except in 2012 and 2015 when the cumulated winter and summer balances underestimate the annual mass loss by -0.83 m and -0.59 m w.e.~~

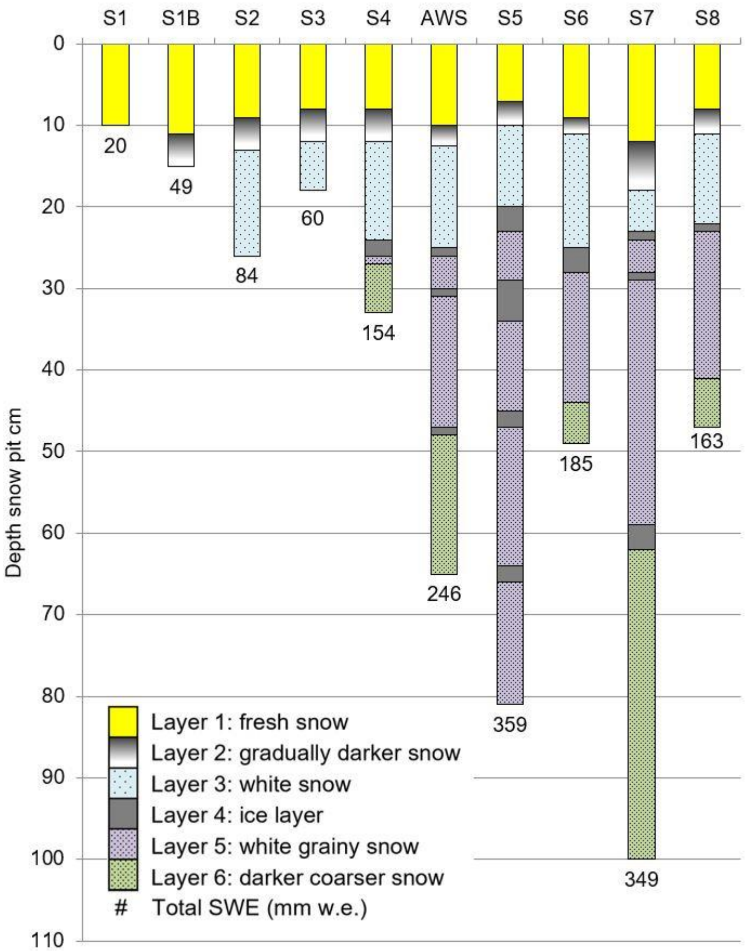

Figure 6: Snow profiles measured at the stakes on Yala Glacier on 23, 24 and 25 April 2017. At the site AWS, a temporary weather station was set up near stake S4. Distinct snow layers can be identified at all measurement sites. At the stakes S5, S6, S7, and S8 sawdust from 19 and 20 November 2016 was found at the bottom of the snow pit, and glacier ice at all lower sites.

During the twelve-year period (2000–2012) Yala Glacier's average glacier thinning was -10.49 ±7.41 m, with an annual thinning rate of -0.87 ±0.62 m a^{-1}, which corresponds to a ~~net~~total mass loss of -8.92 ±6.33 m w.e., and an annual rate of -0.74 ±0.53 m w.e. a^{-1} (Fig. 7~~, Table 4~~). The mean thinning rate along the profile line is ~~higher (-~~-1.1 ±0.13 m a^{-1}~~) but within the uncertainty range of the DEM thinning rate, most likely because accumulation above 5571 m is excluded from the calculation~~. Maximum thickness gain of 17.63 m was measured below the ice cliffs, and the biggest ice wastage was measured above the lake and along the glacier terminus, with a value of -50.66 m. Positive mass~~-~~-balance values lie in the upper part of the glacier. However, when averaging the values over elevation bands, we see a mass gain only in the highest elevation bands, which is filled with the mode value from the accumulation area (Fig. 8). From 2011 to 2017, Yala Glacier's cumulative balance and mean annual rate were -4.80 ±0.69 m w.e. and -0.80 ±0.28 m w.e. a^{-1}, respectively. From 2000 to 2017, Yala Glacier lost -12.86 m w.e. with an annual rate of -0.76 ±0.53 m w.e. a^{-1}. Rikha Samba Glacier lost from 2011 to 2017 -2.34 ±0.79 m w.e with an annual rate of -0.39 ±0.32 m w.e. a^{-1}.

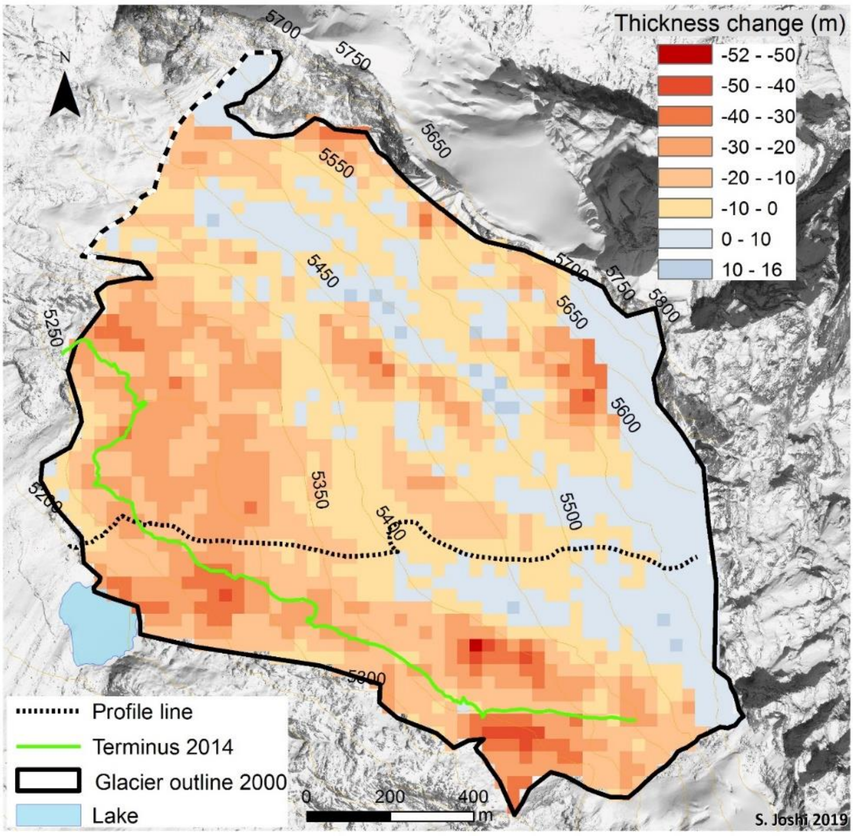

Figure 7: Thickness changes of Yala Glacier in metres after DEM differencing of GeoEye-1 (Jan 2012) and SRTM3 (Feb 2000) DEM and ~~dGPS~~dGNSS profile in 2012.

~~**Table 4: Comparison of glacier surface lowering and in-situ mass balance measurements from various studies.**~~

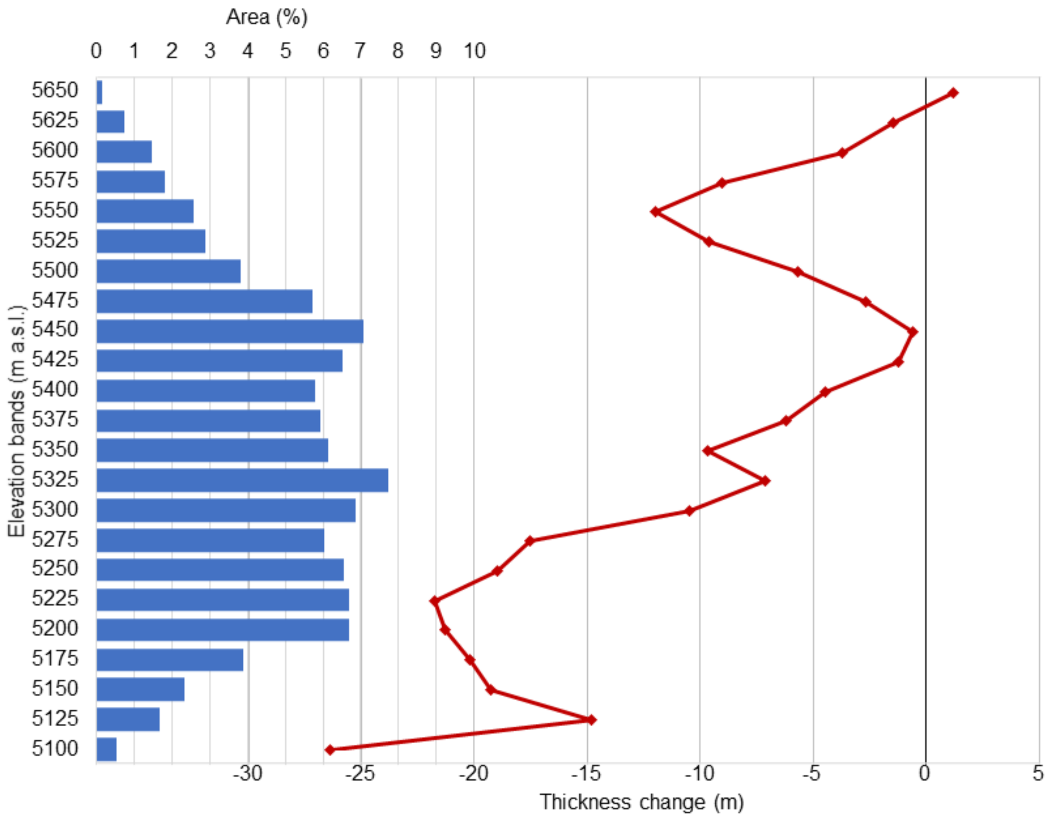

Figure 8: The mean thickness changes of Yala Glacier for 25 m elevation bands with hypsography, from 2000 to 2012. The reduced thickness change at an elevation of 5125 m is likely a result of the thinner ice thickness in the steeper part of the glacier in 2000. The increased thinning between 5525 and 5575 m a.s.l. might be caused by increased ablation at steep slopes and ice cliffs.

4.2 Glacier length changes and flow

The glacier length changes for Yala and Rikha Samba glaciers are reported in Table 4 and displayed in Fig. 9 and 10. Yala Glacier retreated from 1974 to 2016 by -346 m, with an annual rate of -8.2 m a^{-1}. The fastest retreat with a rate of -14.1 m a^{-1} happened between 2000 and 2012, when the glacier retreated 169 m over a large rock step behind the lake. The smallest rates of -3.8 m and -3.9 m a^{-1} were measured from 1974 to 1981 and 2014 to 2016. For Rikha Samba Glacier, between 1989 and 2013 the average retreat rate and total retreat was -18.0 m a^{-1}, and -431 m, respectively. We measured maximum retreat rates of -31.8 m a^{-1}, from 2011 to 2016, when the glacier retreated by -159 m. The smallest retreat rates of -12.4 m a^{-1} were measured during a retreat of 149 m from 1989 to 2001.

Table 4: Frontal variations of Yala and Rikha Samba glaciers.

Time period	Frontal variation (m)	Uncertainty (m)	Annual rate (m a^{-1})	Source
Yala Glacier				
1974–1981	-26.9	±5	-3.8	Hexagon KH-9 / GEN map
1981–2000	-129.0	±31	-6.8	GEN map / Landsat 7
2000–2012	-169.1	±30	-14.1	Landsat 7 /dGNSS
2012–2014	-13.0	±1	-6.5	dGNSS / dGNSS
2014–2016	-7.7	±1	-3.9	dGNSS / dGNSS
1974–2016	**-345.8**	±5	**-8.2**	Hexagon KH-9 / dGNSS
Rikha Samba Glacier				
1989–2001	-149	±30	-12.4	Landsat 4 / Landsat 7
2001–2006	-71	±30	-14.2	Landsat 7 / Landsat 5
2006–2011	-159	±30	-31.8	Landsat 5 / Landsat 5
2011–2013	-52	±15	-26.0	Landsat 5 / dGNSS
1989–2013	**-431**	±34	**-18.0**	Landsat 4 / dGNSS

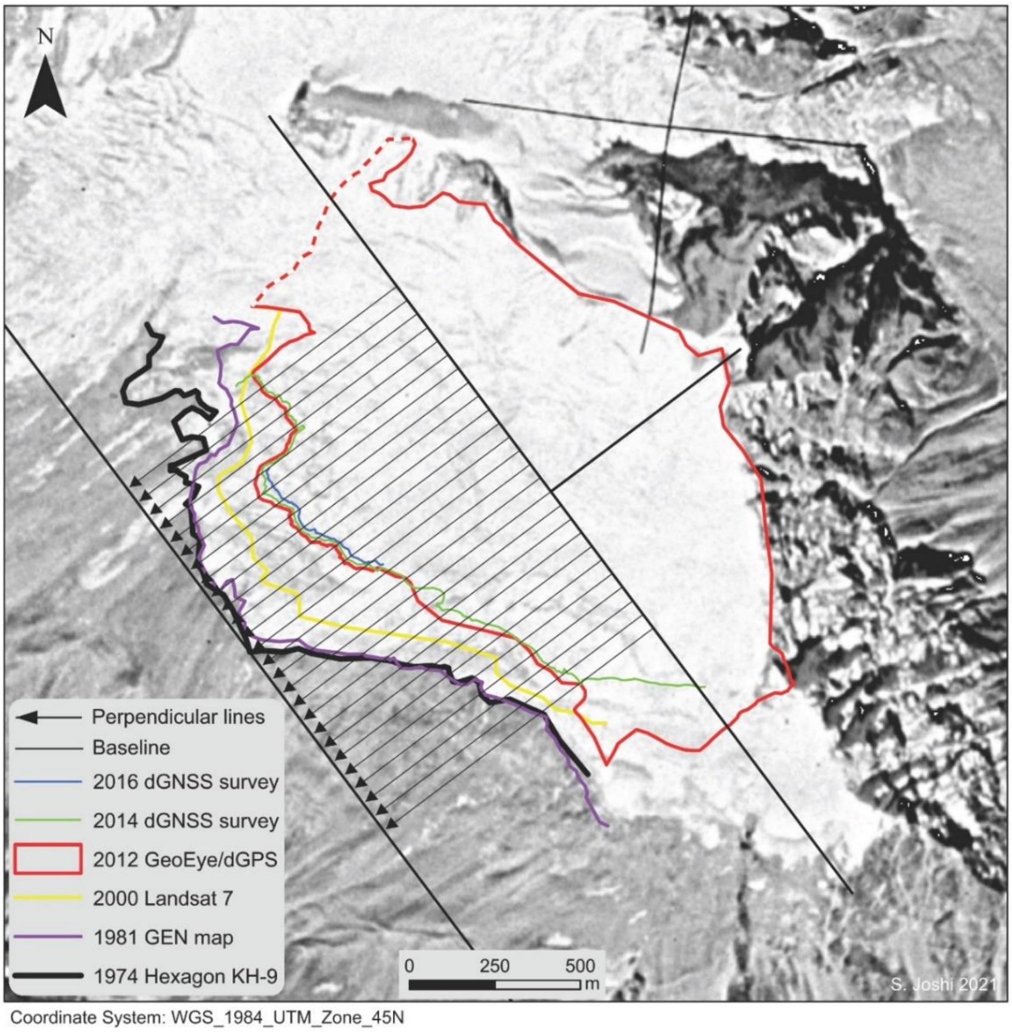

690 **Figure 9: Frontal variations of Yala Glacier from 1974 to 2016. The general flow direction is indicated by a straight black line starting at the highest point of the glacier (north-east corner). An arbitrary baseline marks the maximum extent of 1974. Twenty-six parallel arrows in flow direction at 50 m intervals were used to calculate average frontal variations but to exclude outliers only the 9 lines crossing the terminus from 2016 were used for the analysis. The background image is the Hexagon KH-9 from 1974.**

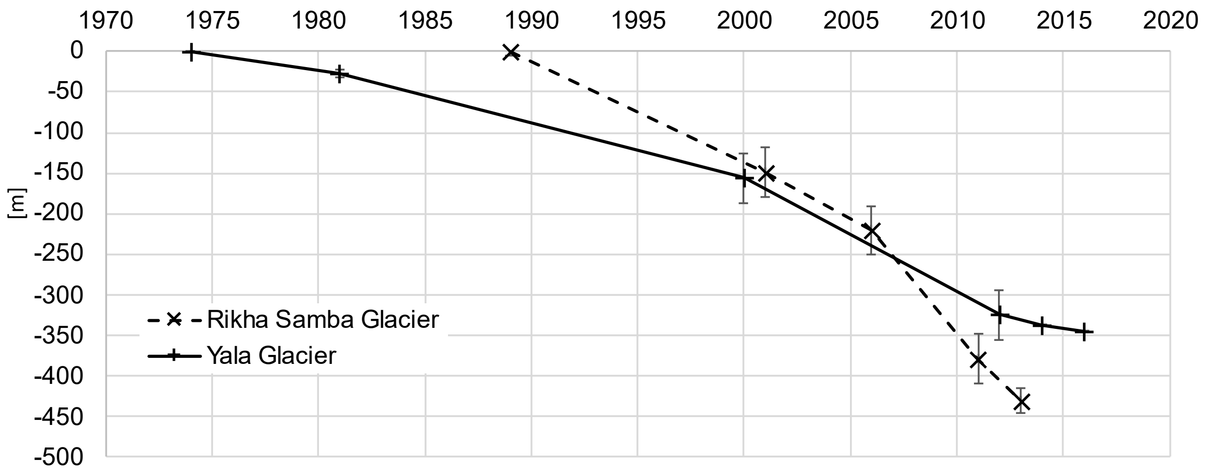

Figure 10: Cumulative glacier retreat of Yala and Rikha Samba glaciers, with uncertainty range.

Glacier flow was measured on Yala Glacier between 8 May 2012 and 5 May 2014. The mean horizontal flow was 5.8 ±0.4 m a^{-1}, with a minimum and maximum velocity of 4.6 ±0.4 m a^{-1} and 7.8 ±0.4 m a^{-1}, respectively (Fig. 11, Table 5). The glacier surface lowered at each measured stake, on average by 3.4 ±0.4 m a^{-1}. While reinstalling stakes in the lowest part of the glacier, it was observed that flow velocities were typically less than 5 m a^{-1}.

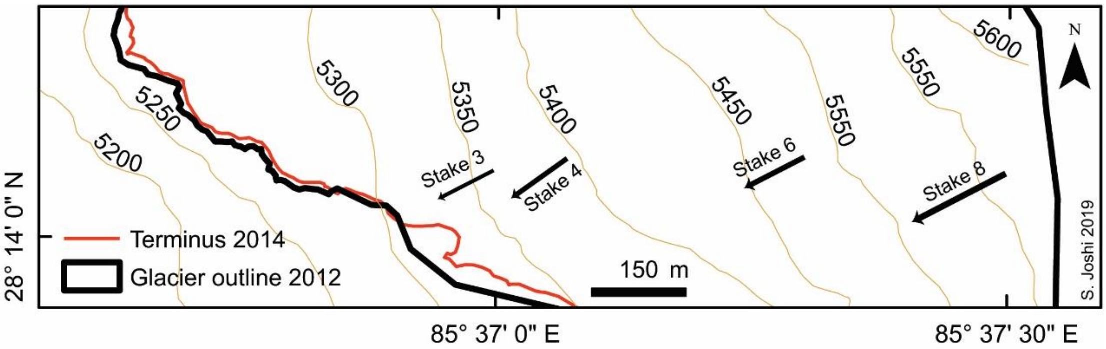

Figure 11: Glacier flow from 8 May 2012 to 5 May 2014 at the stakes 3, 4, 6 and 8, with annual rates between 4.6 and 7.8 m a^{-1}. The black arrows show the flow direction and the lengths indicate the annual speed of glacier surface flow, which is depicted 10 times longer than the real flow (Figure adapted from Sugiyama et al., 2013).

Table 5: Glacier flow in metres and direction of Yala Glacier at the stakes S3, S4, S6 and S8 from 8 May 2012 to 5 May 2014.

Stake	Horizontal flow (m)	Annual flow (m a^{-1})	Flow direction	Altitude in 2012	Altitude in 2014	Vertical flow (m)	Annual (m a^{-1})
3	9.1	4.6 ±0.4	S63W	5249	5242	7.0	3.5 ±0.4
4	11.2	5.6 ±0.4	S56W	5286	5279	7.1	3.6 ±0.4
6	10.0	5.0 ±0.4	S62W	5373	5366	7.1	3.6 ±0.4
8	15.6	7.8 ±0.4	S63W	5457	5450	6.2	3.1 ±0.4
Average		**5.8 ±0.4**					**3.4 ±0.4**

5 Discussion

5.1 Yala Glacier

5.1.1 Annual mass-balance rates

Yala Glacier's annual geodetic mass-balance rate is -0.74 ±0.53 m w.e. a^{-1} from 2000–2012 (Table 6). The thinning rate along the profile line is with -1.1 ±0.13 m a^{-1} higher but within the uncertainty range of the DEM thinning rate, most likely because accumulation above 5571 m a.s.l. is excluded from the calculation. The profile line has been surveyed repeatedly, the first time by Sugiyama et al. (2013) in 2009 and in subsequent years by our team. The future analysis of the geodetic mass balances along the profile lines and transects is planned as supporting and independent method for the analysis of the mass balance (Wagnon et al., 2020, 2013). The average annual rate of the in situ mass balance from 2011 to 2017 is with -0.80 ±0.28 m w.e. a^{-1} larger than the geodetic mass-balance rate from 2000 to 2012. From 2000 to 2017, Yala Glacier lost -12.86 m w.e. with an annual rate of -0.76 ±0.53 m w.e. a^{-1}. For Yala Glacier, Ragettli et al. (2016) calculated a mass-balance rate of -0.76 ±0.24 m w.e. a^{-1} from DEM differencing for 2006 to 2015, which is within the uncertainty range calculated in this study. Brun et al., (2017) calculated an annual geodetic mass-balance rate of -0.44 ±0.18 m w.e. a^{-1}, from 2000 to 2016, which is lower than what we measured, but withing the uncertainty range. Fujita and Nuimura (2011) and Sugiyama et al. (2013) calculated geodetic mass-balance rates of -0.80 ±0.16 m and -0.64 ±0.20 m w.e. a^{-1}, respectively, from 1996 to 2009, which are within the uncertainty ranges but for different time periods. Based on a modelling study Fujita and Nuimura (2011) find that Yala Glacier is will disappear over time.

Table 6: Comparison of glacier surface lowering and in situ mass-balance measurements from various studies. Conversions of thickness change (*) calculated assuming a density of 850 kg m^{-3} and annual uncertainties calculated based on authors' values and Zemp et al. (2013).

Duration	Total years	Glacier	Annual thickness change (m a^{-1})	Annual mass~~-~~-balance rate (m we a^{-1})	Method	Source
2000–2012	12	Yala	-0.87 ±0.62	-0.74 ±0.53*	DEM differencing	This study
2000–2012	12	Yala profile	-1.1 ±0.13	-0.94 ±0.11*	DEM differencing	This study
2011–2017	6	Yala		-0.~~74~~80 ±0.28	~~Direct measurements~~Glaciological method	This study
2006–2015	9	Yala	-0.89 ±0.23	-0.76 ±0.24	DEM differencing	Ragettli et al., (2016)
2000–2016	16	Yala	-0.52 ±0.21	-0.44 ±0.18*	DEM differencing	Brun et al., (2017); WGMS ~~2019~~2020a
1996–2009	13	Yala profile	-0.75 ±0.24	-0.64 ±0.20*	~~dGPS~~dGNSS and GPR Survey	Sugiyama et al., 2013
1996–2009	13	Yala		-0.80 ±0.16	DEM differencing	Fujita and Nuimura, 2011
2006–2015	9	7 glaciers in Langtang	-0.45 ±0.18	-0.38 ±0.17	DEM differencing	Ragettli et al. (2016)
2000–2016	16	3 glaciers in Langtang		-0.58 ±0.08	DEM differencing	Maurer et al., 2019
2011–2017	6	Rikha Samba		-0.39 ±0.32	~~Direct measurements~~Glaciological method	This study
2000–2016	16	Rikha Samba	-0.44 ±0.27	-0.37 ±0.23*	DEM differencing	Brun et al., (2017); WGMS ~~2019~~2020a
1998–2010	12	Rikha Samba		-0.48 ±0.10	DEM differencing	Fujita and Nuimura, 2011
2011–2017	6	Mera		-0.31 ±0.17	~~Direct measurements~~Glaciological method	Wagnon et al., 2020
2011–2017	6	Pokalde		-0.75 ±0.28	~~Direct measurements~~Glaciological method	Wagnon et al.,~~2013; WGMS 2019~~ 2020
2000–2011	11	Everest Region		-0.26 ±0.13	DEM differencing	Gardelle et al., 2013
2000–2008	8	Everest Region		-0.45 ±0.60	DEM differencing	Nuimura et al., 2012
2002–2007	5	Everest Region		-0.79 ±0.52	DEM differencing	Bolch et al., 2011
~~2002–2014~~2011–2017	~~12~~6	Chhota Shigri		-0.~~56~~43 ±0.40	~~Direct measurements~~Glaciological method	~~Azam~~Mandal et al., 2020~~2016~~
2000–2016	16	Himalayan glaciers clean		~~=~~-0.38 ±0.08	DEM differencing	Maurer et al., 2019

5.1.2 Seasonal mass balance

On Yala Glacier the negative summer balance determines the annual balance. For every winter season we measured positive mass balances, and during summer only little or no accumulation in higher elevations (Fig. 2, 4 and Table 2). The slight mass gain in winter mainly happened from January to May when snowfall set in. In early October 2013 and 2014, the Central Himalayas received large amounts of precipitation brought by the cyclones Phailin and Hudhud (Shea et al. 2015b; Necker et al., 2015). These precipitation events in form of snow contributed to the summer balance since the measurements were taken after the cyclones passed, making the summer balance less negative.

In winter 2014/15 an exceptional amount of precipitation was measured at various AWSs. Local people in Langtang reported many Yaks dying in the snow, and during the Nepal earthquake in April 2015 extreme avalanches with anomalous amounts of snow were triggered (Fujita et al., 2017). For this winter, above average accumulation (0.54 m w.e.) was measured and calculated, despite a delay of measurements by a month in early June. Triggered by the earthquake and aftershocks, the Langtang Valley was heavily affected by snow and ice avalanches, landslides, as well as rockfalls on the glacier in the immediate vicinity of the study area (Kargel et al., 2016, Fujita et al., 2017). Direct effects of the earthquake on the glacier could not be measured, however AWSs on and near the glacier were destroyed likely because of air blasts from ice avalanches. The effect of the air blasts on the snow cover of Yala Glacier is not known, however, it is possible that snow was blown away and partly sublimated. The air in the valley was filled with dust and it is probable that more dust than usual settled on Yala Glacier, increasing ablation particularly in summer 2015. The seasonal mass-balance measurements in June 2015 were taken under precarious conditions, and only stake measurements could be taken up to an elevation of 5217 m a.s.l., resulting in a higher uncertainty for the seasonal mass balances in 2014/15 and a possibly underrepresented accumulation in winter 2014/15. These circumstances explain the discrepancy in the cumulative seasonal and the annual mass balance by -0.59 m w.e. in the mass-balance year 2014/15 (Fig. 4). In autumn 2012, we calculated the least negative summer balance (-0.35 m w.e.), based on only three measurements and likely underestimating ablation. This could explain the underestimated annual mass loss of -0.83 m w.e. in the cumulative seasonal balance compared to the annual balance of 2011/12. Measurements taken in autumn were generally more reliable because less snow was present on the glacier surface, reducing the uncertainty related to the snow cover. Although Yala Glacier is a summer-accumulation type glacier, most of the accumulation was measured in the winter season because the accumulation area is too small and at a too low elevation to benefit from snowfall during the monsoon months. Together with the overall negative balances it indicates that Yala Glacier is out of balance and shrinking.

5.1.3 Glacier length changes, flow and downwasting

At Yala Glacier, Ono (1985) dated Little Ice Age moraines and documented annual ice push moraines, and Yamada et al. (1992) and Kappenberger et al. (1993) observed terminus retreat since the 1970s with a minor advance in the early 1980s and stagnation, respectively, followed by retreat. In the 1990s Fujita et al. (1998) noted an accelerated retreat. From 2000 to 2012, we measured the highest retreat rate of -14.1 m a^{-1} when the glacier retreated over a steep rock step from about 5100 m to 5175 m a.s.l. From 2012 to 2016, Yala Glacier retreated with a slower annual rate of -5.2 m a^{-1} in mostly flat terrain, partly in shallow water.

Horizontal flow was measured with a theodolite from 28 September to 27 October 1982 (Ageta et al., 1984), and from 22 May to 7 October 1996 (Fujita et al., 1998) and a decreasing velocity was observed (Fig. 12). In both studies, the annual flow rate was assumed to be the same as for the measurement periods, despite varying seasons. Sugiyama et al. (2013) measured the top three stakes on 26 September 2008 and 31 October 2009, and the lower two stakes for four days from 31 October to 4 November 2009 with a dGNSS, which were presumably extrapolated to calculate the annual rate, assuming a constant flow. The flow velocity and direction measured in this study from 2012 to 2014 compares to the measurements from 2008 to 2009.

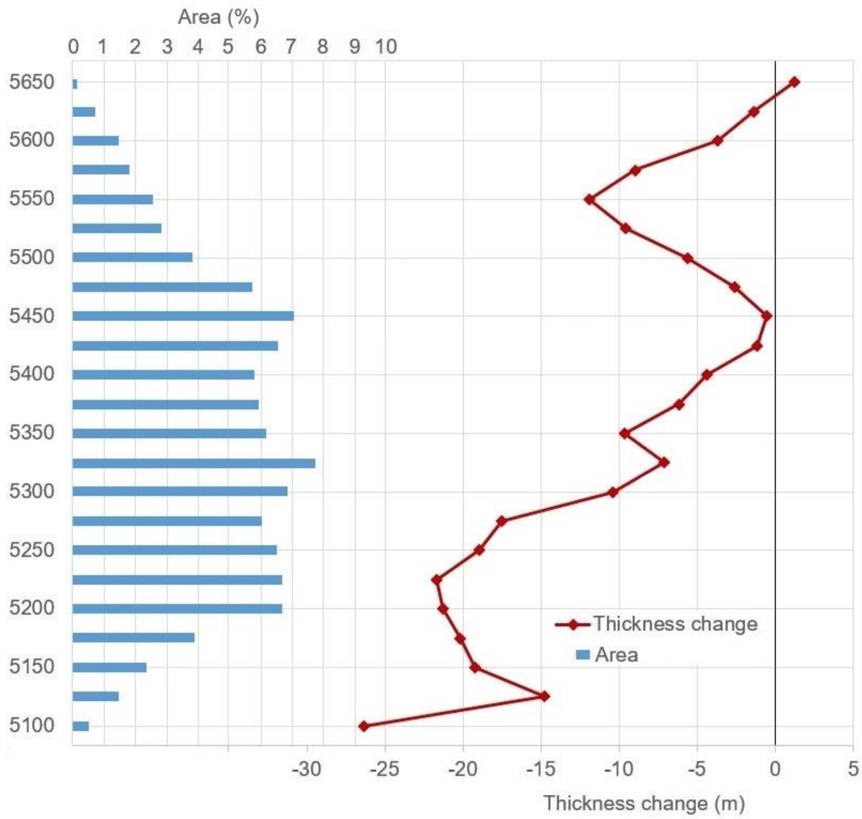

~~**Figure 8: The mean thickness changes of Yala Glacier for 25 m elevation bands with hypsography, from 2000 to 2012. The reduced thickness change at an elevation of 5125 m is likely a result of the thinner ice thickness in the steeper part of the glacier in 2000. The increased thinning between 5525 and 5575 m a.s.l. might be caused by increased ablation at steep slopes and ice cliffs.**~~

~~The annual and cumulative balances of both glaciers show a similar pattern (Fig. 9, Table 2 and 3), however, the mean annual rate and cumulative balance of Yala Glacier from 2011 to 2017 are more negative (-0.74 ±0.28 m w.e. a^{-1}, -4.44 ±0.69 m w.e.) than of Rikha Samba Glacier (-0.39 ±0.32 m w.e. a^{-1}, -2.34 ±0.79 m w.e). From 2000 to 2017, Yala Glacier lost -12.50 m w.e. with an annual rate of -0.74 ±0.53 m w.e. a^{-1}.~~

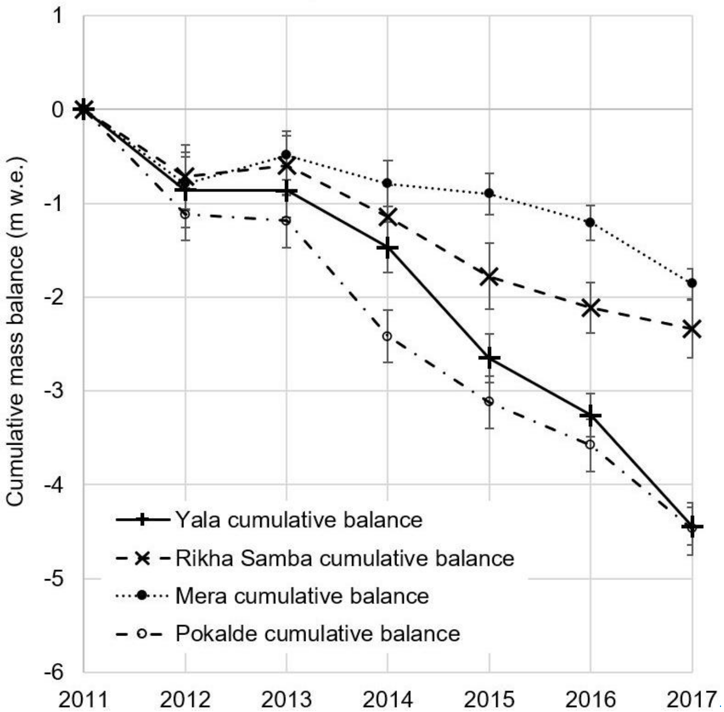

~~**Figure 9: Cumulative mass balances of Yala, Rikha Samba, Mera and Pokalde Glacier. The data for Mera and Pokalde Glacier is from Wagnon et al. 2013, Sherpa et al. 2017, WGMS, 2020, and Wagnon et al. 2020.**~~

4.2 Glacier length changes and flow

The glacier length changes for Yala and Rikha Samba Glacier are reported in Table 5 and displayed in Fig. 10 and 11. Yala Glacier retreated from 1974 to 2016 by -346 m, with an annual rate of -8.2 m a^{-1}. The fastest retreat with a rate of -14.1 m a^{-1} happened between 2000 and 2012, when the glacier retreated 169 m over a large rock step behind the lake. The smallest rates of -3.8 m and -3.9 m a^{-1} were measured from 1974 to 1981 and 2014 to 2016. Rikha Samba Glacier showed much larger retreat rates than Yala Glacier, with an average of -18.0 m a^{-1}, and a total retreat of -431 m between 1989 and 2013. We measured maximum retreat rates of -31.8 m a^{-1}, from 2011 to 2016, when the glacier retreated by -159 m. The smallest retreat rates of -12.4 m a^{-1} were measured during a retreat of 149 m from 1989 to 2001.

Table 5: Frontal variations of Yala and Rikha Samba Glacier.

Time period	Frontal variation (m)	Uncertainty (m)	Annual rate (m a^{-1})	Source
Yala Glacier				
1974–1981	-26.9	±5	-3.8	Hexagon KH-9 / GEN map
1981–2000	-129.0	±31	-6.8	GEN map / Landsat 7
2000–2012	-169.1	±30	-14.1	Landsat 7 /dGPS
2012–2014	-13.0	±1	-6.5	dGPS / dGPS
2014–2016	-7.7	±1	-3.9	dGPS / dGPS
1974–2016	**-345.8**	**±5**	**-8.2**	Hexagon KH-9 / dGPS
Rikha Samba Glacier				
1974–1994	-215.8		-10.8	Fujita et al. 2001
1994–1998	-72.8		-18.2	Fujita et al. 2001
1998–1999	-11.5		-11.5	Fujita et al. 2001
1989–2001	-149	±30	-12.4	Landsat 4 / Landsat 7
2001–2006	-71	±30	-14.2	Landsat 7 / Landsat 5
2006–2011	-159	±30	-31.8	Landsat 5 / Landsat 5
2011–2013	-52	±15	-26.0	Landsat 5 / dGPS
1989–2013	**-431**	**±34**	**-18.0**	Landsat 4 / dGPS

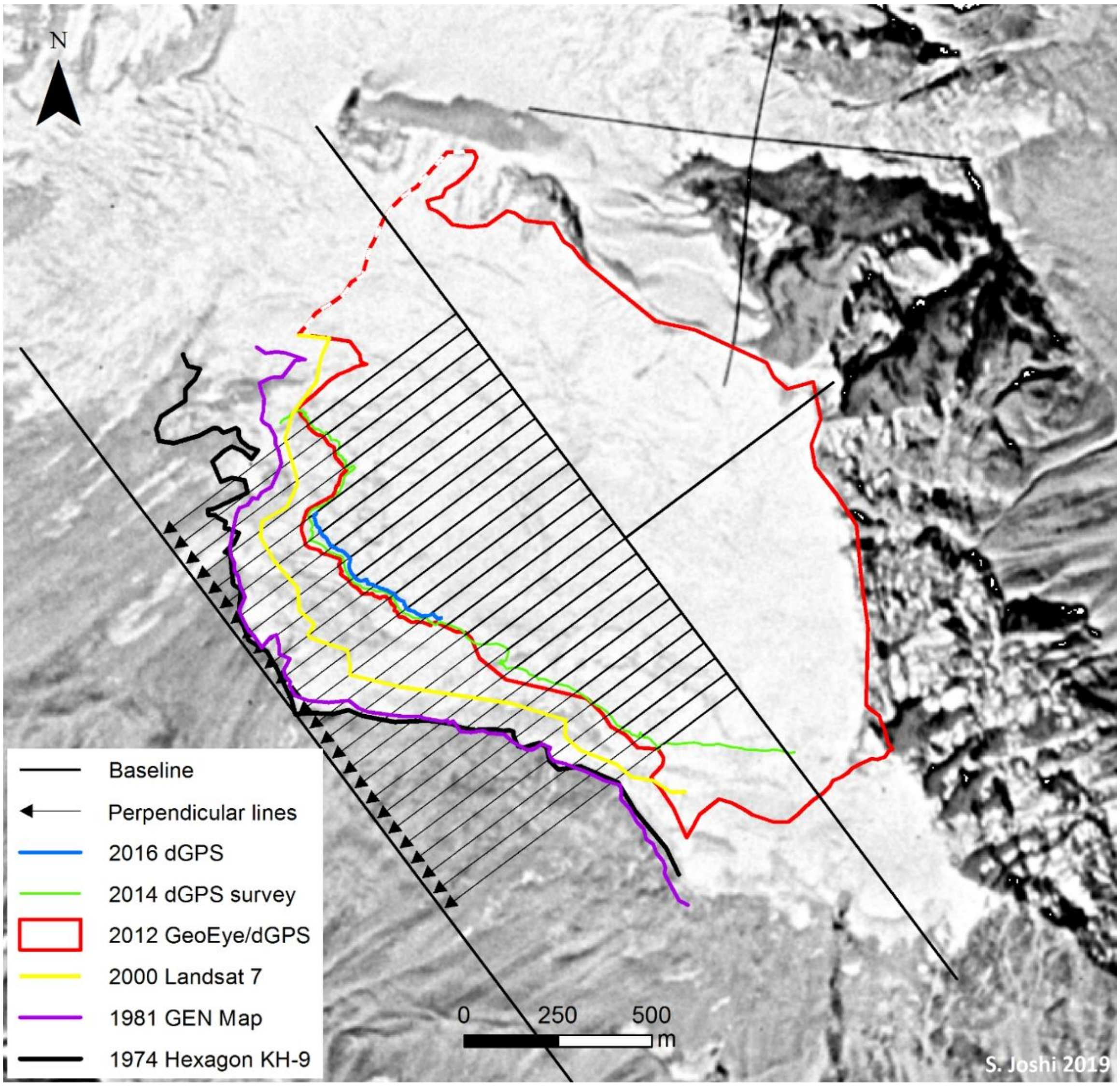

~~Figure 10: Frontal variations of Yala Glacier from 1974 to 2016. The general flow direction is indicated by a straight black line starting at the highest point of the glacier (north east corner). An arbitrary baseline is at the maximum extent of 1974 (black outline), and 26 parallel arrows in flow direction at 50 m intervals we used to calculate average front variations, but only the 9 bold lines were used for the analysis to exclude outliers. The background image is the Hexagon KH-9 from 1974.~~

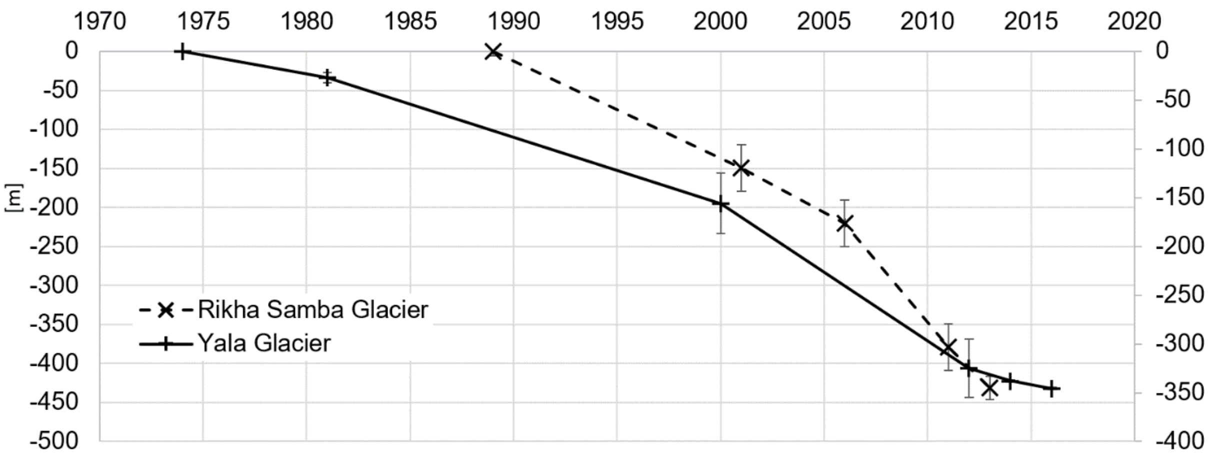

~~Figure 11: Cumulative glacier retreat of Yala and Rikha Samba Glacier, with uncertainty range.~~

~~Glacier flow was measured on Yala Glacier between 8 May 2012 and 5 May 2014. The mean horizontal flow was 5.8 ±0.4 m a^{-1}, with a minimum and maximum velocity of 4.6 ±0.4 m a^{-1} and 7.8 ±0.4 m a^{-1}, respectively (Fig. 12, 13, Table 6). The glacier surface lowered at each measured stake, on average by 3.4 ±0.4 m a^{-1}. While reinstalling stakes in the lowest part of the glacier, it was observed that flow velocities were typically less than 5 m a^{-1}.~~

However, the glacier is slower than in the 1980s and 1990s, and the direction slightly varied, as already shown by Sugiyama et al. (2013).

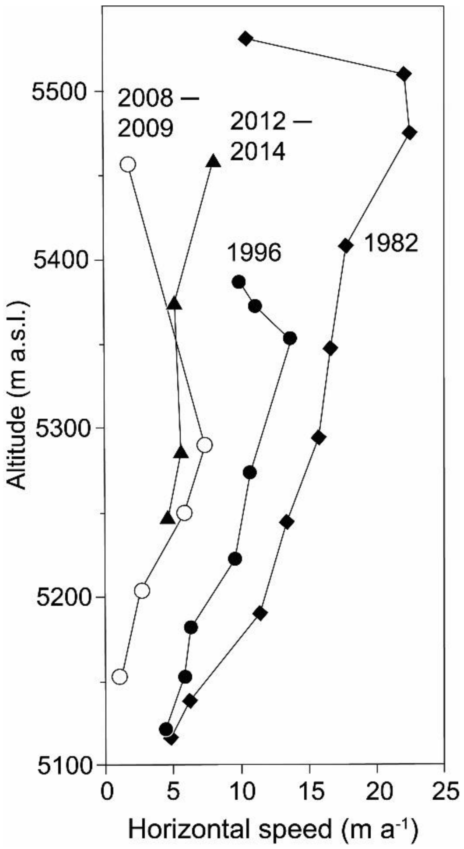

Figure 12: Altitudinal distribution of the surface flow speeds of Yala Glacier, surveyed in 1982 ~~(solid diamonds,~~by Ageta et al. (1984), ~~in~~ 1996 ~~(solid circles,~~by Fujita et al. (1998), 2008 to 2009 ~~(open circles,~~by Sugiyama et al~~.,~~. (2013) and from 2012 to 2014 ~~(solid tringle,~~in this study~~) (modified Fujita et al. 1998).~~

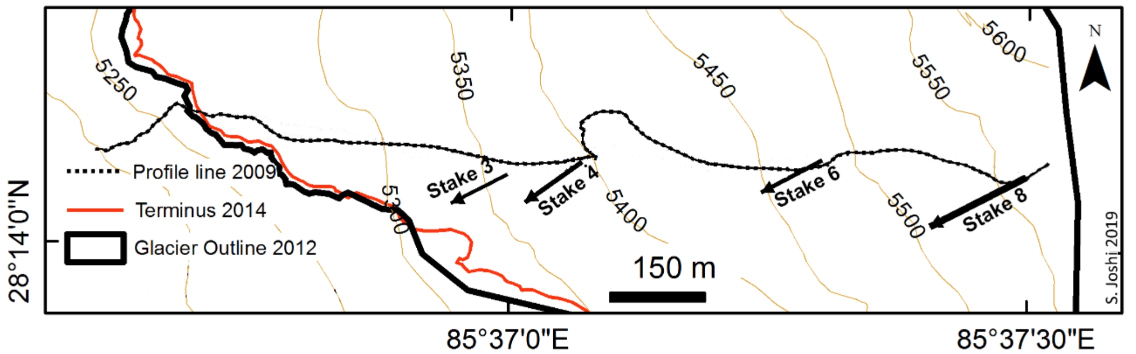

~~Figure 13: Glacier flow~~ (adapted from ~~8 May 2012 to 5 May 2014 at the stakes 3, 4, 6 and 8, with annual rates between 4.6 and 7.8 m. The black arrows show the flow direction and the lengths indicate the annual speed of glacier surface flow, which is depicted 10 times longer than the real flow. The densely dashed line is the profile line from Sugiyama et al. 2013 (Figure modified from Sugiyama et al. 2013~~Fujita et al. 1998).

From 2011 onwards, we observed that concave shapes on the glacier surface have become more pronounced, ice velocities decreased, and the glacier surface was downwasting as observed at other glaciers (Ragettli et al., 2016; Sommer et al. 2020). The downwasting is a consequence of the decreased ice velocities, and indicates changes in the glacier dynamics. The downwasting of Yala Glacier compromised the consistent representativeness of stake measurements at several locations. For example, between stakes S1 and S1B and near S5, Yala Glacier has very concave surfaces with bowl-shaped areas and transitions to steep slopes. Here the ablation is likely enhanced because of the reflection of radiation (Hock, 2005). At some locations the glacier surface topography changed to a degree that the stake had to be shifted. These small-scale spatial variabilities could cause a bias, which should be corrected later with help of complementing geodetic surface analyses (Zemp et a., 2013).

5.1.4 Steep slopes and ice cliffs

The ice cliffs and steep slopes at Yala Glacier are mainly exposed to south-west, occur over the entire glacier range, and likely experience increased melt due to their orientation and large surface area. Already Ageta et al. (1984) described the ice cliffs, and old photos document part of the glacier terminus as ice cliff, at times with an apron (Shiraiwa, 1993). The effect of vertical ablation through melt, sublimation and ice breaking off could be substantial, as observed at glacier ice cliffs in the Antarctic McMurdo Dry Valleys (Chinn, 1987; Lewis et al., 1999), on Kilimanjaro (Winkler et al., 2010), and debris-covered glaciers (e.g. Sakai et al., 2002; Steiner et al., 2015). However, ice-cliff and steep-slope ablation cannot be quantified with the conventional glaciological method and ablation might be underestimated. Additionally, it is difficult to quantify the relevance of steep slopes in terms of area because the slope surface area is not well represented in the map view of a DEM, and increases with steepness (Supplement section S4). At Yala Glacier, assessed with a DEM of 30 m resolution, the area of slopes in average steeper than 50° make up 5 % of the total glacier area in map view. But these steep slopes only represent slopes of at least 36 m height (Table S4 and S5, Fig. S8), and the actual surface area exposed to ablation is much larger than represented by the DEM (Table S6 and Fig. S9). Analysed with the SRTM-3 DEM, Bajracharya et al. (2014) found that more than 50 % of the glacier area in Nepal is oriented south-west, south, or south-east. Yet, to quantifying steep slopes with a DEM with a resolution of 90 m, slopes with angles equal or larger than 48° must have a minimum slope height of 100 m, and steeper slopes of smaller height cannot be represented (Table S4 and S5, Fig. S8). Hence, the surface area of Nepal's ice cliffs and steep ice slopes is underrepresented and cannot be quantified in such DEM analyses.

Complementing geodetic mass-balance measurements for the same timeframe help to correct the glacier-wide annual mass balances of Yala Glacier for biases such as introduced by steep slopes and ice cliffs (Zemp et al., 2013; Wagnon et al., 2020). To better understand and assess specifically the influence of the steep slopes and ice cliffs of the mass balance, geodetic thickness-change analyses based on high-resolution surface elevations for short time intervals could be used, in combination with energy-balance models (Joerg and Zemp, 2014).

5.2 Rikha Samba Glacier

For Rikha Samba Glacier, Fujita and Nuimura (2011) and Brun et al. (2017) calculated geodetic mass-balance rates of -0.48 m w.e. a^{-1} (1998–2010) and -0.37 ±0.23 m w.e. a^{-1} (2000–2016). These values are close to the annual average rate of -0.39 ±0.32 m w.e. a^{-1} (2011–2017) calculated in this study, however, the time periods vary and Fujita and Nuimura (2011) largely excluded elevations above 6000 m a.s.l. From 1974 to 1994, Fujita et al. (2001) measured a retreat of 216 m with a slow retreat rate of -10.8 m a^{-1}. The rate accelerated to -18.2 m a^{-1} from 1994 to 1998 when the glacier retreated 73 m. From 1989 to 2006, we measured a glacier retreat of totally 220 m with retreat rates of -12.4 m a^{-1} and 14.2 m a^{-1}, from 1989 to 2001 and 2001 to 2006, respectively (Table 4, Fig. 10). From 2006 to 2011 and 2013 the terminus retreated rapidly 159 m and 52 m, with rates of -31.8 m a^{-1} and -26.0 m a^{-1}, respectively. ~~**Table 6: Glacier flow in metres and direction of Yala Glacier at the stakes S3, S4, S6 and S8 from 8 May 2012 to 5 May 2014.**~~

~~Stake~~	~~Horizontal flow (m)~~	~~Annual flow (m a⁻¹)~~	~~Flow direction~~	~~Altitude in 2012~~	~~Altitude in 2014~~	~~Vertical flow (m)~~	~~Annual (m a⁻¹)~~
~~3~~	~~9.1~~	~~4.6 ±0.4~~	~~S63W~~	~~5249~~	~~5242~~	~~7.0~~	~~3.5 ±0.4~~
~~4~~	~~11.2~~	~~5.6 ±0.4~~	~~S56W~~	~~5286~~	~~5279~~	~~7.1~~	~~3.6 ±0.4~~
~~6~~	~~10.0~~	~~5.0 ±0.4~~	~~S62W~~	~~5373~~	~~5366~~	~~7.1~~	~~3.6 ±0.4~~
~~8~~	~~15.6~~	~~7.8 ±0.4~~	~~S63W~~	~~5457~~	~~5450~~	~~6.2~~	~~3.1 ±0.4~~
~~Average~~		~~5.8 ±0.4~~					~~3.4 ±0.4~~

~~5 Discussion~~

~~5.1 Annual glacier-wide mass balances, ELA and AAR~~

~~In the Himalayan region various studies observed an accelerated thinning trend over the past decades and heterogeneous thinning patterns (e.g. Maurer et al., 2019; Ragettli et al., 2016; Nuimura et al., 2012; Bolch et al., 2011; Gardelle et al., 2013).~~In a modelling study, Fujita and Nuimura (2011) find that Rikha Samba will not disappear under the current climate.

5.3 Comparison of in situ glacier mass balances in the Himalaya

~~For 18 Himalayan glaciers Azam et al. (2018) assessed a mean rate of -0.49 m w.e. a⁻¹ for directly measured glacier mass balance for the period from 1975 to 2015. Maurer et al. (2019) calculated a Himalayan-wide geodetic mass balance of –0.38 ±0.08 m w.e. a⁻¹ for clean ice from 2000 to 2016. The mass balance rate of Rikha Samba Glacier is within a similar range, however, the one of Yala glacier is more negative. For Chhota Shigri Glacier in the Western Himalaya, Azam et al. (2016) found a mass balance rate of -0.56 ±0.40 m a.s.l. from 2002 to 2014 in direct measurements.~~

In Nepal, the mean annual mass-balance rates of the small low-lying Yala and Pokalde ~~Glacier~~glaciers (Fig 1) from 2011 to 2017 are similar (~~Table 4, -~~0.~~74~~80 ±0.28 m and -0.75 ±0.28 m w.e. a^{-1}, Table 6). Rikha Samba and Mera ~~Glacier~~glaciers are both higher lying glaciers with a larger elevation range and smaller mass-balance rates (-0.39 ±0.32 m and -0.31 ±0.17 m w.e. a^{-1}; Wagnon et al., 2020). These tendencies are reflected in the cumulative mass balances that are negative for Mera and Rikha Samba ~~Glacier~~glaciers, and even more negative for Yala and Pokalde ~~Glacier~~glaciers (Fig. ~~9~~13). Mera Glacier has ~~the largest~~a large elevation range (4940–6420 m a.s.l.) and similar upper limits as Rikha Samba Glacier (5416–6515 m a.s.l), but a lower ELA$_0$ (~5515 m a.s.l.), and a large accumulation area with an AAR$_0$ of about 0.60. Rikha Samba Glacier has a smaller elevation range (1100 m vs. 1460 m), and a smaller average mass-balance gradient at the ELA than Mera Glacier (0.36 m vs. 0.45 m w.e. (100 m)$^{-1}$), which indicates the ~~likely~~ more continental ~~condition~~conditions on the north side of the Himalayan main divide, opposed to Mera Glacier on the south side of the main divide.

~~For Rikha Samba Glacier, Fujita and Nuimura (2011) and Brun et al. (2017) calculated mass balance rates of -0.48 m w.e. a⁻¹ (1998–2010) and -0.37 ±0.23 m w.e. a-1 (2000–2016), which are close to the values calculated in this study, however, the time periods vary, and Fujita and Nuimura (2011) largely excluded elevations above 6000 m a.s.l.~~ Fujita and Nuimura (2011) calculated so-called preferable ELAs for the glacier extents of Yala and Rikha Samba in 2009 and 2010, which are 5260 m and 5545 m a.s.l., respectively, and are lower than the calculated ELA$_0$ of 5378 m and 5758 m a.s.l. in this study. Varying glacier areas and elevation ranges are likely reasons for the differences.

In winter, wind and sublimation are important ablation processes on the glaciers. Wagnon et al. (2013) address the high wind speeds from westerly winds at Mera Glacier (5360 m a.s.l on glacier station) in winter, which causes in combination with sublimation a substantial part of the winter ablation. Stitger et al. (2018) and Litt et al. (2019) assessed sublimation on Yala Glacier and confirm its strong ablating influence, especially during favourable conditions such as high wind speed, low atmospheric vapour pressure and low near-surface vapour pressure. The study of Shea et al. (2015b) shows similarly high winter wind speeds at Rikha Samba Glacier (5310 m a.s.l, off-glacier station) as at Mera Glacier, but at Yala Glacier (5060 m a.s.l., off-glacier station) only slightly higher wind speeds than on annual average. It seems reasonable that wind and sublimation are important ablation processes for Rikha Samba Glacier in winter. At Yala Glacier, in winter when accumulation dominates over ablation the effect of wind and sublimation is probably smaller compared to Mera and Rikha Samba glaciers. Fujita et al. (1997b) point out that winter precipitation is more important in Langtang than in Khumbu, which is confirmed by the AWS data described by Shea et al. (2015b) and could partly explain the winter accumulation on Yala Glacier. Shiraiwa (1993) highlights the influence of both the summer monsoon and westerly winter circulation on the annual balance. To better understand the relationship between the climate and the mass balance of Yala an Rikha Samba glaciers, the analysis of homogenised climate data from nearby weather stations or reanalysis data would be useful.

Chhota Shigri Glacier (Fig. 1) is a glacier in the Western Himalaya under the influence of the Indian summer monsoon in summer, and western disturbances in winter, with a relatively long in situ mass-balance series (Mandal et al., 2020). The cumulative mass balance and the annual mass-balance rate of the glacier (-2.59 m w.e. and -0.43 ±0.40 m w.e.a^{-1}) from 2011 to 2017 are in a similar range like Rikha Samba and Mera glaciers. Chhota Shigri Glacier also has a large elevation range of about 1760 m, but lies on a lower elevation (4072 m to 5830 m a.s.l.). The mean ELA and AAR of 5047 m a.s.l. and 0.49, respectively, indicate that Chhota Shigri Glacier is relatively healthy despite the lower elevation range, due to the colder climate and winter precipitation from westerly disturbances.

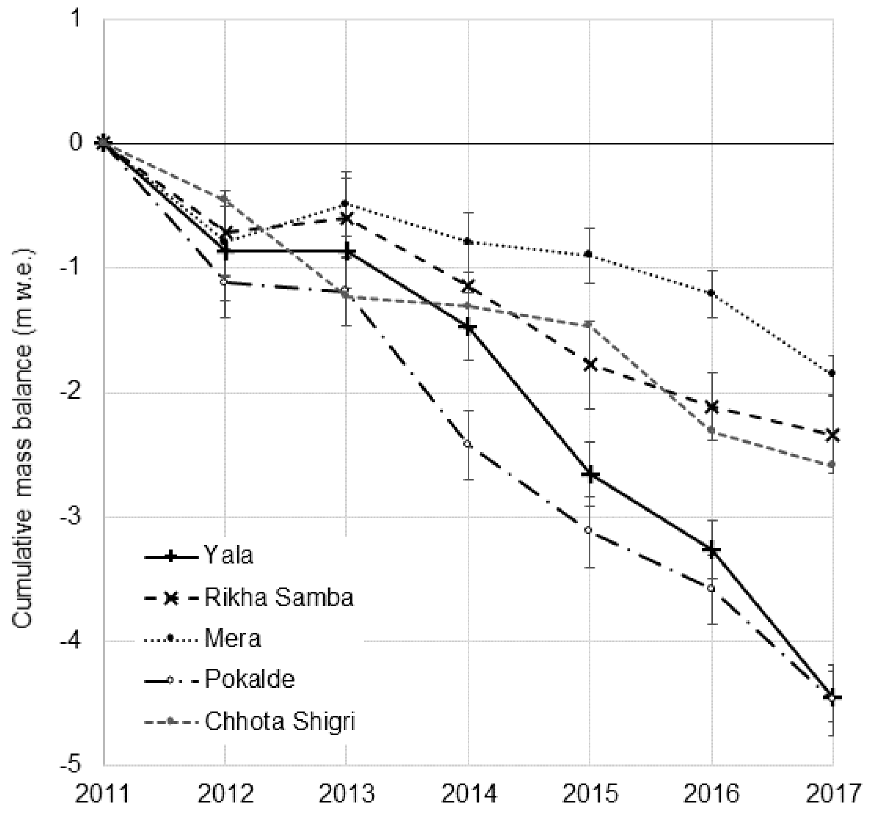

Figure 13: Cumulative mass balances of Yala, Rikha Samba, Mera, Pokalde and Chhota Shigri glaciers. The data for Mera, Pokalde and Chhota Shigri glaciers is from Wagnon et al. (2013), Sherpa et al. (2017), WGMS (2020a), Wagnon et al. (2020) and Mandal et al. (2020).

5.4 Bias by small low-lying glaciers

The mass-~~For Yala Glacier, Ragettli et al. (2016) calculated a mass balance rate of -0.76 ±0.24 m w.e. a-1 from DEM differencing for 2006 to 2015, which is nearly the same as calculated in this study. Fujita and Nuimura (2011) and Sugiyama et al. (2013) calculated mass balance rates of -0.80 ±0.16 m and -0.64 ±0.20 m w.e. a-1, respectively, from 1996 to 2009, and Brun et al., (2017) calculated an annual rate of -0.44 ±0.18 m w.e. a-1, from 2000 to 2016, which are within the uncertainty ranges but for different time periods. Yala Glacier's annual mass balance rate of -0.74 ±0.53 m w.e. a-1 from 2000–2012 is higher than the average rates measured in the Everest Region by Gardelle et al. (2013; 2000–2011: -0.26 ±0.13 m w.e. a-1) and Nuimura et al. (2012; 2000–2008: -0.45 ±0.60), and similar to the value calculated by Bolch et al. (2011; 2002–~~

~~2007: -0.79 ±0.52 m w.e. a^{-1}). However, over a region, mass balances can be very heterogeneous. Ragettli et al. (2016) assessed the geodetic mass balances of two clean and five debris-covered glaciers in Langtang and found a very heterogeneous pattern and a mean annual mass balance rate of -0.45 ±0.18 m w.e. a^{-1}. Maurer et al. (2019) calculated a median balance of about -0.54 m w.e. a^{-1} for the clean glaciers in the subregion including Langtang, and a mean rate of -0.58 ±0.08 m w.e. a^{-1} for three debris covered glaciers in Langtang from 2000 to 2016, which is a bit more negative than calculated for the same glaciers by Ragettli et al. (2016).~~

~~The mass~~ balance bias by low-lying glaciers with a small elevation range is demonstrated by Yala and Pokalde ~~Glacier. Both are small glaciers on a lower~~ glaciers. Both glaciers have a bias towards negative mass balances in terms of representativeness for the mass balance of a region. Yala and Pokalde glaciers are both small, on a low altitude with a small elevation range (5168 m–5661 m, and 5430 m–5690 m a.s.l., respectively) similar like AX010 Glacier in the Shorong Himal, Nepal (Fig. 1), and are very sensitive to temperature especially in the monsoon season (Fujita and Nuimura, 2011; Ragettli et al., 2016). Immerzeel et al. (2012), found that from 1957 to 2002 in Langtang 77 % of precipitation fell between June and September, and Ageta and Higuchi (1984) reported about 80 % of the annual precipitation in the same months for east Nepal. Shea et al. (2015b) estimated the height of the 0° C isotherm in Langtang between 3000 m a.s.l. in winter and 6000 m a.s.l. during monsoon. Hence, ~~the~~ glaciers at lower altitudes receive precipitation predominantly in form of rainfall during the monsoon season and snow accumulation is minimal. The very negative balances of ~~the two small~~ Yala and Pokalde glaciers can be explained by the small amount of accumulation during the main precipitation season in monsoon. ~~Yala and Pokalde Glacier likely have a bias towards negative mass balances, like AX010 Glacier in the Shorong Himal, Nepal and are very sensitive to temperature (Fujita and Nuimura, 2011; Ragettli et al., 2016). Such bias results in the overestimation of negative mass balances in the region (Gardner et al., 2013).~~

In comparison, Ragettli et al. (2016) calculated a balanced geodetic mass ~~budget~~balance of -0.02 ±0.13 m w.e. a^{-1} for the clean Kimoshung Glacier (Fig. 1) in close vicinity of Yala Glacier about 3.5 km away, and explain the difference with the very different hypsometry. Compared to Yala Glacier, Kimoshung Glacier has a steep narrow tongue and a large accumulation area (AAR of 0.86~~%)~~)) at high altitude, which is less exposed to air temperatures above 0° C and making the glacier less sensitive to temperature. The accumulation area is ~~possibly~~probably sheltered from ~~the~~ strong westerly winter winds by a mountain ridge running from ~~northwest~~north-west to ~~southeast~~south-east, reducing ablation by wind and sublimation, but receiving precipitation largely in form of snow.

Geodetic mass-balance analyses from the Himalayan region show heterogenous patterns, with average values less negative than for Yala Glacier, although mostly within the uncertainty ranges. Ragettli et al. (2016) assessed the geodetic mass balances of two clean and five debris-covered glaciers in Langtang and found a very heterogeneous distribution and a mean annual mass-balance rate of -0.38 ±0.17 m w.e. a^{-1} from 2006 to 2015, which is lower than Yala Glacier's annual geodetic mass-balance rate of -0.74 ±0.53 m w.e. a^{-1} from 2000 to 2012. Maurer et al. (2019) calculated a median geodetic balance of about -0.54 m w.e. a^{-1} for the clean glaciers in a subregion including Langtang, and a mean rate of -0.58 ±0.08 m w.e. a^{-1} for three debris covered glaciers in Langtang from 2000 to 2016, which is a bit more negative than calculated for the same glaciers by Ragettli et al. (2016). The average geodetic mass-balance rates measured in the Everest Region by Gardelle et al. (2013; 2000–2011: -0.26 ±0.13 m w.e. a^{-1}) and Nuimura et al. (2012; 2000–2008: -0.45 ±0.60), are lower than measured at Yala Glacier. Bolch et al. (2011) found a slightly higher mass balance rate (2002–2007: -0.79 ±0.52 m w.e. a^{-1}) but within the uncertainty ranges of the other studies. For 18 Himalayan glaciers Azam et al. (2018) assessed a mean rate of -0.49 m w.e. a^{-1} for directly measured glacier mass balance for the period from 1975 to 2015. Maurer et al. (2019) calculated a Himalayan-wide geodetic mass balance of −0.38 ±0.08 m w.e. a^{-1} for clean ice from 2000 to 2016. ~~These issues highlight~~The mass-balance rate of Rikha Samba Glacier is within a similar range, however, the one of Yala Glacier is more negative.

The bias introduced by small low-lying glaciers result in the overestimation of negative mass balances in the region (Gardner et al., 2013). It highlights the importance of investigating large glacier elevation ranges, measuring mass balances in the accumulation areas and precipitation data in high altitudes.

5.5 Interannual variability of winter precipitation and long-term trends of accumulation

Climate data indicate a large interannual variability of winter precipitation but long-term trends of solid and liquid precipitation on high elevations are not well known, and winter mass balances measurements are still rare in the Nepal Himalaya. The interannual variability of winter precipitation is much larger than of summer precipitation, and affected the seasonal mass balances on Yala Glacier. Derived from precipitation data from the Indian Embassy and the Airport in Kathmandu, Seko and Takahashi (1991) found that winter precipitation (October–April) exceeds summer precipitation (May–September) during 10 years in the period from 1911 to 1986. Since 1985, the interannual variability was largest in the month of October (Fujita et al., 1997b) and extreme snowfall has been reported from cyclones in October for several years, such as in 1985 (Seko and Takahashi, 1991; Iida et al., 1987), Phailin in 2013 (Shea et al., 2015b), Hudhud in 2014 (Neckel et al., 2015), and the 1995 India cyclone in November 1995 (Kattelmann and Yamada, 1996). This precipitation variability has a significant effect on the mass balance of glaciers in the Nepal Himalaya (Seko and Takashj, 1991). Early or large amounts of winter snowfall protect the glacier from ablation by the high albedo, like the snowfall from the cyclones Phailin and Hudhud in October 2013 and 2014. In early 2015, exceptional amounts of precipitation likely dampened the effects of the extremely negative summer balance with less than average precipitation.

On Yala Glacier positive point ~~net~~ mass-balance data from the ~~eighties~~1980s and ~~nineties~~1990s are more positive than those measured in this study (Fig. 14), ~~indicating increased temperatures possibly combined with decreasing precipitation. On Yala glacier, positive~~but the related precipitation trends are unknown. Positive annual point balances were measured above 5400 m a.s.l. in all years except ~~2015 and 2017. In the eighties and nineties, Japanese and Swiss researchers measured snow layers with a range of methods~~2014/15 and 2016/17. Steinegger et al. (1993) measured deposited snow in a crevasse at 5580 m a.s.l. and identified annual layers from 1981 to 1989 based on the dirt layers, and converted them to water equivalent. Iida et al. (1987) studied snow and dirt layer formation processes, analysed a snow profile at 5333 m a.s.l. and used precipitation data to assign clean and dirt layers to specific periods in the mass~~-~~–balance years 1983 and 1984. Ozawa and Yamada (1989) and Yamada (1991) evaluated snow profiles from various elevations to calculate the net ~~balance from~~accumulation for the ~~mass balance~~ years ~~1986~~1985/86 and ~~1987~~1986/87, and Yoshimura et al. (2006) retrieved an ice core at 5350 m a.s.l. and identified annual layers from 1984 to 1994 with help of snow algae. Shiraiwa et al. (1992) analysed snow profiles at various elevations, identified surface balances from monsoon 1990 and the following winter balance up to May 1991. Even though the measurements are difficult to compare because of varying methodologies, it can be seen that accumulation was highest in the ~~eighties~~1980s, and also measured at lower elevations. In the ~~nineties~~1990s the accumulation decreased, however, accumulation was still measured at elevations where in this study no positive balances were measured. The authors of the earlier studies identified annual layers with confidence, and only Iida et al. (1987) discussed additional dirt layers formed after strong winter snowfall events. In this study the accumulation measurements were challenging because often sawdust layers were gone or older layers hard to assign. In the winter snow at Yala Glacier, we often observed white and grey snow layers, with ice lenses or layers in between (Fig. 6). The ice layers and lenses, superimposed ice and occasional ice fingers indicated melt and refreezing processes, which likely already start in March when incoming solar radiation and temperature increase and April when solar radiation is close to its maximum (Takahashi et al., 1987a; Shea et al., 2015b). Snow from monsoon was usually more metamorphed with darker and coarser grains. Watanabe et al. (1984) reported from April to June melting up to at least 5500~~-~~ m a.s.l., and an abundance of water from rain and melt in the temperate accumulation area during the Himalayan Glacier Boring Project 1981–1982, which promotes the snow metamorphosis process. In some years we observed icicles hanging from distinct layers in ice cliffs, indicating melt and refreezing processes and impermeable ice layers in the snowpack.

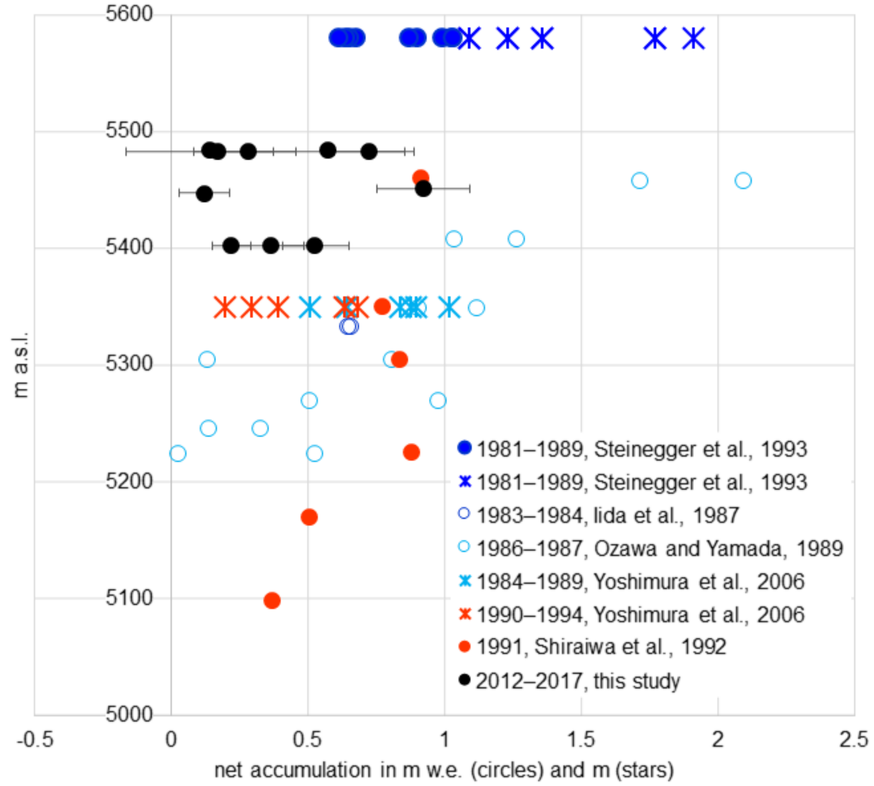

Figure 14: Positive point mass balances in the accumulation area from mass-balance years in the 1980s (blue), 1990s (red) and from this study (black). The data was compiled from annual snow pit measurements, multiannual snow profiles, ice cores and crevasses, using dirt, algae or ice layers to distinguish annual layers. Most measurements were converted into water equivalents (circles), and some are only available as snow depth (stars).

~~Overall, it was challenging to identify annual snow accumulation without help of sawdust layers.~~ The decreased accumulation over the past decades is likely due to the raising temperatures, possibly a decrease in precipitation as observed in the Everest region by Salerno et al. (2015). On the south slopes of Mt. Everest above 5000 m a.s.l., they found that the minimum temperature increased outside of the monsoon season and liquid precipitation decreased significantly from 1993 to 2013. Provided this also applies to other parts of the Central Himalaya, the impact of reduced snowfall could possibly contribute to ~~a large degree to~~ the negative mass balances of Yala, Rikha Samba and other glaciers.

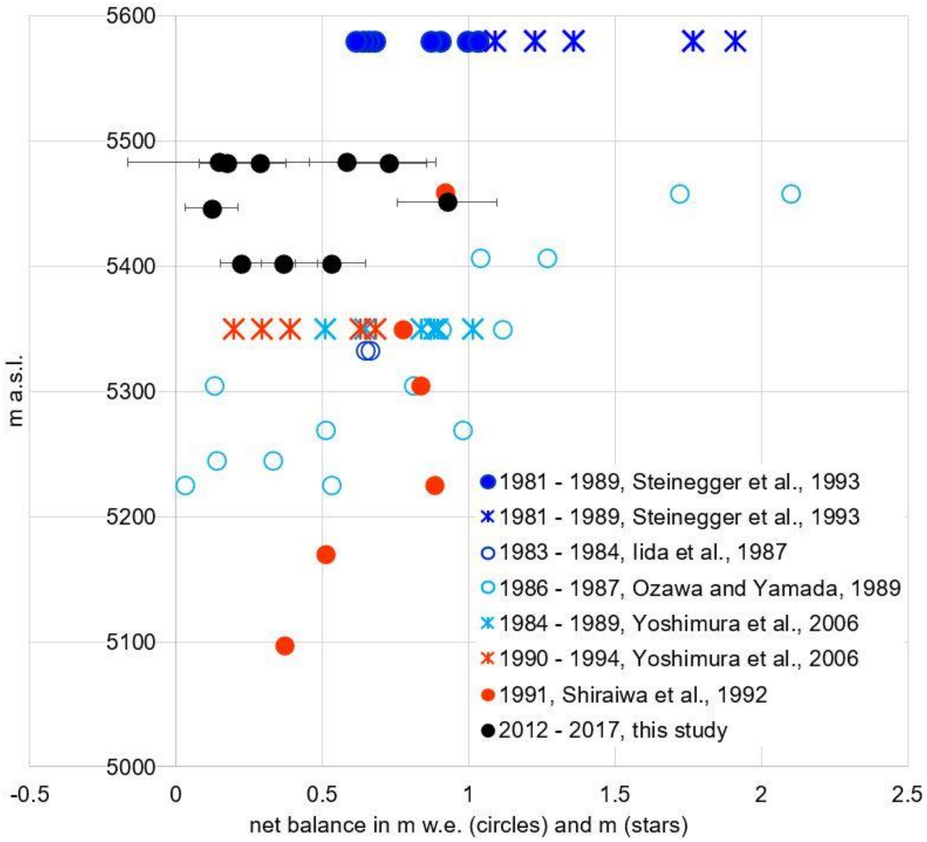

~~**Figure 14: Positive point net balances in the accumulation area from mass balance years in the 1980ies (blue), 1990ies (red) and from this study (black). The data has been**~~

5.6 Extrapolation of in situ measurements to the accumulation area

In the ablation area of Yala and Rikha Samba glaciers sufficient in situ measurements largely allowed the interpolation of the data by using elevation dependent mass-balance gradient. In the accumulation area, measurements were often challenging and associated with higher uncertainties. The main issues were difficult access, and cumulative ablation that temporarily exceeded the cumulative accumulation (Supplement section S1). On one hand this ablation removed the marked reference surfaces for the accumulation measurements, and on the other hand the uncertainty is increase for ablation measured with stakes installed in an unstable firn and snow underground. Additionally, no accumulation data could be collected at the highest elevations.

To extrapolate the mass balance to higher elevations, we made a few considerations: the glacier mass-balance programmes were running only within the first decade, and a re-evaluation and possible correction of the glacier-wide mass balance with help of other methods is likely in the future (Zemp et al., 2013; Cullen et al., 2016; Wagnon et al., 2020). Therefore, we chose simple extrapolation approaches.

At Yala Glacier, extrapolating the ablation gradient to the accumulation area introduced a systematic error for a small glacier area (15 % of the total area) with a small elevation range (~160 m). The largest errors are expected in the highest elevation bands, where accumulation is overestimated (Fig. S3 and S4). At the steep south-west-oriented slopes of Yala Glacier, the ablation is likely increased and underestimated in the glacier-wide mass balance. At Rikha Samba Glacier, using the same extrapolation method like at Yala Glacier would have very much overestimated the accumulation in a large area (36 % of the total area) with a large elevation range (~650 m). Instead, we estimated a fixed value for the accumulation area, which introduced a random error. Geodetic mass-balance analyses complementing in situ mass-balance data for the same time interval help reducing uncertainties and are an integral part of glacier mass-balance programmes following the international glacier monitoring strategy (WGMS, 2020b; Haeberli et al., 2000).

~~**compiled from annual snow pit measurements, multiannual snow profiles, ice cores and crevasses, using dirt, algae or ice layers to distinguish annual layers. Most measurements were converted into water equivalents (circles), and some are only available as snow depth (stars).**~~

~~The downwasting of Yala Glacier compromised the consistent representativeness of stake measurements at several locations. For example, between stakes S1 and S1B and near S5, Yala Glacier has very concave surfaces with bowl-shaped areas and transitions to steep slopes. Here the ablation is likely enhanced because of the reflection of radiation (Hock, 2005). Since 2011 onwards, we observed that concave shapes have become more pronounced, ice velocities decreased generally, and the glacier surface downwasted as observed at other glaciers (Ragettli et al., 2016; Sommer et al. 2020). The decreased ice velocities are likely a consequence of the downwasting. At some locations the glacier surface topography changed to a degree that the stake had to be shifted. These small-scale spatial variabilities could cause a bias, which might be later reduced with help of complementing geodetic surface analyses.~~

~~The ice cliffs of Yala Glacier are mainly oriented southwest, and slopes steeper than 50° make up approximately 5 % of the map view glacier area and occur over the entire glacier range. Already Ageta et al. (1984) described the ice cliffs and old photos document part of the glacier terminus as ice cliff, at time with an apron (Shiraiwa, 1993). The effect of vertical ablation through melt, sublimation and ice breaking off could be substantial, as observed at glacier ice cliffs in the Antarctic McMurdo Dry Valleys (Chinn, 1987; Lewis et al., 1999), on Kilimanjaro (Winkler et al., 2010), and debris-covered glaciers (e.g. Sakai et al., 2002; Steiner et al., 2015). Ice cliff ablation cannot be quantified with the conventional glaciological method and might lead to underestimating ablation. With geodetical thickness change analyses based on high resolution surface elevations for the entire glacier area the effect could be quantified (Joerg and Zemp, 2014). The mass balance measurements of Yala Glacier are likely and largely representative for comparable slopes in Nepal. However, the mass balance of clean glaciers' ice cliffs remains unknown. While more than 50 % of the glacier area in Nepal is oriented southwest, south, or southeast, less than 1 % of the map view area are slopes steeper than 50° (Bajracharya et al., 2014). Yet, the steeper the ice slopes the smaller is the surface area in a DEM, hence the surface area of Nepal's ice cliffs and steep ice slopes is underrepresented in such DEM analyses.~~

~~5.2 Seasonal mass balance~~

~~Yala Glacier is considered a summer-accumulation type glacier (Acharya and Kayastha, 2018), and the summer balance determines the annual balance. However, we measured positive mass balances for every winter season, and only little or no accumulation in higher elevations during summer (Fig. 2, 4 and Table 2). Fujita et al. (1997b) point out that winter precipitation is more important in Langtang than in Khumbu, which is confirmed by the climate station data described by Shea et al. (2015b) and could partly explain the winter accumulation. Shiraiwa (1993) highlights the influence of both the summer monsoon and westerly winter circulation on the annual balance. Wagnon et al. (2013) address the high wind speeds from westerly winds associated with the jet stream at Mera Glacier (5360 m a.s.l on glacier station) in winter, which causes in combination with sublimation a substantial part of the winter ablation. Stitger et al. (2018) and Litt et al. (2019) assessed sublimation on Yala Glacier and confirm its strong ablating influence, especially during in favourable conditions such as high wind speed, low atmospheric vapour pressure and low near-surface vapour pressure. The study of Shea et al. (2015b) shows similarly high winter wind speeds at Rikha Samba Glacier (5310 m a.s.l, off-glacier station) as at Mera Glacier, but at Yala Glacier (5060 m a.s.l., off-glacier station) only slightly higher wind speeds than on annual average. It seems reasonable that wind and sublimation are important ablation processes for Rikha Samba Glacier in winter. At Yala Glacier, in winter when accumulation dominates over ablation the effect of wind and sublimation is probably smaller compared to Mera and Rikha Samba Glacier. Derived from precipitation data from the Indian Embassy and the Airport in Kathmandu, Seko and Takahashi (1991) found that winter precipitation (October–April) exceeds summer precipitation (May–September) during 10 years in the period from 1911 to 1986. Salerno et al. (2015) found increased winter temperatures and decreased precipitation above 5000 m a.s.l. in the Everest region. Additionally, the interannual variability of winter precipitation is much larger than of summer precipitation, which is explained by post-monsoon cyclones and passage of western disturbances with sometimes large amounts of snowfall.~~

~~This variability has a significant effect on the mass balance of glaciers in the Nepal Himalaya (Seko and Takahashj, 1991). Since 1985, the interannual variability was largest in the month of October (Fujita et al., 1997b) and extreme snowfall has been reported from cyclones in October for several years, such as in 1985 (Seko and Takahashi, 1991; Iida et al., 1987), Phailin in 2013 (Shea et al., 2015b), Hudhud in 2014 (Neckel et al., 2015), and the 1995 India cyclone in November 1995 (Kattelmann and Yamada, 1996). Early or large amounts of winter snowfall protect the glacier longer from ablation by the high albedo. In winter 2014/15, the exceptional amounts of precipitation likely dampened the effects of the extremely negative summer balance with less than average precipitation. Still there are only few seasonal mass balance measurements in the Himalayas and many studies have the main focus on ablation processes. Certainly, the glaciers, especially in humid climates are more sensitive to temperature changes. However, it would be useful to better understand the impact of the highly variable winter precipitation on the winter balance. For the next few decades such winter accumulation could be important for the survival of low-lying glaciers and are important contributors for water from snow cover in pre-monsoon.~~

~~5.3 Frontal variation and flow~~

~~On Rikha Samba Glacier, Fujita et al. (2001) measured a retreat of 216 m from 1974–1994 with the slow retreat of -10.8 m a^{-1} (Table 5). From 1994–1998 the glacier retreated 73 m with an accelerated rate of -18.2 m a^{-1}, followed by a decreased rate. From 2006 to 2011 and 2013 the terminus retreated rapidly 159 m and 52 m, with rates of -31.8 m a^{-1} and -26.0 m a^{-1}, respectively.~~

~~At Yala Glacier, Ono (1985) dated LIA moraines and documented annual ice push moraines, and Yamada et al. (1992) and Kappenberger et al. (1993) observed terminus retreat since the 70ies with a minor advance in the early 80ies and stagnation, respectively, followed by continuous retreat. Fujita et al. (1998) noted an accelerated shrinkage in the 90ies, which continued from 2000 to 2012 with a rate of -14.1 m a^{-1} when the glacier retreated over a steep rock step from about 5100 m to 5175 m a.s.l. From 2012 to 2016 Yala Glacier retreated with an annual rate of -5.2 m a^{-1} in mostly flat terrain, partly in shallow water.~~

~~Horizontal flow was also measured with a theodolite from 28 September to 27 October 1982 (Ageta et al., 1984), and from 22 May to 7 October 1996 (Fujita et al., 1998) and a decreasing velocity was observed (Fig. 12). In both studies, the annual flow rate was assumed to be the same as for the measurement periods, despite varying seasons. Sugiyama et al. (2013) measured the top three stakes on 26 September 2008 and 31 October 2009, and the lower two stakes for four days from 31 October to 4 November 2009 with a dGPS, which were presumably extrapolated to calculate the annual rate, assuming a constant flow. The flow velocity and direction measured in this study from 2012 to 2014 compares to the measurements from 2008 to 2009. However, the glacier is slower than in the 80ies and 90ies, and the direction slightly varied, as already shown by Sugiyama et al. (2013).~~

6 Conclusions

We measured the in situ mass balance of Yala and Rikha Samba glaciers for the mass-balance years 2011/12 to 2016/17. Additionally, we measured the seasonal in situ mass balance of Yala Glacier and analysed the geodetic mass balance from 2000 to 2012. Glacier length changes have been analysed for both glaciers based on field measurements, maps and satellite images.

- Both Yala and Rikha Samba ~~Glacier have been continuously shrinking and retreating~~glaciers shrank and retreated in the last couple of decades. The geodetic mass balance of Yala Glacier showed a mass loss of -10.49 ±~~-~~7.41 m w. e. from 2000~~-~~ to 2012, ~~and~~at an annual rate of -0.74 ±0.53~~-~~ m w.e. a^{-1}~~, which indicates an unfavourable climate for the glacier.~~. The ~~glacier retreat of 346 m from~~ cumulative in situ mass balances for Yala and Rikha Samba glaciers were -4.80 ±0.69 m w.e. and 2.34 ±0.79 m w.e., and the annual mass-balance rates -0.80 ±0.28 m w.e. a^{-1} and -0.39 ±0.32 m w.e. a^{-1}, respectively. From 1974 to 2016~~ indicates that this unfavourable climate trend persisted in the preceding~~

~~decades. Yala Glacier is not in balance with the climate, and a modelling study by Fujita and Nuimura (2011) confirms~~, Yala Glacier retreated 346 m, and from 1989 to 2013 Rikha Samba Glacier retreated 431 m. Under the recent climate it can be expected that Yala Glacier will ~~likely continue shrinking and retreating in the coming decades.~~disappear over time but not Rikha Samba Glacier (Fujita and Nuimura, 2011).

- ~~At Yala Glacier, the annual balance is determined by the summer balance, however, positive balances were measured in all winters. A better understanding of~~For both investigated glaciers, the ~~mass balance processes and highly variable precipitation~~measurements in the ablation area were sufficient to calculate mass-balance gradients. However, lacking reliable measurements in ~~winter would help to better understand the water regulating function of glaciers, especially for~~ the ~~many smaller glaciers in lower altitude ranges in the Central Himalayas. This study also confirms the bias towards negative mass balances for small glaciers in lower elevation ranges. There are no~~ high elevations prevented the calculation of accumulation ~~measurements above 5500 m a.s.l. and thus, no gradient could be identified, and balances are likely slightly overestimated. Additional~~ gradients. On one hand, parts of the accumulation areas were not accessible, on the other hand the in situ measurements in the accumulation area had higher ~~elevations are challenging but would be useful, to limited degree with snow pits, but for example also terrestrial laser scanning or unmanned aerial vehicles. Vertical ablation at~~ uncertainties. The related uncertainties can be addressed in future with complementing geodetic mass-balance analyses for the same time interval.
- The mass balance of the steep ~~and mainly southwest~~ south-west-facing slopes ~~and ice cliffs~~on Yala Glacier could not be quantified~~, but possibly play a role for the glacier-wide mass balance. Once better data for DEM generation are available especially from laser scans (Joerg and Zemp, 2014), the geodetic mass balance of the entire glacier should be analysed to identify the systematic bias, e.g. caused by steep~~ and may result in an underestimated ablation, which can be addressed with geodetic mass-balance analyses. The relevance of the steep glacier slopes ~~and cliffs, or accumulation above 5500 m, and possibly improve the uncertainty assessment. Generally,~~in terms of area cannot be quantified neither for Yala Glacier, nor the glaciers in Nepal in general with DEMs of 30 m and 90 m resolution, respectively.
- Yala Glacier experienced downwasting, indicated by the observed changing surface topography ~~of Yala Glacier has changed a lot~~ between 2011 and 2017 and ~~very small~~decreasing ice flow velocities~~ were measured.~~. Over the course of the years, most of the stakes could not be reinstalled at the original coordinates, either because of new crevasses, or significant changes of the surface features at the original site. ~~These are strong indications for the glacier downwasting and changed glacier characteristics. In an attempt to keep the glacier monitoring going for the next decades, we installed four new stakes at locations with possibly larger ice thicknesses. An updated high-resolution DEM would do better justice to the changed glacier topography, and a repeated GPR survey might be beneficial to quantify the remaining ice volume.~~The downwasting and small accumulation area at low elevation compromise the long-term monitoring of Yala Glacier.

~~In the coming years, ideally distributed physically based mass balance models are developed for both glaciers to improve the annual glacier-wide mass balance calculation. The model likely would use a classic energy balance approach and could be calibrated and corrected based on the direct and geodetic measurements. Ideally, it would take into account the increased melt at steeper, exposed areas, and increased deposition of snow in flatter, sheltered areas at Yala Glacier.~~

~~The long-term glacier monitoring of Rikha Samba Glacier is very important because of its larger and higher elevation range, which ensures the survival of the glacier, opposed to Yala Glacier. The processes on Rikha Samba Glacier are not yet well understood. However, winter ablation by wind and sublimation are likely important processes, similar to Mera Glacier.~~

~~As the next obvious step, the glacier mass balances should be compared to climatic data. We tried to compare the mass balances from the summer and winter seasons with climate station data, however, because of the data gaps it was impossible. Reanalysis data that have been downscaled with field-based data would be most suitable for that purpose.~~

~~The Langtang Valley is a well investigated study catchment with multiple types of measurements and monitoring stations. There are several datasets from automatic weather and hydrological stations from various time periods, however, with many gaps due to the challenging environment. The systematic homogenisation of the climatic data according to WMO standards would be beneficial for the assessment of climate reanalysis data, and local, regional and global modelling analyses of e.g. glacier mass balances or runoff.~~

- ~~We recommend future complementing~~ The mean annual mass-balance rate of Yala Glacier is more negative compared to regional geodetic mass-balance analyses. The reason is the small area and elevation range of Yala Glacier and the setting on a low elevation.

The glacier mass-balance programmes for the two glaciers have been designed using a comprehensive monitoring strategy following the international glacier monitoring strategy within GTN-G (WGMS, 2020b; Haeberli et al., 2000). Provisions have been made for future geodetic mass balance ~~measurements as part of standard glacier monitoring programmes, which also help addressing systematic errors (Zemp et al., 2013). The development of distributed physically based modelling approaches would improve interpolation for glacier wides mass~~analyses by acquiring stereo images for DEM generation early on. AWSs at both study sites collect data to further assess the relationship between the mass balance~~, which likely will result in a reanalyse of the reported mass~~ and the climate, and modelling studies are ongoing for Rikha Samba Glacier.

7 Recommendations

The mass-balance ~~data.~~ programmes at Yala and Rikha Samba glaciers are set up for a long-term sustainable continuation. Based on this study we recommend a focus on following points:

- The long-term monitoring of glaciers with a high and large elevation range is important. Rikha Samba Glacier is such a glacier and its long-term survival is better compared to the small low-lying Yala Glacier.
- More ~~mass balance~~ measurements are needed in accumulation areas~~, and generally on glaciers with large elevation ranges. These data should be complemented with climate and in particular precipitation data from high elevations, with a focus on precipitation variability and patterns outside the monsoon season~~. At Rikha Samba Glacier measurements up to 6000 m a.s.l. are feasible with the glaciological method. However, at Yala Glacier possibilities are limited.
- Geodetic mass-balance analyses overlapping the time interval of the glaciological measurements of Yala and Rikha Samba glaciers are needed (Zemp et al., 2013). The complementing approach assures keeping the annual signal of the glaciological measurements, and reduce uncertainties introduced for example by unmeasured parts of the accumulation area or steep glacier slopes.
- The comparison of mass-balance data with climate data is needed to better understand ~~precipitation trends, the impact for low lying glaciers and runoff in the pre-monsoon season.~~the climate signal of the mass-balance data. Homogenised data from AWSs or reanalysis climate data ~~would support these efforts.~~ could be used for that purpose.

Data availability

The data ~~have been submitted to the World Glacier Monitoring Service, is~~are available from the Fluctuations of Glaciers Database http://dx.doi.org/10.5904/wgms-fog-2021-xx~~2020-08~~ (WGMS, ~~2020a) and is published in the Global Glacier Change Bulletin No. 3 (2016-2017) World Glacier Monitoring Service, Zurich, Switzerland (WGMS, 2020b~~2021). The Supplement contains additional information related to this article.

Contributions

DS designed the study and monitoring programme, collected and analysed data, and wrote the manuscript as main author. SPJ collected data and analysed the geodetic mass balance, velocities and frontal variations, and wrote the respective sections. TRG and GS collected and analysed the in situ mass~~-~~-balance data and contributed to text editing.

Competing interests

The authors declare that they have no conflict of interest

Acknowledgements

We would like to thank the Government of Norway for supporting and funding this research, as well as ~~our~~ICIMOD's national partners of Nepal, including the Department of Hydrology and Meteorology, Kathmandu University, and Tribhuvan University. This study was partially supported with core funds of ICIMOD contributed by the governments of Afghanistan, Australia, Austria, Bangladesh, Bhutan, China, India, Myanmar, Nepal, Norway, Pakistan, Switzerland, and the United Kingdom. Thanks to all field assistants, trainees and the Trekking Agencies Glacier Safari Treks, ~~Guides for all Seasons and~~ Himalayan Research Expeditions and Guides for all Seasons for their support for the glacier measurements and logistic support. We thank Koji Fujita ~~very much~~ for his support and the dGPS Magellan ProMark 3 data from May 2012, and the GEN map of Yala Glacier. Thanks to Joe Shea, Inka Koch and Santosh Nepal from ICIMOD and Suresh C. Pradhan from DHM for providing temperature and precipitation ~~data of~~information from the Langtang ~~area and Kyangjing station~~Valley. We thank Christa Stephan for providing the orthomap of Langtang, and Pushpalal Ball from the Department of Survey for help to digitize existing topographic data and maps. We thank Tino ~~Piecozonka~~Pieczonka, Nicolai Holzer and Tobias Bolch for the training and support on the geodetic mass balance analysis~~, and we thank~~. Thanks to Patrick Wagnon for supporting the field measurements in May 2013 and taking measurements in June 2015 together with Joe Shea, his support for geodetic dGNSS measurements and ~~advice~~analysis, and reviewing an earlier version of ~~the paper~~this article. We thank Matthias Huss for his support for the uncertainty assessment of the glaciological measurements, and Martin Hoelzle for reviewing the article thoroughly and providing support. We thank the scientific editor Reinhard Drews, reviewer Argha Banerjee and an anonymous reviewer for taking the time to help improve the article with constructive feedback.

References

Abdullah, T., Romshoo, S. A., and Rashid, I.: The satellite observed glacier mass changes over the Upper Indus Basin during 2000–2012, Sci. Rep., 10, 14285, https://doi.org/10.1038/s41598-020-71281-7, 2020.

Acharya, A. and Kayastha, R. B.: Mass and Energy Balance Estimation of Yala Glacier (2011–2017), Langtang Valley, Nepal, Water, 11, https://doi.org/10.3390/w11010006, 2019.

Ageta, Y. and Higuchi, K.: Estimation of Mass Balance Components of a Summer-Accumulation Type Glacier in the Nepal Himalaya, Geogr. Ann. Ser. A Phys. Geogr., 66, 249–255, https://doi.org/10.1080/04353676.1984.11880113, 1984.

Ageta, Y., Hajime, I. A., and Watanabe, O.: Glaciological Studies on Yala Glacier in Langtang Himal, Bull. Glaciol. Res., 2, 41–47, 1984.

Azam, M. F., Wagnon, P., Ramanathan, A., Vincent, C., Sharma, P., Arnaud, Y., Linda, A., Pottakkal, J. G., Chevallier, P., Singh, V. B., and Berthier, E.: From balance to imbalance: a shift in the dynamic behaviour of Chhota Shigri glacier, western Himalaya, India, J. Glaciol., 58, 315–324, https://doi.org/10.3189/2012JoG11J123, 2012.

Azam, M. F., Wagnon, P., Vincent, C., Ramanathan, A., Linda, A., and Singh, V. B.: Reconstruction of the annual mass balance of Chhota Shigri glacier, Western Himalaya, India, since 1969, Ann. Glaciol., 55, 69–80, https://doi.org/10.3189/2014AoG66A104, 2014.

Azam, M. F., Ramanathan, A.L., Wagnon, P., Vincent, C., Linda, A., Berthier, E., Sharma, P., Mandal, A., Angchuk, T., Singh, V. B., and Pottakkal, J. G.: Meteorological conditions, seasonal and annual mass balances of Chhota Shigri Glacier, western Himalaya, India, Ann. Glaciol., 57, 328–338, https://doi.org/10.3189/2016AoG71A570, 2016.

Azam, M. F., Wagnon, P., Berthier, E., Vincent, C., Fujita, K., and Kargel, J. S.: Review of the status and mass changes of Himalayan-Karakoram glaciers, J. Glaciol., 64(243) 61–74, https://doi.org/10.1017/jog.2017.86, 2018.

Bajracharya, S. R., Maharjan, S. B., Shrestha, F., Bajracharya, O. R., and Baidya, S.: Glacier status in Nepal and decadal change from 1980 to 2010 based on Landsat data, ICIMOD, Kathmandu, Nepal, 2014.

Baral, P., Kayastha, R.B., Immerzeel, W.W., Pradhananga, N.S., Bhattarai, B., Shahi, S., Galos, S., Springer, C., Joshi, S.P., and Mool, P.K.: Preliminary results of mass-balance observations of Yala Glacier and analysis of temperature and precipitation gradients in Langtang Valley, Nepal, Ann. Glaciol., 55, 9–14, https://doi.org/10.3189/2014AoG66A106, 2014.

Berthier, E., Arnaud, Y., Vincent, C., and Rémy, F.: Biases of SRTM in high-mountain areas: Implications for the monitoring of glacier volume changes, Geophys. Res. Lett., 33, L08502, https://doi.org/10.1029/2006GL025862, 2006.

Berthier, E., Arnaud, Y., Kumar, R., Ahmad, S., Wagnon, P., and Chevallier, P.: Remote sensing estimates of glacier mass balances in the Himachal Pradesh (Western Himalaya, India), Remote. Sens. Environ., 108, 327–338, https://doi.org/10.1016/j.rse.2006.11.017, 2007.

Bojinski S., Verstraete, M., Peterson, T. C., Richter, C., Simmons, A., Zemp, M.: The concept of Essential Climate Variables in support of climate research, applications, and policy. Bull. Amer. Meteor. Soc., 95, 1431–1443, https://doi.org/10.1175/BAMS-D-13-00047.1, 2014.

Bolch, T., Buchroithner, M., Pieczonka, T., and Kunert, A.: Planimetric and volumetric glacier changes in the Khumbu Himal, Nepal, since 1962 using Corona, Landsat TM and ASTER data, J. Glaciol., 54, 592–600, https://doi.org/10.3189/002214308786570782, 2008.

Bolch, T., Pieczonka, T., and Benn, D. I.: Multi-decadal mass loss of glaciers in the Everest area (Nepal Himalaya) derived from stereo imagery, The Cryosphere, 5, 349–358, https://doi.org/10.5194/tc-5-349-2011, 2011.

Bolch, T., Kulkarni, A., Kääb, A., Huggel, C., Paul, F., Cogley, J. G., Frey, H., Kargel, J. S., Fujita, K., Scheel, M., Bajracharya, S., and Stoffel, M.: The state and fate of Himalayan glaciers, Science, 336, 310–314, https://doi.org/10.1126/science.1215828, 2012.

Bolch, T., Pieczonka, T., Mukherjee, K., and Shea, J.: Brief communication: Glaciers in the Hunza catchment (Karakoram) have been nearly in balance since the 1970s, The Cryosphere, 11, https://doi.org/10.5194/tc-11-531-2017, 531–539, 2017.

Bookhagen, B. and Burbank, D. W.: Toward a complete Himalayan hydrological budget: Spatiotemporal distribution of snowmelt and rainfall and their impact on river discharge, J. Geophys. Res., 115, F03019, https://doi.org/10.1029/2009JF001426, 2010.

Brun, F., Berthier, E., Wagnon, P., Kääb, A., and Treichler, D.: A spatially resolved estimate of High Mountain Asia glacier mass balances from 2000 to 2016. Nature Geosci 10, 668–673, https://doi.org/10.1038/ngeo2999, 2017.

Chinn, T. J. H.: Accelerated ablation at a glacier ice-cliff margin, Dry Valleys, Arct. Antarct. Alp. Res., 19, 71–80, https://doi.org/10.1080/00040851.1987.12002579, 1987.

Cogley, J. G., Kargel, J. S., Kaser, G., and van der Veen, C. J.: Tracking the source of glacier misinformation, Science, 327(5965), 522, https://doi.org/10.1126/science.327.5965.522-a, 2010.

Cogley, J. G., Hock, R., Rasmussen, L. A., Arendt, A. A., Bauder, A., Braithwaite, R. J., Jansson, P., Kaser, G., Möller, M., Nicholson, L., and Zemp, M.: Glossary of glacier mass balance and related terms, IHP-VII Technical Documents in Hydrology

No. 86, IACS Contribution No. 2, UNESCOIHP, Paris, France, available at: https://unesdoc.unesco.org/ark:/48223/pf0000192525 (last access: 7 September 2020), 2011.

Cruz, R. V., Harasawa, H., Lal, M., Wu, S., Anokhin, Y., Punsalmaa, B., Honda, Y., Jafari, M., Li, C., and Huu Ninh, N.: Asia, in: Climate Change 2007: Impacts, Adaptation and Vulnerability. Contribution of Working Group II to the Fourth Assessment Report of the Intergovernmental Panel on Climate Change, edited by: Parry, M.L., Canziani, O.F., Palutikof, J.P., van der Linden, P.J., and Hanson, C.E., Cambridge University Press, Cambridge, UK, 469–506, https://archive.ipcc.ch/publications_and_data/ar4/wg2/en/ch10.html, 2007.

Cuffey, K. M. and Paterson, W. S. ~~Ding, Y., Sikka, D. R.: Synoptic systems and weather, in: The Asian Monsoon, edited by: Wang, B., Springer, Berlin, Heidelberg, Germany, 131–201, https://doi.org/10.1007/3-540-37722-0_4, 2006.~~ B.: The Physics of Glaciers, 4th ed. Butterworth-Heinemann/Elsevier, Oxford, 2010.

Dobhal, D. P., Gergan J. T., and Thayyen, R. J.: Mass balance studies of the Dokriani Glacier from 1992 to 2000, Garhwal Himalaya, India, Bull. Glaciol. Res., 25, 9–17, 2008.

Cullen, N. J., Anderson, B., Sirguey, P., Stumm, D., Mackintosh, A., Conway, J. P., Horgan. H. J., Dadic, R., Fitzsimons, S. J., and Lorrey, A.: An 11-year record of mass balance of Brewster Glacier, New Zealand, determined using a geostatistical approach, J. Glaciol., 63, 199–217, https://doi.org/10.1017/jog.2016.128, 2016.

Dobhal, D. P., Mehta, M., and Srivastava, D.: Influence of debris cover on terminus retreat and mass changes of Chorabari Glacier, Garhwal region, central Himalaya, India, J. Glaciol., 59, 961–971, https://doi.org/10.3189/2013JoG12J180, 2013.

Elsberg, D.H., Harrison, W. D., Echelmeyer, K. A., and Krimmel, R. M.: Quantifying the effects of climate and surface change on glacier mass balance, J. Glaciol., 47, 649–658, https://doi.org/10.3189/172756501781831783, 2001.

Fujii, Y., Nakawo, M., and Shrestha, M. L.: Mass balance studies of the glaciers in Ridden Valley, Mukut Himal, Seppyo, Special Issue, 38, 17–21, https://doi.org/10.5331/seppyo.38.Special_17, 1976.

Fujii, Y., Fujita, K., and Paudyal, P.: Glaciological research in Hidden Valley, Mukut Himal in 1994, Bull. Glaciol. Res., 14, 7–11, 1996.

Fujita, K.: Influence of precipitation seasonality on glacier mass balance and its sensitivity to climate change, Ann. Glaciol., 48, 88–92, https://doi.org/10.3189/172756408784700824, 2008a.

Fujita, K.: Effect of precipitation seasonality on climatic sensitivity of glacier mass balance, Earth Planet. Sci. Lett., 276, 14–19, https://doi.org/10.1016/j.epsl.2008.08.028, 2008b.

Fujita, K. and Nuimura, T.: Spatially heterogeneous wastage of Himalayan glaciers, P. Nat. Acad. Sci. USA, 108, 14011–14014, https://doi.org/10.1073/pnas.1106242108, 2011.

Fujita, K. and Sakai, A.: Modelling runoff from a Himalayan debris-covered glacier, Hydrol. Earth Syst. Sci., 18, 2679–2694, https://doi.org/10.5194/hess-18-2679-2014, 2014.

Fujita, K., Nakawo, M., Fujii, Y., and Paudyal, P.: Changes in glaciers in Hidden Valley, Mukut Himal, Nepal Himalayas, from 1974 to 1994, J. Glaciol., 43, 583–588, https://doi.org/10.3189/S002214300003519X, 1997a.

Fujita, K., Sakai, A., and Chhetri, R. B.: Meteorological observation in Langtang Valley, Nepal Himalayas, 1996, Bull. Glaciol. Res., 15, 71–78, 1997b.

Fujita, K., Takeuchi, N., and Seko, K.: Glaciological observations of Yala Glacier in Langtang Valley, Nepal Himalayas, 1994 and 1996, Bull. Glaciol. Res., 16, 75–81, 1998.

Fujita, K., Nakazawa, F., and Rana, B.: Glaciological observations on Rikha Samba Glacier in Hidden Valley, Nepal Himalayas, 1998 and 1999, Bull. Glaciol. Res., 18, 31–35, 2001.

Fujita, K., Inoue, H., Izumi, T., Yamaguchi, S., Sadakane, A., Sunako, S., Nishimura, K., Immerzeel, W. W., Shea, J. M., Kayastha, R. B., Sawagaki, T., Breashears, D. F., Yagi, H., and Sakai, A.: Anomalous winter-snow-amplified earthquake-induced disaster of the 2015 Langtang avalanche in Nepal, Nat. Hazards Earth Syst. Sci., 17, 749–764, https://doi.org/10.5194/nhess-17-749-2017, 2017.

Gardelle, J., Berthier, E., and Arnaud, Y.: Impact of resolution and radar penetration on glacier elevation changes computed from DEM differencing, J. Glaciol., 58, 419–422, https://doi.org/10.3189/2012JoG11J175, 2012.

Gardelle, J., Berthier, E., Arnaud, Y., and Kääb, A.: Region-wide glacier mass balances over the Pamir-Karakoram-Himalaya during 1999–2011, The Cryosphere, 7, 1263–1286, https://doi.org/10.5194/tc-7-1263-2013, 2013.

Gardner, A. S., Moholdt, G., Cogley, J. G., Wouters, B., Arendt, A. A., Wahr, J., Berthier, E., Hock, R., Pfeffer, W. T., Kaser, G., Ligtenberg, S. R. M., Bolch, T., Sharp, M. J., Hagen, J.-O. O., van den Broeke, M. R., and Paul, F.: A Reconciled Estimate of Glacier Contributions to Sea Level Rise: 2003 to 2009, Science, 340, 852–857, https://doi.org/10.1126/science.1234532, 2013.

GCOS: The Global Observing System for Climate: Implementation Needs, World Meteorological Organization, GCOS-200 (GOOS-214), https://library.wmo.int/doc_num.php?explnum_id=3417, last access: 7 September 2020, 2016.

Gilbert, A., Sinisalo, A., Gurung, T. R., Fujita, K., Maharjan, S. B., Sherpa, T. C., and Fukuda, T.: The influence of water percolation through crevasses on the thermal regime of a Himalayan mountain glacier, The Cryosphere, 14, 1273–1288, https://doi.org/10.5194/tc-14-1273-2020, 2020.

Gurung, S., Bhattarai, B. C., Kayastha, R. B., Stumm, D., Joshi, S. P., and Mool, P. K.: Study of annual mass balance (2011–2013) of Rikha Samba Glacier, Hidden Valley, Mustang, Nepal, Sci. Cold Arid Reg., 8, 311–318, https://doi.org/10.3724/SP.J.1226.2016.00311, 2016.

Haeberli, W., Cihlar, J., and Barry, R. G.: Glacier monitoring within the Global Climate Observing System, Ann. Glaciol., 31, 241–246, https://doi.org/10.3189/172756400781820192, 2000.

Haeberli, W., Hoelzle, M., Paul, F., and Zemp, M.: Integrated monitoring of mountain glaciers as key indicators of global climate change: the European Alps, Ann. Glaciol., 46, 150 – 160, https://doi.org/10.3189/172756407782871512, 2007.

Higuchi, K.: Outline of the Glaciological Expedition of Nepal: Boring Project 1981 and 1982, Bull. Glaciol. Res., 2, 1–13, 1984.

Hock, R.: Glacier melt: a review of processes and their modelling, Prog. Phys. Geogr., 29, 362–391. https://doi.org/10.1191/0309133305pp453ra, 2005.

Holzer, N., Vijay, S., Yao, T., Xu, B., Buchroithner, M., and Bolch, T.: Four decades of glacier variations at Muztagh Ata (eastern Pamir): a multi-sensor study including Hexagon KH-9 and Pléiades data, The Cryosphere, 9, 2071–2088, https://doi.org/10.5194/tc-9-2071-2015, 2015.

Huss, M.: Density assumptions for converting geodetic glacier volume change to mass change, The Cryosphere, 7, 877–887, https://doi.org/10.5194/tc-7-877-2013, 2013.

Huss, M. and Hock, R.: Global-scale hydrological response to future glacier mass loss. Nat. Clim. Chang., 8, 135-140, https://doi.org/10.1038/s41558-017-0049-x, 2018.

IGOS: Integrated Global Observing Strategy Cryosphere Theme Report - For the Monitoring of our Environment from Space and from Earth, World Meteorological Organization, WMO/TD-No. 1405, 114 pp, https://globalcryospherewatch.org/reference/documents/files/igos_cryosphere_report.pdf, last access: 7 September 2020, 2007.

Iida, H., Watanabe, O., and Takiwaka, M.: First Results from Himalayan Glacier Boring Project in 1981–1982, Part II. Studies on internal structure and transformation process from snow to ice of Yala Glacier, Langtang Himal, Nepal, Bull. Glaciol. Res., 2, 25–33, 1984.

Iida, H., Endo, Y., Kohshima, S., Motoyama, H., and Watanabe, O.: Characteristics of snow cover and formation process of dirt layer in the accumulation area of Yala Glacier, Langtang Himal, Nepal, Bull. Glacier Res., 5, 55–62, 1987.

Immerzeel W. W., van Beek, L.P.H., Konz, M., Shrestha, A. B., and Bierkens, M. F. P.: Hydrological response to climate change in a glacierized catchment in the Himalayas, Clim. Change, 110, 721–736, https://doi.org/10.1007/s10584-011-0143-4, 2012.

Immerzeel, W. W., Kraaijenbrink, P. D. A., Shea, J. M., Shrestha, A. B., Pellicciotti, F., Bierkens, M. F. P., and de Jong, S.M.: High-resolution monitoring of Himalayan glacier dynamics using unmanned aerial vehicles, Remote. Sens. Environ., 150, 93–103, https://doi.org/10.1016/j.rse.2014.04.025, 2014.

Immerzeel, W. W., Wanders, N., Lutz, A. F., Shea, J. M., and Bierkens, M. F. P.: Reconciling high-altitude precipitation in the upper Indus basin with glacier mass balances and runoff, Hydrol. Earth Syst. Sci., 19, 4673–4687, https://doi.org/10.5194/hess-19-4673-2015, 2015.

Immerzeel, W. W., Lutz, A. F., Andrade, M., Bahl, A., Biemans, H., Bolch, T., Hyde, S., Brumby, S., Davies, B. J., Elmore, A. C., Emmer, A., Feng, M., Fernández, A., Haritashya, U., Kargel, J. S., Koppes, M., Kraaijenbrink, P. D. A., Kulkarni, A. V., Mayewski, P. A., Nepal, S., Pacheco, P., Painter, T. H., Pellicciotti, F., Rajaram, H., Rupper, S., Sinisalo, A., Shrestha, A. B., Viviroli, D., Wada, Y., Xiao, C., Yao, T., and Baillie, J. E. M.: Importance and vulnerability of the world's water towers, Nature, 577, 364–369, https://doi.org/10.1038/s41586-019-1822-y, 2019.

Joerg, P. C., and Zemp, M.: Evaluating volumetric glacier change methods using airborne laser scanning data. Geogr. Ann. Ser. A Phys. Geogr., 96, 135–145, https://doi.org/10.1111/geoa.12036, 2014.

Kääb, A., Berthier, E., Nuth, C., Gardelle, J., and Arnaud, Y.: Contrasting patterns of early twenty-first-century glacier mass change in the Himalayas, Nature, 488, 495–498, https://doi.org/10.1038/nature11324, 2012.

Kargel, J. S., Leonard, G. J., Shugar, D. H., Haritashya, U. K., Bevington, A., Fielding, E. J., Fujita, K., Geertsema, M., Miles, E. S., Steiner, J., Anderson, E., Bajracharya, S., Bawden, G. W., Breashears, D. F., Byers, A., Collins, B., Dhital, M. R., Donnellan, A., Evans, T. L., Geai, M. L,. Glasscoe, M. T., Green, D., Gurung, D. R., Heijenk, R., Hilborn, A., Hudnut, K., Huyck, C., Immerzeel, W. W., Jian, L. M., Jibson, R., Kääb, A., Khanal, N. R., Kirschbaum, D., Kraaijenbrink, P. D. A., Lamsal, D., Liu, S. Y., Lv, M. Y., McKinney, D., Nahirnick, N. K., Nan, Z. T., Ojha, S., Olsenholler, J., Painter, T. H., Pleasants, M., Pratima, K. C., Yuan, Q. I., Raup, B. H., Regmi, D., Rounce, D. R., Sakai, A., Shangguan, D. H., Shea, J. M., Shrestha, A. B., Shukla, A., Stumm, D., van der Kooij, M., Voss, K., Wang, X., Weihs, B., Wolfe, D., Wu, L. Z., Yao, X. J., Yoder, M. R., and Young, N.: Geomorphic and geologic controls of geohazards induced by Nepal's 2015 Gorkha earthquake, Science, 351, aac8353, https://doi.org/10.1126/science.aac8353, 2016.

Kappenberger, G., Steinegger, U., Braun, L. N., and Kostka, R., Recent glacier tongues in the Langtang Khola Basin, Nepal, determined by terrestrial photogrammetry, Snow and Glacier Hydrology (Proceedings of the Kathmandu Symposium, November 1992), IAHS Publ. no. 218, 95–101, 1993.

Kaser, G., Grosshauser, M., Marzeion, B.: Contribution potential of glaciers to water availability in different climate regimes. P. Nat. Acad. Sci. USA, 107, 20223-20227, https://doi.org/10.1073/pnas.1008162107, 2010.

Kattelmann, R. and Yamada, T.: Storms and Avalanches of November 1995, Khumbu Himal, Nepal. Proceedings of the 1996 International Snow Science Workshop, Banff, Canada, 276–278, 1996.

Koblet, T., Gärtner-Roer, I., Zemp, M., Jansson, P., Thee, P., Haeberli, W., and Holmlund, P.: Reanalysis of multi-temporal aerial images of Storglaciären, Sweden (1959–99) – Part 1: Determination of length, area, and volume changes, The Cryosphere, 4, 333–343, https://doi.org/10.5194/tc-4-333-2010~~-~~, 2010.

Kostka, R., Schneider, E., Mareich, M., Moser, G., Nairz, W., Patzelt, G., and Schneider, C.: Alpenvereinskarte Langthang Himal Ost~~. In Alpenvereinskarte (Ed.), Alpenvereinskarte~~ Nr 0/11, map, Austrian Alpine Club, Freytag - Berndt and Artaria, Wien, Austria, 1990.

Lea, J. M., Mair, D. W. F., and Rea, B. R.: Evaluation of existing and new methods of tracking glacier terminus change, J. Glaciol., 60, 323–332. http://doi.org/10.3189/2014JoG13J061, 2014.

Lewis, K. L., Fountain, A. G., and Dana, G. L.: How important is terminus cliff melt?: a study of the Canada Glacier terminus, Taylor Valley, Antarctica, Glob. Planet. Change, 22,105–115, https://doi.org/10.1016/S0921-8181(99)00029-6, 1999.

Lindenmann, J.: Untersuchung dekadischer Gletschervolumenänderungen im Langtang Himalaya, Nepal, basierend auf DHM-Analysen verschiedener Datensätze inklusive statistischer Unsicherheitsanalyse, M.S. thesis, Glaciology and Geomorphodynamics Group - 3G, University of Zurich, Switzerland, 138 pp., 2012.

Litt, M., Shea, J., Wagnon, P., Steiner, J., Koch, I., Stigter, E., and Immerzeel, W.: Glacier ablation and temperature indexed melt models in the Nepalese Himalaya, Sci. Rep. 9, 5264, https://doi.org/10.1038/s41598-019-41657-5, 2019.

Liu, S., Xie, Z., Song, G., Ma, L., and Ageta, Y.: Glacier on the north side of Mt. Xixiabangma, China, Bull. Glacier Res., 14, 37–43, 1996.

Lutz, A. F., Immerzeel, W. W., Shrestha, A. B., and Bierkens, M.F.P.: Consistent increase in High Asia's runoff due to increasing glacier melt and precipitation, Nature Clim. Change 4, 587–592, https://doi.org/10.1038/nclimate2237, 2014.

Mandal, A., Ramanathan, A., Azam, M. F., Angchuk, T., Soheb, M., Kumar, N., Pottakkal, J. G., Vatsal, S., Mishra, S., and Singh, V. B.: Understanding the interrelationships among mass balance, meteorology, discharge and surface velocity on Chhota Shigri Glacier over 2002–2019 using in situ measurements, J. Glaciol., 66, 727–741, https://doi.org/10.1017/jog.2020.42, 2020.

Marzeion, B., Jarosch, A. H., and Hofer, M.: Past and future sea-level change from the surface mass balance of glaciers, The Cryosphere, 6, 1295–1322, https://doi.org/10.5194/tc-6-1295-2012, 2012.

Maurer, J. M., Schaefer, J. M., Rupper, S., and Corley, A.: Acceleration of ice loss across the Himalayas over the past 40 years, Sci. Adv. 5, eaav7266, https://doi.org/10.1126/sciadv.aav7266, 2019.

Ménégoz, M., Gallée, H., and Jacobi, H. W.: Precipitation and snow cover in the Himalaya: from reanalysis to regional climate simulations, Hydrol. Earth Syst. Sci., 17, 3921–3936, https://doi.org/10.5194/hess-17-3921-2013, 2013.

Murakami, S., Ozawa, H., and Yamada, T.: Permeability coefficient of water in snow and firn at the accumulation area of Yala Glacier, Nepal Himalaya, Bull. Glacier Res., 7, 203–208, 1989.

Neckel, N., Kropáček, J., Schröter, B., and Scherer, D.: Effects of Cyclone Hudhud captured by a high altitude Automatic Weather Station in northwestern Nepal, Weather, 70, 208–2010, https://doi.org/10.1002/wea.2494, 2015.

Nuimura, T., Fujita, K., Yamaguchi, S., and Sharma, R. R.: Elevation changes of glaciers revealed by multitemporal digital elevation models calibrated by GPS survey in the Khumbu region, Nepal Himalaya, 1992–2008, J. Glaciol., 58, 648–656, https://doi.org/10.3189/2012JoG11J061, 2012.

Ono, Y.: Recent fluctuations of the Yala (Dakpatsen) Glacier, Langtang Himal, reconstructed from annual moraine ridges, Innsbruck, Z. Gletscher. Glazial., 21, 251–258, 1985.

Ozawa, H.: Thermal regime of a glacier in relation to glacier ice formation, PhD thesis, Sapporo, Hokkaido University, 73 pp., 1991.

Ozawa, H. and Yamada, T: Contributions of internal accumulation to mass balance and conditions of superimposed ice formation in Yala glacier, Nepal Himalayas. In: Report of the Glaciological Expedition of Nepal Himalayas, 1987–1988: Glacial studies in Langtang Valley, Sapporo, Japan, 31–46, 1989.

Paul, F.: Calculation of glacier elevation changes with SRTM: is there an elevation bias? J. Glaciol., 54, 945–946, https://doi.org/10.3189/002214308787779960, 2008.

Pieczonka, T., Bolch, T. Junfeng, W., and Shiyin, L.: Heterogeneous mass loss of glaciers in the Aksu-Tarim Catchment (Central Tien Shan) revealed by 1976 KH-9 Hexagon and 2009 SPOT-5 stereo imagery, Remote. Sens. Environ., 130, 233–244. https://doi.org/10.1016/j.rse.2012.11.020, 2013.

Pratap, B., Dobhal, D. P., Mehta, M., and Bhambri, R.: Influence of debris cover and altitude on glacier surface melting: a case study on Dokriani Glacier, central Himalaya, India, Ann. Glaciol., 56, 9–16, https://doi.org/10.3189/2015AoG70A971, 2015.

Pratap, B., Sharma, P., Patel, L., Singh, A. T., Gaddam, V. K., Oulkar, S., and Thamban, M.: Reconciling High Glacier Surface Melting in Summer with Air Temperature in the Semi-Arid Zone of Western Himalaya, Water, 11, 1561, https://doi.org/10.3390/w11081561, 2019.

Rabus, B., Eineder, M., Roth, A., and Bamler, R.: The shuttle radar topography mission—a new class of digital elevation models acquired by spaceborne radar, ISPRS J. Photogramm. Remote Sens., 57, 241–262, https://doi.org/10.1016/S0924-2716(02)00124-7, 2003.

Racoviteanu, A. E., Armstrong, R., and Williams, M. W.: Evaluation of an ice ablation model to estimate the contribution of melting glacier ice to annual discharge in the Nepal Himalaya, Water Resour. Res., 49, 5117–5133, https://doi.org/10.1002/wrcr.20370, 2013.

Ragettli, S., Bolch, T., and Pellicciotti, F.: Heterogeneous glacier thinning patterns over the last 40 years in Langtang Himal, Nepal, The Cryosphere, 10, 2075–2097, https://doi.org/10.5194/tc-10-2075-2016, 2016.

Rasmussen, R., Baker, B., Kochendorfer, J., Meyers, T., Landolt, S., Fischer, A. P., Black, J., Thériault, J. M., Kucera, P., Gochis, D., Smith, C., Nitu, R., Hall, M., Ikeda, K., and Gutmann, E.: How Well Are We Measuring Snow: The NOAA/FAA/NCAR Winter Precipitation Test Bed, B. Am. Meteorol. Soc., 93, 811–829, https://doi.org/10.1175/BAMS-D-11-00052.1, 2012.

Salerno, F., Guyennon, N., Thakuri, S., Viviano, G., Romano, E., Vuillermoz, E., Cristofanelli, P., Stocchi, P., Agrillo, G., Ma, Y., and Tartari, G.: Weak precipitation, warm winters and springs impact glaciers of south slopes of Mt. Everest (central Himalaya) in the last 2 decades (1994–2013), The Cryosphere, 9, 1229–1247, https://doi.org/10.5194/tc-9-1229-2015, 2015.

Sakai, A., Nakawo, M. and Fujita, K.: distribution characteristics and energy balance of ice cliffs on debris-covered Glaciers, Nepal Himalaya, Arct. Antarct. Alp. Res., 34, 12–19, https://doi.org/10.1080/15230430.2002.12003463, 2002.

Schwitter, M. P. and Raymond, C. F.: Changes in the longitudinal profiles of glaciers during advance and retreat, J. Glaciol., 39, 582–590, https://doi.org/10.3189/S0022143000016476, 1993.

Seko, K. and Takahashi, S.: Characteristics of Winter Precipitation and its Effect on Glaciers in the Nepal Himalaya, Bull. Glaciol. Res., 9, 9–16, 1991.

Shea, J. M., Immerzeel, W. W., Wagnon, P., Vincent, C., and Bajracharya, S.: Modelling glacier change in the Everest region, Nepal Himalaya, The Cryosphere, 9, 1105–1128, https://doi.org/10.5194/tc-9-1105-2015, 2015a.

Shea, J. M., Wagnon, P., Immerzeel, W. W., Biron, R., Brun, F., and Pellicciotti, F.: A comparative high-altitude meteorological analysis from three catchments in the Nepalese Himalaya, Int. J. Water Res. Environ. Eng., https://doi.org/10.1080/07900627.2015.1020417, 2015b.

Sherpa, S. F., Wagnon, P., Brun, F., Berthier, E., Vincent, C., Lejeune, Y., Arnaud, Y., Kayastha, R.B., and Sinisalo, A.: Contrasted surface mass balances of debris-free glaciers observed between the southern and the inner parts of the Everest region (2007–15), J. Glaciol., 63, 637–651, https://doi.org/10.1017/jog.2017.30, 2017.

Shrestha, M.L., Fujii, Y., and Nakawo, M.: Climate of Hidden Valley, Mukut Himal during the Monsoon in 1974, Seppyo, 38 105–108, https://doi.org/10.5331/seppyo.38.Special_105, 1976.

Shiraiwa, T.: Glacial fluctuations and cryogenic environments in the Langtang Valley, Nepal Himalaya, PhD thesis, Hokkaido University, Sapporo, Japan, 230 pp., http://doi.org/10.11501/3071619, 1993.

Shiraiwa, T.: Glacial fluctuations and cryogenic environments in the Langtang Valley, Nepal Himalaya, Contribution from the Institute of Low Temperature Science, Series A, 38, 1-98, http://hdl.handle.net/2115/20256, last access: 7August 2020, 1994.

Shiraiwa, T. and Watanabe, T.: Late Quaternary Glacial Fluctuations in the Langtang Valley, Nepal Himalaya, Reconstructed by Relative Dating Methods, Arct. Antarct. Alp. Res., 23, 404–416, https://doi.org/10.1080/00040851.1991.12002860, 1991.

Shiraiwa, T., Kenichi, U., and Yamada, T.: Distribution of mass input on glaciers in the Langtang Valley, Nepal Himalayas, Bull. Glacier Res., 10, 21–30, 1992.

Sommer, C., Malz, P., Seehaus, T.C., Lippl, S., Zemp, M. and Braun, M. H.: Rapid glacier retreat and downwasting throughout the European Alps in the early 21st century. Nat. Commun., 11, 3209, https://doi.org/10.1038/s41467-020-16818-0, 2020.

Steinegger, U., Braun, L. N., Kappenberger, G., and Tartari, G.: Assessment of Annual Snow Accumulation over the Past 10 Years at High Elevations in the Langtang Region, Snow and Glacier Hydrology (Proceedings of the Kathmandu Symposium, November 1992), IAHS Publ. no. 218, 155–166, 1993.

Steiner, J. F., Pellicciotti, F., Buri, P., and Miles, E. S.: Modelling ice-cliff backwasting on a debris- covered glacier in the Nepalese Himalaya, J. Glaciol., 61, 889–907, https://doi.org/10.3189/2015JoG14J194, 2015.

Stigter, E. E., Litt, M., Steiner, J. F., Bonekamp, P. N. J., Shea, J. M., Bierkens, M. F. P., and Immerzeel, W. W.: The Importance of Snow Sublimation on a Himalayan Glacier, Front. Earth Sci., 6, https://doi.org/10.3389/feart.2018.00108, 2018.

Sugiyama, S., Kukui, K., Fujita, K., Tone, K., and Yamaguchi, S.: Changes in ice thickness and flow velocity of Yala Glacier, Langtang Himal, Nepal, from 1982 to 2009, Ann. Glaciol., 54, 157–162, https://doi.org/10.3189/2013AoG64A111, 2013.

Takagi, H., Kazunori, A., Danhara, T., and Hideki, I.: Timing of the Tsergo Ri landslide, Langtang Himal, determined by fission-track dating of pseudotachylyte, J. Asian Earth Sci., 29, 466–472, https://doi.org/10.1016/j.jseaes.2005.12.002, 2007

Takahashi, S., Motoyama, H., Kawashima, K, Morinaga, Y., Seko, K, Iida, H., Kubota, H., and Turadahr, N. R.: Meteorological features in Langtang Valley, Nepal Himalayas, 1985–1986, Bull. Glaciol. Res., 5, 35–40, 1987a.

Takahashi, S., Motoyama, H., Kawashima, K, Morinaga, Y., Seko, K, Iida, H., Kubota, H., and Turadahr, N. R.: Summery of meteorological data at Kyangchen in Langtang Valley, Nepal Himalayas, Bull. Glaciol. Res., 5, 121–128, 1987b.

Tawde, S. A., Kulkarni, A.V., and Bala, G.: An estimate of glacier mass balance for the Chandra basin, western Himalaya, for the period 1984–2012, Ann. Glaciol., 58, 99–109, https://doi.org/10.1017/aog.2017.18, 2017.

Tian, L., Zong, J., Yao, T., Ma,L., Pu, J., and Zhu, D.: Direct measurement of glacier thinning on the southern Tibetan Plateau (Gurenhekou, Kangwure and Naimona'Nyi glaciers), J. Glaciol., 60, 879–888, https://doi.org/10.3189/2014JoG14J022, 2014.

Trewin, B., Cazenave, A., Howell, S., Huss, M., Isensee, K., Palmer, M. D., Tarasova, O., and Vermeulen, A.: Heasline Indicators for Global Climate Monitoring, Bull. Amer. Meteor. Soc., 102, E20-E37, https://doi.org/10.1175/BAMS-D-19-0196.1, 2021.

Tshering, P. and Fujita, K.: First in situ record of decadal glacier mass balance (2003–2014) from the Bhutan Himalaya, Ann. Glaciol., 57, 289–294, https://doi.org/10.3189/2016AoG71A036, 2016.

Vincent, C., Ramanathan, Al., Wagnon, P., Dobhal, D. P., Linda, A., Berthier, E., Sharma, P., Arnaud, Y., Azam, M. F., Jose, P. G., and Gardelle, J.: Balanced conditions or slight mass gain of glaciers in the Lahaul and Spiti region (northern India, Himalaya) during the nineties preceded recent mass loss, The Cryosphere, 7, 569–582, https://doi.org/10.5194/tc-7-569-2013, 2013.

Wagnon, P., Linda, A., Arnaud, Y., Kumar, R., Sharma, P., Vincent, C., Pottakkal, J. G., Berthier, E., Ramanathan, A., Hasnain, S.I., and Chevallier, P.: Four years of mass balance on Chhota Shigri Glacier, Himachal Pradesh, India, a new benchmark glacier in the western Himalaya, J. Glaciol., 53, 603–611, https://doi.org/10.3189/002214307784409306, 2007.

Wagnon, P., Vincent, C., Arnaud, Y., Berthier, E., Vuillermoz, E., Gruber, S., Ménégoz, M., Gilbert, A., Dumont, M., Shea, J. M., Stumm, D., and Pokhrel, B. K.: Seasonal and annual mass balances of Mera and Pokalde glaciers (Nepal Himalaya) since 2007, The Cryosphere, 7, 1769–1786, https://doi.org/10.5194/tc-7-1769-2013, 2013.

Wagnon, P., Brun, F., Khadka, A., Berthier, E., Shrestha, D., Vincent, C., Arnaud, Y., Six, D., Dehecq, A., Ménégoz, M., and Jomelli, V.: Reanalysing the 2007–19 glaciological mass-balance series of Mera Glacier, Nepal, Central Himalaya, using geodetic mass balance, J. Glaciol., 1–9, https://doi.org/10.1017/jog.2020.88, 2020.

Wagnon, P., Brun, F., Khadka, A., Berthier, E., Shrestha, D., Vincent, C., Arnaud, Y., Six, D., Dehecq, A., Ménégoz, M., and Jomelli, V.: Reanalysing the 2007–19 glaciological mass-balance series of Mera Glacier, Nepal, Central Himalaya, using geodetic mass balance, J. Glaciol., 1–9, https://doi.org/10.1017/jog.2020.88, 2020.

Watanabe, O., Takenaka, S., Iida, H., Kamiyama, K., Thapa, K. B., and Mulmi, D. D.: First results from Himalayan glacier boring project in 1981–1982, Part I. Stratigraphic analyses of full-depth cores from Yala Glacier, Langtang Himal, Nepal, Bull. Glacier Res., 2, 7–23, 1984.

Weidinger, J. T., Schramm, J. M., and Nuschej, F.: Ore mineralization causing slope failure in a high-altitude mountain crest—on the collapse of an 8000 m peak in Nepal, J. Asian Earth Sci., 21, 295–306, https://doi.org/10.1016/S1367-9120(02)00080-9, 2002.

Winkler, M., Kaser, G., Cullen, N., Mölg, T., Hardy, D., & Pfeffer, W.: Land-based marginal ice cliffs: Focus on Kilimanjaro, Erdkunde, 64, 179–193. https://doi.org/10.3112/erdkunde.2010.02.05, 2010.

~~WGMS: Global Glacier Change Bulletin No. 1 (2012–2013), edited by: Zemp, M., Gärtner-Roer, I., Nussbaumer, S. U., Hüsler, F., Machguth, H., Mölg, N., Paul, F., and Hoelzle, M.: ICSU(WDS)/IUGG(IACS)/ UNEP/UNESCO/WMO, World Glacier Monitoring Service, Zurich, Switzerland, Publication based on database version: doi:10.5904/wgms-fog-2015-11, Zurich, Switzerland, available at: http://wgms.ch/ggcb/ (last access: 7 September 2020), 2015.~~

~~WGMS: Global Glacier Change Bulletin No. 2 (2014–2015), edited by: Zemp, M., Nussbaumer, S. U., Gärtner-Roer, I., Huber, J., Machguth, H., Paul, F., and Hoelzle, M.: ICSU(WDS)/IUGG(IACS)/UNEP/UNESCO/WMO, World Glacier Monitoring Service. Publication based on database version: https://doi.org/10.5904/wgms-fog-2017-10, Zurich, Switzerland, available at: http://wgms.ch/ggcb/ (last access: 7 September 2020), 2017.~~

WGMS: Fluctuations of Glaciers Database, World Glacier Monitoring Service, digital media, http://dx.doi.org/10.5904/wgms-fog-2020-08, 2020a.

WGMS: Global Glacier Change Bulletin No. 3 (2016–2017), edited by: Zemp, M., Gärtner-Roer, I., Nussbaumer, S.U., Bannwart, J., Rastner, P., Paul, F., and Hoelzle, M., ISC(WDS)/IUGG(IACS)/UNEP/UNESCO/WMO, World Glacier Monitoring Service, Zurich, Switzerland, available at: http://wgms.ch/downloads/WGMS_GGCB_03.pdf, last access: 7 September 2020, 2020b.

WGMS: Fluctuations of Glaciers Database, World Glacier Monitoring Service, digital media, http://dx.doi.org/10.5904/wgms-fog-2021-xx, 2021.

Yamada, T., Motoyama, H., and Thapa, K.B.: Mass balance study of a glacier system from hydrological observations in Langtang Valley, Nepal Himalaya, Ann. Glaciol., 6, 318–320, https://doi.org/10.3189/1985AoG6-1-318-320, 1985.

Yamada, T., Shiraiwa, T., Iida, H., Kadota, T., Watanabe, T., Rana, B., Ageta, Y., and Fushimi, H.: Fluctuations of the glaciers from the 1970s to 1989 in the Khumbu, Shorong and Langtang regions, Nepal Himalayas, Bull. Glaciol. Res., 10, 11–19, 1992.

Yokoyama, K.: Ground Photogrammetry of Yala Glacier, Langtang Himal, Nepal Himalaya, Bull. Glaciol. Res., 2, 99–105, 1984.

Yoshimura, Y., Kohshima, S., Takeuchi, N., Seko, K., and Fujita, K.: Snow algae in a Himalayan ice core: new environmental markers for ice-core analyses and their correlation with summer mass balance, Ann. Glaciol., 43, 148–153, https://doi.org/10.3189/172756406781812276, 2006.

Zemp, M., Thibert, E., Huss, M., Stumm, D., Rolstad Denby, C., Nuth, C., Nussbaumer, S. U., Moholdt, G., Mercer, A., Mayer, C., Joerg, P. C., Jansson, P., Hynek, B., Fischer, A., Escher-Vetter, H., Elvehøy, H., and Andreassen, L. M.: Reanalysing glacier mass balance measurement series, The Cryosphere, 7, 1227–1245, https://doi.org/10.5194/tc-7-1227-2013, 2013.

Zemp, M., Huss, M., Eckert, N., Thibert, E., Paul, F., Nussbaumer, S. U., and Gärtner-Roer, I.: Brief communication: Ad hoc estimation of glacier contributions to sea-level rise from the latest glaciological observations, The Cryosphere, 14, 1043–1050, https://doi.org/10.5194/tc-14-1043–2020, 2020.

~~Supplement~~

~~For manuscript:~~

~~Mass balances~~S1 A brief description of ~~Yala~~summer-accumulation type glaciers and ~~Rikha Samba Glacier, Nepal~~related mass balance measurements

On summer-accumulation type glaciers the main ablation and accumulation season coincide in the monsoon season (Fig. S1.; Ageta and Higuchi, 1984). Summer-accumulation type glaciers with a balanced mass budget experience the majority of snowfall on high elevations during the monsoon season. In autumn and winter, snow accumulation is usually low but depends on the interannually very variable precipitation events as a result of westerly disturbances and cyclones (Fujita et al., 1997). Melt starts in the pre-monsoon season and continues throughout the monsoon season. In autumn and winter melt is minimal.

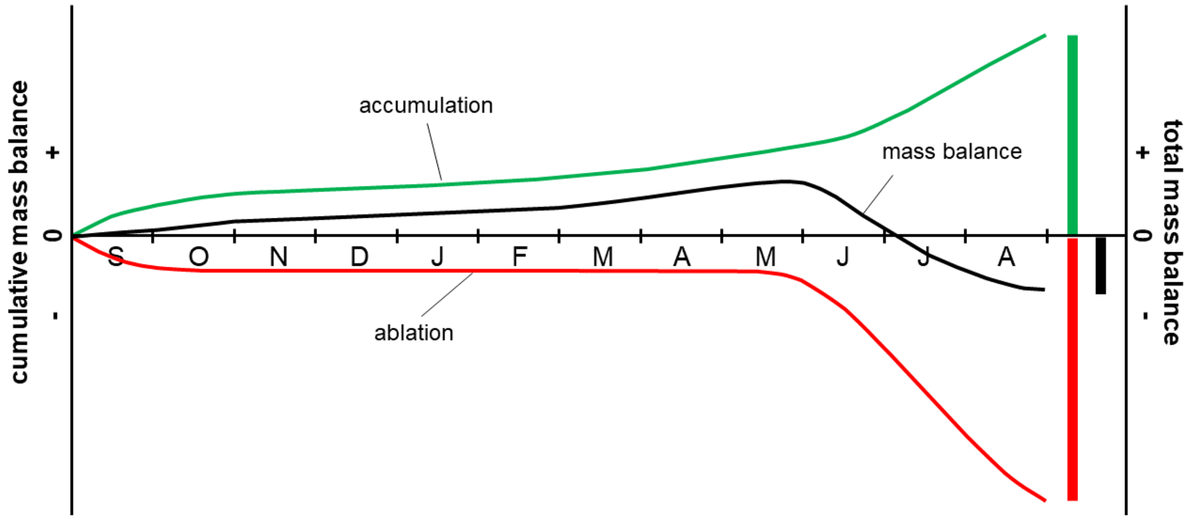

Figure S1: An example of the cumulative ablation, accumulation and mass balance of a summer-accumulation type glacier over the course of a mass balance year (adapted from ~~2000~~Ageta and Higuchi, 1984).

During monsoon, the altitude of the transient snowline on the glacier fluctuates and is very sensitive to ~~2017~~the temperature, especially during precipitation events. At the end of the monsoon season the altitude of the snowline depends on both the preceding temperatures and precipitation. Consequently, on summer-accumulation type glaciers the snowline at the end of the monsoon season does not necessarily coincide with the approximate equilibrium line and is not a reliable proxy for the equilibrium line altitude (ELA).

Ablation on glacier ice is usually measured with stakes, and accumulation with snow pits including snow depth, density and profile measurements (Kaser et al., 2003). In case of accumulation measurements snow cores are practical and more feasible than snow pits if the snow is hard and metamorphized from melt and refreezing processes during monsoon. Snow profiles are important to identify ice layers and characteristics snow layers. When snow is probed, it is important to take multiple measurements and to consider ice layers found in snow profiles to assess the representativeness of the measurements.

Measuring and analysing the point mass balance in the ablation area tends to be straightforward. In the ablation area, the ice is possibly covered with snow. The ablation on the ice can be measured with stakes. If snow is present, the snow accumulation can be measured with snow pits. For the point mass balance calculation, the ablation and accumulation are added up.

Measuring the mass balance in the accumulation season can be difficult. New snow from the current mass balance year is lying on top of snow and firn layers from previous mass balance years. An annual dust layer separating new snow from snow from previous mass balance years is often absent or unreliable. The reasons are the moist monsoon months when little dust is in the atmosphere to be deposited on the snow, and fresh snowfall preventing the accumulation of a distinct dust layer. To mark the current glacier surface in the field, an unsolvable powder (e.g. sawdust or blue carpenter chalk) is spread on the surface, covered by snow to protect from ablation. The location is marked with a stake.

The challenges of mass balance measurements in the accumulation area depend to a large degree on the timing of ablation and accumulation. If the cumulative accumulation is always larger than the cumulative ablation during the entire measurement period, the mass balance can be measured with snow pits or snow cores, provided the previous year's glacier surface can be identified (Scenario 1 in Fig. S2). This is the case in large parts of accumulation areas of glaciers with a large elevation range in the accumulation area.

Measurements are challenging if the cumulative ablation exceeds the cumulative accumulation during parts of the monitoring period (Scenarios 2 and 3 in Fig. S2). This can be the case in areas close to the equilibrium line where warm temperatures cause increased melt, or at locations where the glacier is exposed to ablation by wind drift. On one hand, the ablation cannot be reliably measured with stakes installed in an unstable firn underground that compacts over time and may push or pull the stake up or down. On the other hand, accumulation can be difficult to be quantified because ablation removed the marked reference glacier surface. The uncertainty of mass balance measurements is larger in such areas than in ablation areas, and an overestimated positive mass balance is likely.

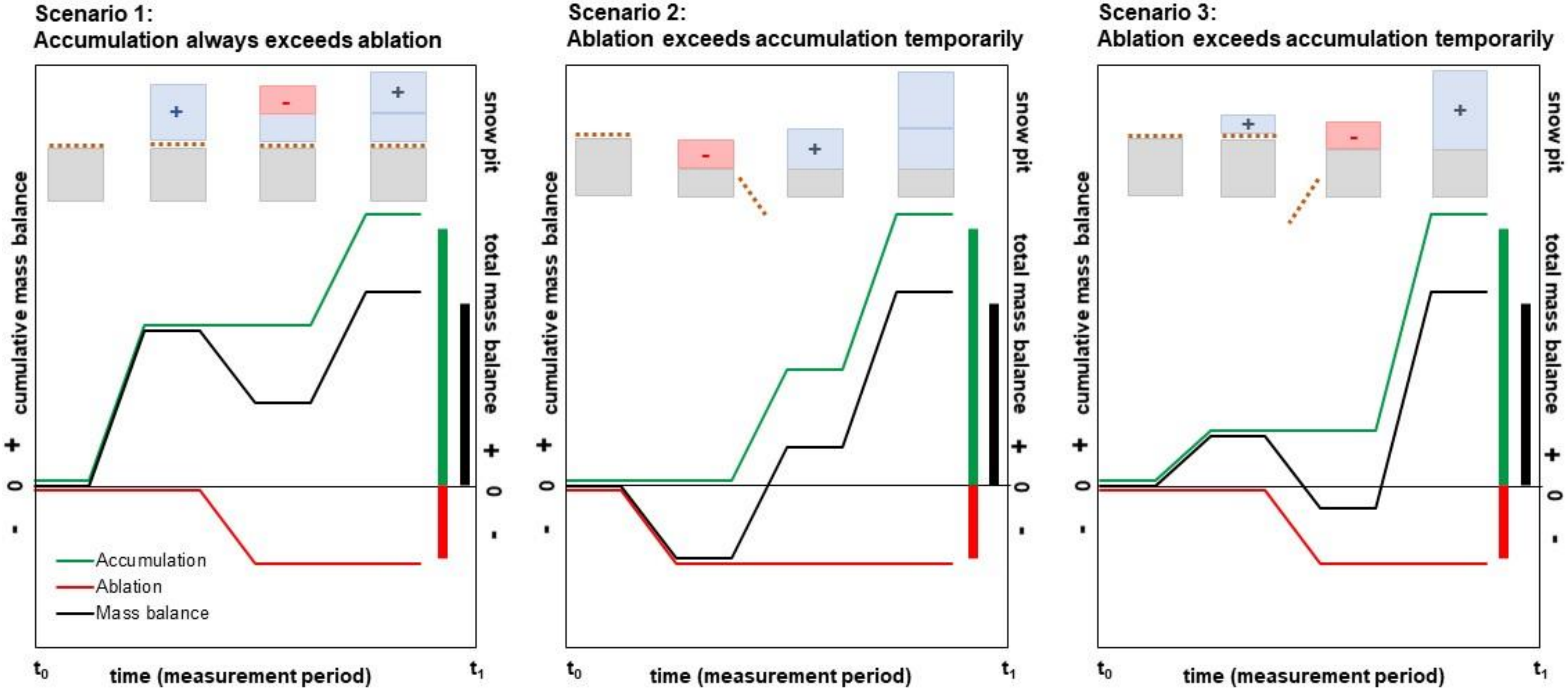

Figure S2: Three schematic scenarios of the evolvement of accumulation, ablation and mass balance in parts of an accumulation area during one measurement season (bottom graphs), and the impact on the snow and firn layers in a snow pit (top sketches). In the sketch, snow and firn from the previous measurement period are marked grey and the layer marking the surface artificially is the dashed brown line. Snow accumulation and snow ablation are marked blue and red, respectively. In all three scenarios the total amount of accumulation, ablation and mass balance are the same. But in scenarios two and three the temporarily exceeding ablation removes the marked layer on the reference surface, making the measurement and analysis challenging.

S2 Differential GNSS measurements, evaluated maps and used satellite products

Table S1: ~~dGPS~~Differential GNSS data collected and its usage for Yala and Rikha Samba ~~Glacier~~glaciers. The accuracy of the ~~dGPS~~dGNSS measurements mainly depends on access and measurement duration.

Yala Glacier			
Date	**Product**	**Usage**	**Accuracy measurements**
8.5.2012	~~dGPS~~differential GNSS (Magellan, ProMark-3)	stake locations velocity surface profiles	±0.3 m ±0.4 m ±0.4 m
3.11.2012	Garmin GPSmap 60CSx	terminus	<10 m
6.5.2014 5.5.2014 5.5.2014	~~dGPS~~differential GNSS (Topcon)	stake locations velocity terminus	±0.3 m ±0.4 m ±1-2 m
8.5.2016	~~dGPS~~differential GNSS (Topcon)	terminus ~~stake locations~~	±1-3 m ~~±0.3 m~~
25.4.2017	~~dGPS~~differential GNSS (Topcon)	stake locations	±0.3 m
Rikha Samba Glacier			
30.9.2013 3.10.2013	~~dGPS~~differential GNSS (Topcon)	terminus stake locations	±1-2 m ±0.3 m
3-7.10.2015	~~dGPS~~differential GNSS (Topcon)	stake locations	±0.3 m

Table S2: Maps and data sources evaluated for glacier surface and area change analysis for Yala Glacier. The estimated accuracy of topographic ~~map is based on map scale (e.g. in 1:50,000 map = 50m).~~maps is based on the map scale (e.g. in 1:50,000 map = 50 m). The maps known in Nepal as Schneider maps are labelled as "Alpenvereinskarte" (Alpine Club Map), and named after "Schneider's method" for the aerial photograph interpretation. The map was published within the framework of the Alpenvereinskartographie by the Austrian Alpine Club (Oesterreichischer Alpenverein) in 1990.

Publishing year	Name	Map ID	Scale	Accuracy	Map source	Reference	Usage
1965	Survey of India Map	71 H/12	1:63,360	±48–63 m (estimated)	Aerial photos 1957/58, field surveys; scanned map	Survey of India	Problems with transformation and scale, not used
1990	Schneider Map / Austrian Alpine Club Map	Langthang Himal Ost 0/11	1:50,000	±40–50 m (estimated)	Aerial photos 1970/71, field surveys; scanned map	Kostka et al., 1990	Transformation problem, not used
1984	GEN map	Yala Glacier	1:5,000	XY: ±4–5 m Z: ±0.45 m (estimated), terminus ~2-3 m	Ground photogrammetry, field surveys 1981; scanned map	Yokoyama, 1984, provided by K. Fujita	Terminus; for area and surface change not used due to transformation problems
1995	Nepal Topographic Map/ Finn Map	2885-15	1:50,000	>10 m (estimated)	Aerial photo 1992, field surveys; vector map		Transformation problems, not used
2014	ICIMOD glacier inventory	Yala Glacier	~1:50,000	±30 m, terminus and outline ±15 m	Landsat 7 ETM+, vector map	Bajracharya et al. 2014	Terminus Glacier outlines modified

Table S3: Overview of used remote sensing data for Yala and Rikha Samba ~~Glacier~~glaciers.

Year	Sensor	Scene ID	Geometric resolution	Usage
Yala Glacier				
23.11.1974	Hexagon KH-9	DZB1209-500101L006001 DZB1209-500101L007001	±7.6 m (varying from 6 – 9 m)	Frontal variations
2000	SRTM3	2128125658	±90 m	DEM (SRTM-3) GCP generation (z)
Feb 2000	Landsat 7 ETM+		±30 m	Frontal variations Glacier outline
15.1.2012	GeoEye-1 (stereo)	2012011505005761603031609567	±0.5 m (Pan) ±1.65 m (Multispectral)	DEM (DEM2012) Orthoimage for glacier outline
2013	Landsat-8	LC81410402013322LGN00	±15 m (Pan) ±30 m (Multispectral)	GCP generation (x,y)
Rikha Samba Glacier				
7.3.1989	Landsat MSS 4		±60 m	Terminus
2000	SRTM1	SRTM_53_07 SRTM_54_07	±30 m	DEM, voids filled with SRTM3 data
29.9.2001	Landsat 7 ETM+		±30 m	Terminus
7.2.2006	Landsat 5 TM		±30 m	Terminus
25.4.2010 27.4.2010	RapidEye	4452325_2010-04-25 4452325_2010-04-27	±5 m	Outline
5.2.2011	Landsat 5 TM		±30 m	Terminus

S3 Mass balances and uncertainties for elevation bands at Yala and Rikha Samba glaciers

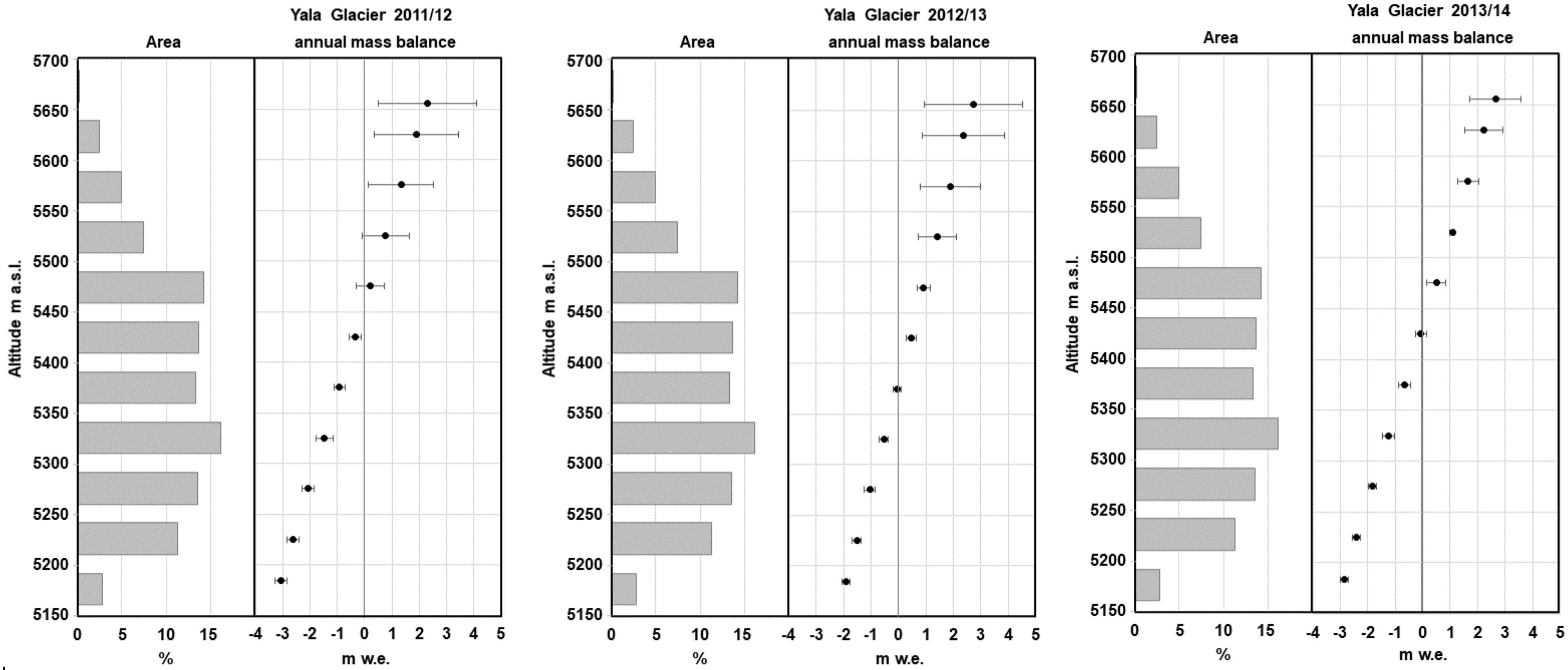

Figure S3: The annual mass balances and uncertainties for 50 m elevation bands of Yala Glacier for the mass balance years 2011/12, 2012/13 and 2013/14. Please note, for the FoG database, the uncertainty is submitted as single value valid for the positive and negative uncertainty.

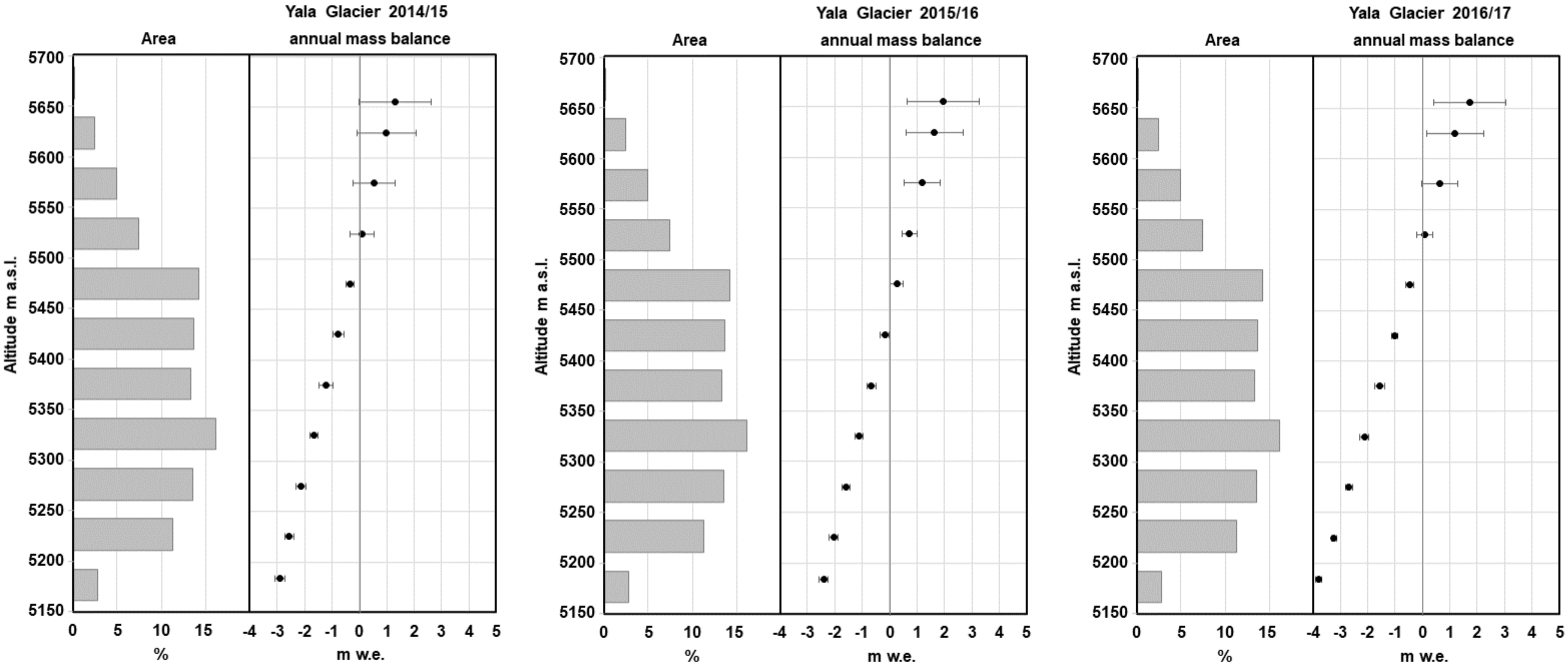

Figure S4: The annual mass balances and uncertainties for 50 m elevation bands of Yala Glacier for the mass balance years 2014/15, 2015/16 and 2016/17. Please note, for the FoG database, the uncertainty is submitted as single value valid for the positive and negative uncertainty.

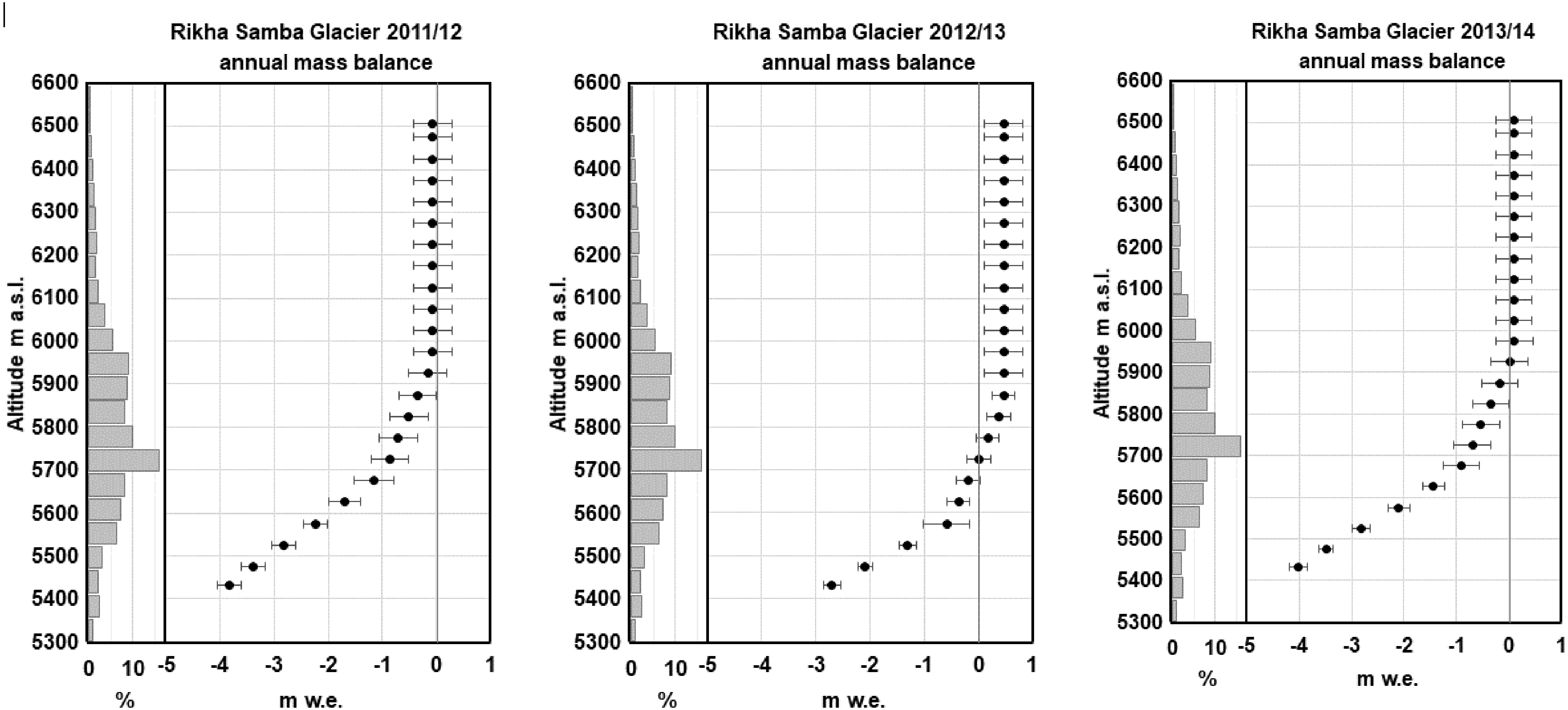

Figure S5: The annual mass balances and uncertainties for 50 m elevation bands of Rikha Samba Glacier for the mass balance years 2011/12, 2012/13 and 2013/14.

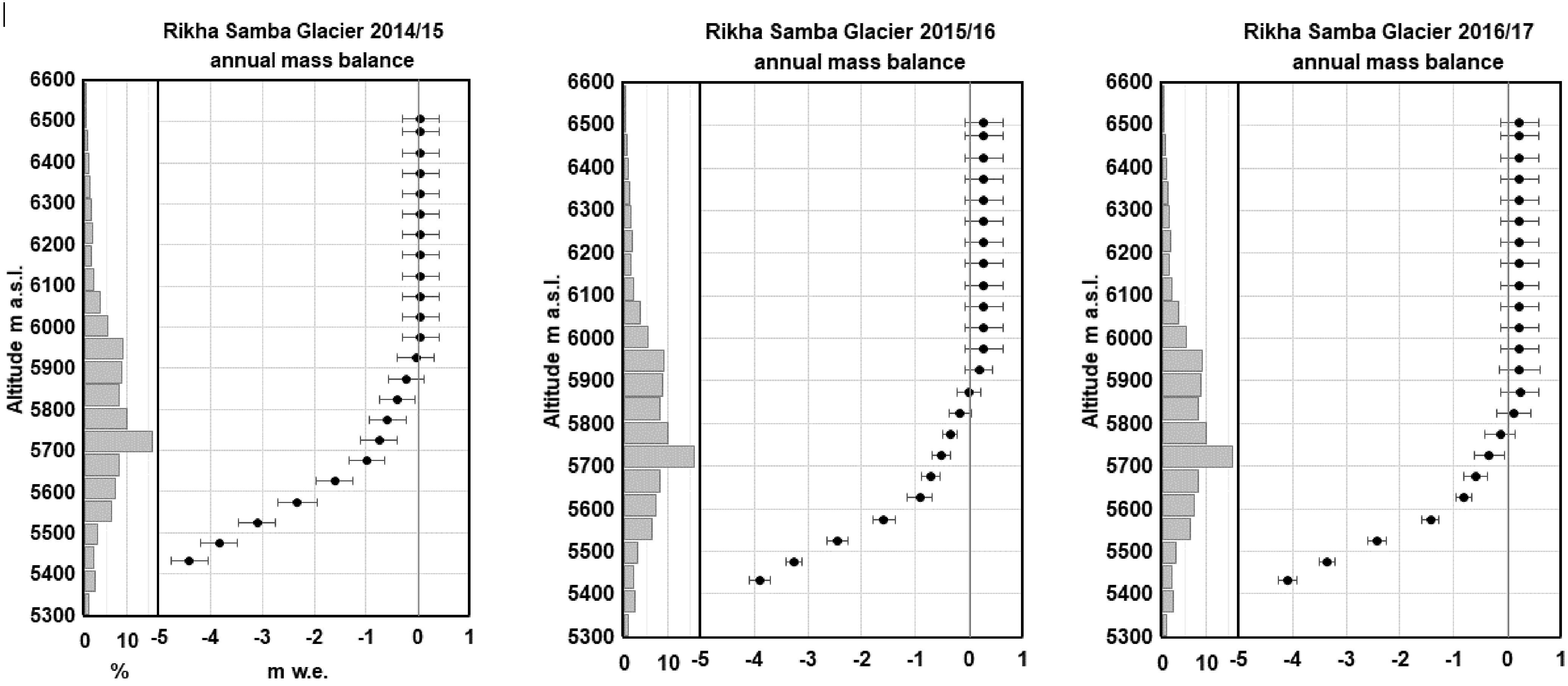

Figure S6: The annual mass balances and uncertainties for 50 m elevation bands of Rikha Samba Glacier for the mass balance years 2014/15, 2015/16 and 2016/17.

S4 The representation of the surface area, angle and height of slopes in DEMs of various resolutions

In digital elevation models (DEM) the surface area of steep slopes is underrepresented (Fig. S7), and vertical or near vertical ice cliffs cannot be represented in a DEM at all. The steeper the slopes, the smaller is the surface area in a DEM, in particular for DEM's with a coarse resolution.

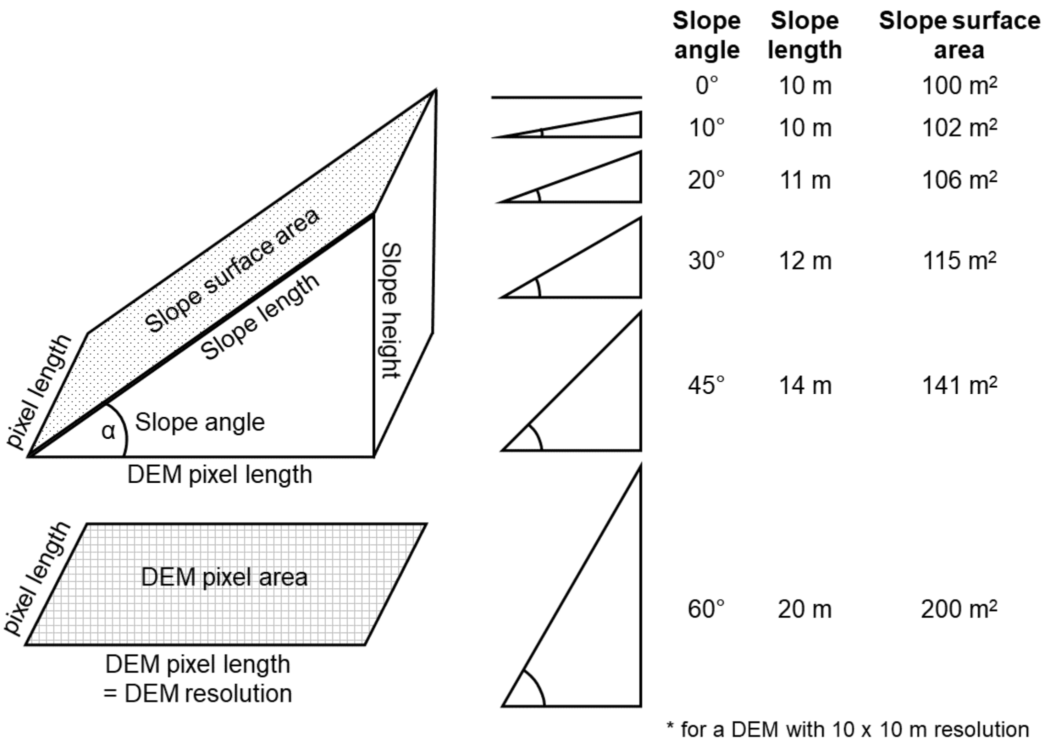

Figure S7: With an increasing slope angle the slope surface area and length increases, while the represented area in a DEM remains the same. Schema with terms (left) and examples of slopes and corresponding slope lengths and slope surface areas based on a DEM with a resolution of 10 m (right).

High resolution DEM's can represent small as well as big slope angles and slopes heights (Table S4 and S5, Figure S8). DEM's with a coarse resolution can only represent slopes with smaller angles and bigger heights.

Table S4: Minimum slope heights for various DEM resolutions (5 m, 10 m, 30 m and 90 m) that can be represented for specific slope angles.

-	Minimum slope height (m) for:			
Slope angle	**DEM resolution 5 m**	**DEM resolution 10 m**	**DEM resolution 30 m**	**DEM resolution 90 m**
0°:	0	0	0	0
10°:	1	2	5	16
20°:	2	4	11	33
30°:	3	6	17	52
40°:	4	8	25	76
45°:	5	10	30	90
50°:	6	12	36	107
60°:	9	17	52	156
70°:	14	27	82	247
80°:	28	57	170	510
85°:	57	114	343	1029
89°:	286	573	1719	5156

Table S5: Maximum slope angle that can be represented in a DEM with a given resolution for a minimum slope height.

	Maximum slope angle for:			
Slope height	**DEM resolution 5 m**	**DEM resolution 10 m**	**DEM resolution 30 m**	**DEM resolution 90 m**
5 m:	45°	27°	10°	3°
10 m:	63°	45°	18°	6°
20 m:	76°	63°	34°	13°
30 m:	81°	72°	45°	18°
50 m:	83°	79°	59°	29°
100 m:	87°	84°	73°	48°

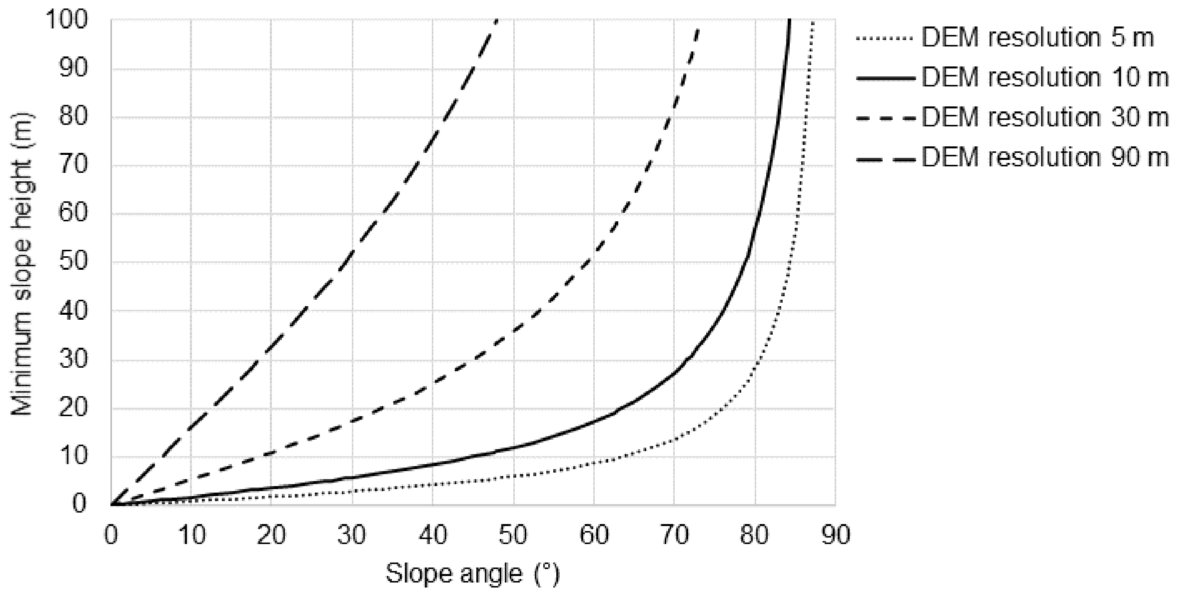

Figure S8: The curves show the minimum slope height required to represent slopes of a given angle in DEMs with a resolution of 5 m, 10 m, 30 m and 90 m.

The slope surface areas of flat slopes are better represented in a DEM than the surfaces areas of steep slopes (Table S6). For example, in a DEM with a resolution of 10 m one pixel has an area of 100 m^2. A slope of 10° has a surface area of 102 m^2 and a slope with an angle of 60° has an area of 200 m^2, which is almost double the area. Slopes of 76° and 83° have a surface area of 400 m^2 and 800 m^2, respectively. The higher the resolution of a DEM, the better is the slope surface area represented also for steeper slopes (Fig S9).

Table S6: The surface area of slopes with varying angles and the respective related height change for a DEM with a resolution of 10 m.

Slope angle (°)	Slope length (m)	Slope surface area (m^2)	Area in DEM (m^2)	Area gain* (surface vs map view) (%)	Height change (m)
0	10	100	100	0	0
10	10	102	100	2	2
20	11	106	100	6	4
30	12	115	100	15	6
40	13	131	100	31	8
45	14	141	100	41	10
50	16	156	100	56	12
60	20	200	100	100	17
70	29	292	100	192	27
80	58	576	100	476	57
85	115	1,147	100	1047	114

* surface gain irrespective of DEM resolution

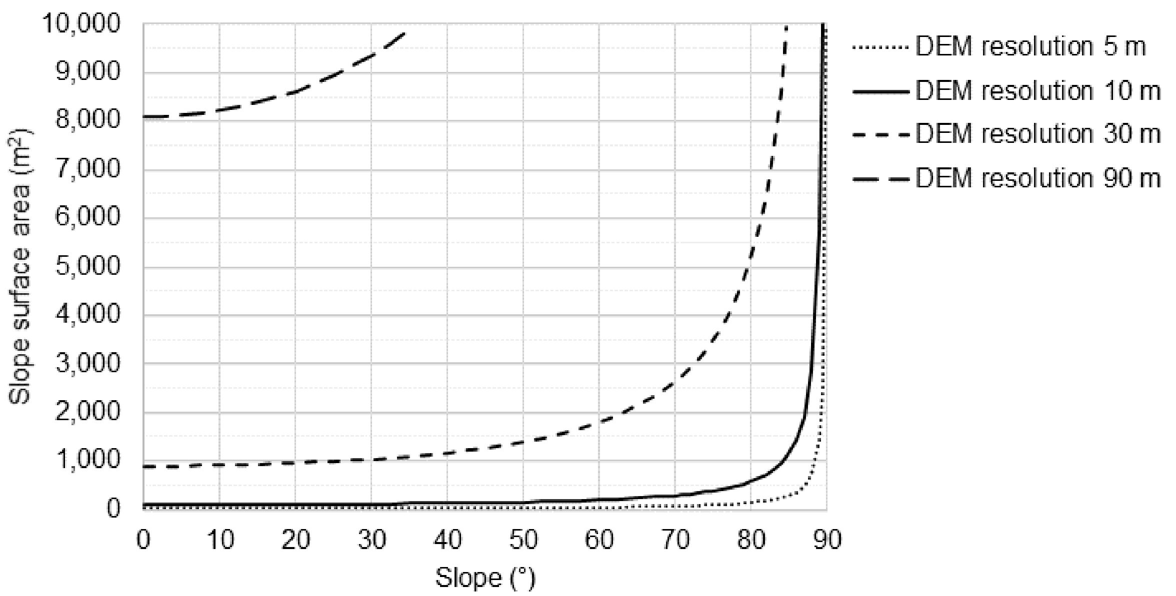

Figure S9: The slope surface area increases with increasing slope angle at different rates for DEMs with resolutions of 5 m, 10 m, 30 m and 90 m.

S5 References

Ageta, Y. and Higuchi, K.: Estimation of Mass Balance Components of a Summer-Accumulation Type Glacier in the Nepal Himalaya, Geogr. Ann. Ser. A Phys. Geogr., 66, 249–255, https://doi.org/10.1080/04353676.1984.11880113, 1984.

Fujita, K., Sakai, A., and Chhetri, R. B.: Meteorological observation in Langtang Valley, Nepal Himalayas, 1996, Bull. Glaciol. Res., 15, 71–78, 1997.

Kaser, G., Fountain, A., and Jansson, P.: A manual for monitoring the mass balance of mountain glaciers. Technical Report 59, International Hydrological Programme. IHP-VI. UNESCO, Technical Documents in Hydrology, 2003.